# Vertical Cloud Layer Statistics Derived From Echo Intensities Received By A 35 - GHz Radar
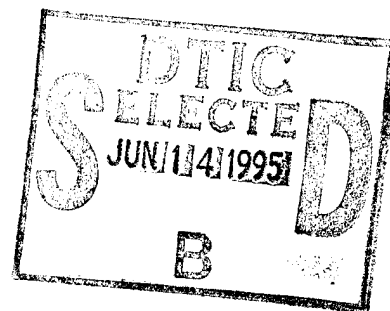
James H. Willand and Albert R. Boehm

Hughes STX Corporation
109 Massachusetts Avenue
Lexington, MA  02173

7  March, 1995

**Scientific Report No. 4**
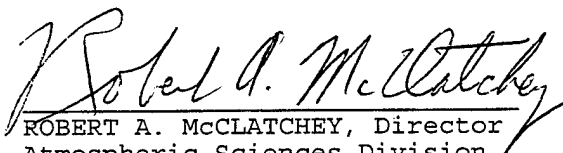
DTIC
SELECTED
JUN 14 1995
B

DTIC QUALITY INSPECTED 3

19950612 019

"This technical report has been reviewed and is approved for publication"

DONALD D. GRANTHAM, Chief
Contract Manager
Atmospheric Structure Branch

ROBERT A. McCLATCHEY, Director
Atmospheric Sciences Division

# REPORT DOCUMENTATION PAGE

Public reporting burden for this collection of information is estimated to average 1 hour per response, including the time for reviewing instructions, searching existing data sources, gathering and maintaining the data needed, and completing and reviewing the collection of information. Send comments regarding this burden estimate or any other aspect of this collection of information, including suggestions for reducing this burden, to Washington Headquarters Services, Directorate for Information Operations and Reports, 1215 Jefferson Davis Highway, Suite 1204, Arlington, VA 22202-4302, and to the Office of Management and Budget, Paperwork Reduction Project (0704-0188), Washington, DC 20503.

| 1. AGENCY USE ONLY (Leave blank) | 2. REPORT DATE <br> 7 March 1995 | 3. REPORT TYPE AND DATES COVERED <br> Scientific Report # 4 |
|---|---|---|

**4. TITLE AND SUBTITLE**

VERTICAL CLOUD LAYER STATISTICS DERIVED FROM ECHO INTENSITIES RECEIVED BY A 35 - GHZ RADAR

**5. FUNDING NUMBERS**

F19628-93-C-0051
PE 62101F
PR 6670
TA GS
WU AC

**6. AUTHOR(S)**

James H. Willand and Albert R. Boehm

**7. PERFORMING ORGANIZATION NAME(S) AND ADDRESS(ES)**

Hughes STX Corporation
109 Massachusetts Avenue
Lexington, MA 02173

**8. PERFORMING ORGANIZATION REPORT NUMBER**

Hughes STX Scientific Report #4

**9. SPONSORING/MONITORING AGENCY NAME(S) AND ADDRESS(ES)**

Phillips Laboratory
29 Randolph Road
Hanscom AFB, MA 01731-3010
Contract Technical Manager: Donald D. Grantham/GPAA

**10. SPONSORING/MONITORING AGENCY REPORT NUMBER**

PL-TR-95-2034

**11. SUPPLEMENTARY NOTES**

**12a. DISTRIBUTION/AVAILABILITY STATEMENT**

Approved for public release: distribution unlimited.

**12b. DISTRIBUTION CODE**

**13. ABSTRACT** (Maximum 200 words)

This report presents an assortment of useful vertical cloud layer statistics that were derived from echo intensities received by a 35-GHz radar. Both monthly and seasonal (summer and winter) vertical cloud layer statistics are presented showing:
1) probabilities of clouds aloft,
2) diurnal cloud layer analysis,
3) probabilities of vertical cloud-free line-of-site between two heights,
4) cloud layer correlation's between two heights;

and seasonal statistics for:
5) serial correlation's of clouds at specified altitudes,
6) probabilities of vertical cloud thicknesses,
7) probabilities of cloudy or clear run lengths, and
8) a method for converting cloudy or clear run length probabilities to persistence probabilities.

Data collection and cloud extraction methods are explained and methods used for deriving the statistics are documented.

**14. SUBJECT TERMS**

Cloud statistics, persistence, cloud thickness, correlation, CFLOS.

**15. NUMBER OF PAGES**

94

**16. PRICE CODE**

| 17. SECURITY CLASSIFICATION OF REPORT <br> Unclassified | 18. SECURITY CLASSIFICATION OF THIS PAGE <br> Unclassified | 19. SECURITY CLASSIFICATION OF ABSTRACT <br> Unclassified | 20. LIMITATION OF ABSTRACT <br> Unlimited |
|---|---|---|---|

NSN 7540-01-280-5500

# TABLE OF CONTENTS

# LIST OF ILLUSTRATIONS

# LIST OF ILLUSTRATIONS

Page

# LIST OF ILLUSTRATIONS

# LIST OF ILLUSTRATIONS

## ACKNOWLEDGMENTS

# 1. INTRODUCTION

This report presents several types of cloud layer statistics derived from echo intensities received by a 35-GHz radar. The statistics presented include probability of clouds aloft, diurnal cloud layer analysis, probability of vertical cloud-free line-of-sight (CFLOS) between two heights, cloud layer correlations between two heights, serial correlations of clouds at specified altitudes, probability of vertical cloud thickness, and probabilities of cloudy or clear run lengths. The methods used to derive these statistics are also documented.

With present advances toward computerized systems for simulating clouds, cloud layers, and precipitation, it has become increasingly desirable to have access to more meaningful cloud layer statistics. For example, Gringorten (1982), pointed out the requirement "... to know the probability of a CFLOS between two points when both points are aloft or if cloud layers envelope levels of the atmosphere partially, fully or not at all."

Conventional weather observations fail to accurately define cloud layer statistics. For example, when broken to overcast, low or middle cloud layer conditions prevail, the presence of higher clouds is often obscured from surface observers. On the other hand, middle and low cloud amounts obtained from satellite observations can be inaccurate when these lower cloud layers are obscured by the presence of broken or overcast high clouds. Cloud layer amounts deduced by surface weather observations made during night time hours may be underestimated. Also, conventional observations frequently do not accurately specify the vertical distribution of clouds. That is, sometimes when clouds are reported to be in a single layer they may actually extend vertically into other layers.

The vertically pointing 35-GHz radar has the unique capability to accurately describe the clouds and precipitation that lie along its beam through the atmosphere regardless of the number of cloud layers present. Since only heavy rain will significantly degrade this capability, the 35-GHz radar is a

prime candidate for deriving useful vertical cloud layer statistics. In this report, we shall show, for the first time, cloud layer statistics derived from such a radar. Although the cloud layer statistics are for only one point on Earth (Sudbury, MA), they should give us insight as to their shapes and characteristics at other locations.

## 2. DATA COLLECTION

Figure 1 shows the data collection and analysis configuration for reducing the 35-GHz radar data to the form of cloud layer statistics. The diagram not only documents the names of programs used and products generated in the data reduction process, but also serves as an outline of the contents of this report. Thus, this section (2) discusses the 35-GHz radar and data archiving. The data analysis section (section 3) discusses the data extraction technique and the cloud layer statistical products generated in this study. Section 4 provides details of the algorithms used in the analysis.

### 2.1 The 35-GHz Radar

Radars operating at frequencies between 35 GHz and 30 GHz have been used for cloud detection since the 1950's. A summary of previous studies pertaining to 35-GHz radars can be found in Biswas and Hobbs (1986). The AN/TPQ-11 35-GHz radar used for data collected in this study was housed at the Air Force Systems Command, Phillips Laboratory Radar site in Sudbury, Massachusetts. The approximate latitude and longitude position of the radar was 42.38° N and 71.42° W. The radar is a microwave, pulse-modulated, two-dish set propagating through the atmosphere vertically with a frequency band from 34.512-35.208 GHz. The radar specifications are shown in Table 1.

According to Biswas (1988), the .26-degree beam width translates into beam diameters of ~4.5 meters at a range of 1 km, ~25 meters at 5 km, and ~40 meters at 8 km.

The continuous records obtained from the radar over a given time interval provide detailed information on the presence,

2
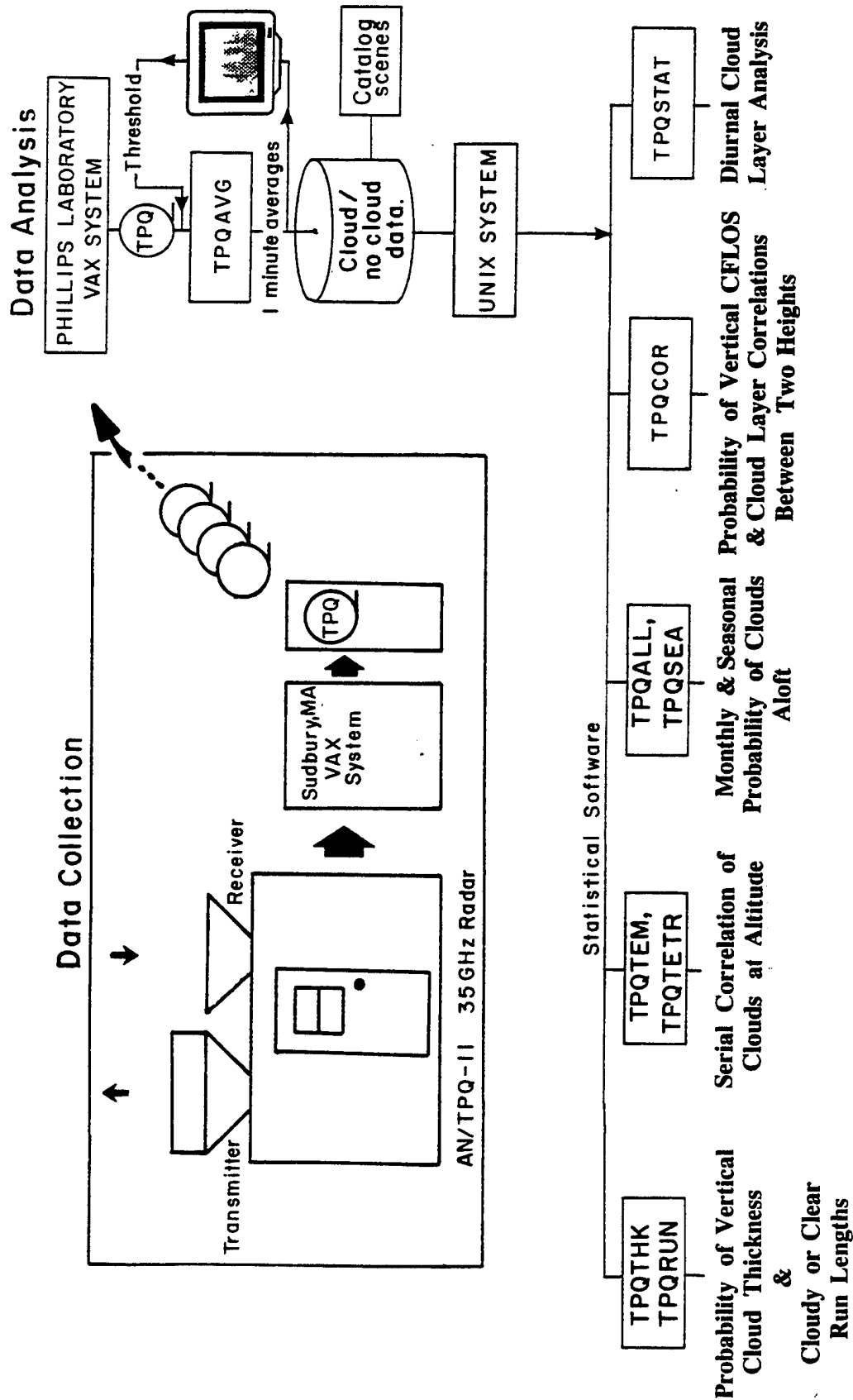
Figure 1. Data Collection and Analysis Configuration for Reducing Echo Intensities From a 35-GHz Radar to Vertical Cloud Layer Statistics.

## Table 1. Specifications for the Sudbury 35-GHz Radar

| | |
|---|---|
| Frequency | 35 GHz |
| Wavelength | 0.86 cm |
| Peak power | 80 kW |
| Pulse repetition frequency | 4000 Hz |
| Pulse duration | 1.0 or .5 $\mu$s |
| Pulse length, (cell width) | 150 or 75 m |
| Receiver band width | 5 MHz |
| Minimum measurable signal | -85 dBm |
| Beam width | 0.26 degrees (at one half power point) |

internal structure, and characteristics of clouds moving over the beam at discrete levels in the atmosphere up to 60,000 feet. The quantitative data also detect inversion layers and cloud bases and tops and give insight into meteorological phenomenon such as wind shear and melting zones (Petrocchi, 1966).

## 2.2 Data Collection and Archiving

At the beginning of 1990, the Phillips Laboratory Atmospheric Structures Branch (GPAA) of Hanscom AFB initiated a project to collect 35-GHz radar data to be used for the purpose of defining climatological cloud layer statistics. The data collection was the responsibility of the Phillips Laboratory Atmospheric Structures Branch personnel stationed at the radar site in Sudbury, Massachusetts. Data collection began on April 26, 1990, and ended on July 17, 1992, providing 28 months of data or a 2.25 year period of record. During this period several important changes in the manner of data collection took place. For example, the 35-GHz radar transmitter contains a high-powered thyratron pulse-generating circuit that excites a magnetron. The magnetron is the source of the microwaves that propagate through the atmosphere. However, these magnetrons tend to "burn out" after one or two months of constant use. Magnetrons are expensive. Therefore, rather than collecting data at a rate of every second or so over a 24-hour period for an entire month,

which would be ideal for deriving climatological cloud layer statistics, we settled for data samples of various durations observed during episodes of 24 hours or less on about 15 days a month.

Initially, the beam of the radar was programmed to penetrate the atmosphere to approximately 60,000 feet in the spring and summer months and to approximately 30,000 feet in the fall and winter. However, it was felt that the resolution change in beam extension would adversely affect the quality of the statistical data being processed. Therefore, data collected for the period from late October 1990 through April 4, 1991, were excluded from the data analysis in this study. On April 5, 1991, the beam was programmed to always propagate through the atmosphere to 60,000 feet.

Data from the entire 2.25-year period of record were stored on 48 10-inch magnetic tapes. For the initial period of record from April 26, 1990 through May 8, 1991, the data were formatted onto tapes at a density of 1,600 bpi. Four vertical radar shots, (about a little over one second per shot) were packed into a binary fixed physical record of 512 bytes. The format detail of each logical record for a single shot is: Julian day, hour, minute, and second; each is a 2-byte quantity followed by 120 bytes of digitized radar intensities for 120 cells. Thus, 8 bytes plus 120 bytes or 128 bytes multiplied by 4 shots comprise the 512-byte physical record. Two shots were packed into the 512-byte physical record on the remaining tapes to accommodate the increase in data resolution which took place on May 9, 1991. These later tapes contained data at a tape density of 6,250 bpi. All 48 tapes were sent to the Atmospheric Structure Branch at the Phillips Laboratory for subsequent processing. As mentioned above, tapes containing data for October 1990 through April 4, 1991, were damaged and the data were irrecoverable.

For the record, the following list is a summary of the dates pertaining to data collection episodes.

| | |
|---|---|
| Apr. | April 26, 1990. Begin acquiring and archiving 35-GHz data at a 150-meter cell width and 120 cells per beam or "shot." Thus, 150 meters x 120 cells results in a maximum beam extension through the atmosphere of 18,000 meters or 18 kms (59,040 feet). |
| May | Normal data collection. |
| June | "          "          "     . |
| July | "          "          "     . |
| Aug. | "          "          "     . |
| Sept. | "          "          "     . |
| Oct. | October 24, 1990.  Changed to a 75-meter cell width but kept the number of cells at 120 per shot (beam extension to 9 kms or 29,520 feet). |
| Nov. | Normal data collection. Off scale. |
| Dec. | "          "          "     . "     "     . |
| Jan. 01, 1991 | "          "          "     . "     "     . |
| Feb. | "          "          "     . "     "     . |
| Mar. | "          "          "     . "     "     . |
| Apr. | April 5, 1991.  Changed back to a 150-meter cell width and 120 cells per shot (beam extension to 18 kms or 59,040 feet). |
| May | May 9, 1991.  Changed to a 75-meter cell width but increased cell resolution from 120-240 cells per shot (beam extension to 18 kms or 59,040 feet). Changed tape density to 6,250 bpi. |
| June | Normal data collection. |
| July | July 1991. No data collected. |
| Aug. | Damaged data tape. Data irrecoverable. |
| Sept. | "          "     "     . "          "          . |
| Oct. | "          "     "     . "          "          . |
| Nov. | "          "     "     . "          "          . |
| Dec. | Normal data collection. |
| Jan. 01, 1992 | "          "          "     . |
| Feb. | "          "          "     . |

Mar.             "        "        "       .

Apr.             "        "        "       .

May              "        "        "       .

June             One day of data.

July             July 17, 1992. End of 35-GHz radar data
                 acquisition at Sudbury, Massachusetts.

## 3. DATA ANALYSIS

Several computer programs were developed by Hughes STX to process, analyze, and display the 35-GHz radar data. The names and roles of eight of the more prominent programs used in the data reduction are shown in Figure 1. As shown, the processing begins with a data extraction program called TPQAVG which was developed on the Phillips Laboratory VAX system. Statistical software routines TPQALL, TPQSEA, TPQCOR, TPQSTAT, TPQTEM, TPQTETR, TPQTHK, and TPQRUN were developed to produce the cloud layer statistics listed beneath each program's box. The remainder of Section 3 will be devoted to describing the functions and products of each of these programs.

### 3.1 Cloud Data Extraction and Compression

Magnetic tapes received from the 35-GHz radar data collection site in Sudbury contained anywhere from 3-10 files of data per tape. Each file, in turn, contained observation episodes of many one second shots over some continuous time period, which varied from 10 minutes to as long as 3 days worth of data. In the data extraction and compression phase of the data processing activities, TPQAVG was called upon to extract a given file of radar data from a particular tape. The extracted data from each shot included Julian day, hour, minute, and second followed by 120 values of radar echo intensities. A range normalization of the echo intensities received for the 120 cells was then undertaken to convert the data in each cell to values of dBZ. Thus, from Petrocchi, (1990)

$$dBZ_m = \frac{cell_m}{sl} + p_0 + rck + rn_m + .5 + pcorr, \qquad (1a)$$

where

$dBZ_m$ is the normalized intensity (Z) in decibels (dB), i.e., logarithmic scale.

$cell_m$ = unnormalized echo intensity.

$sl$ = 2.68      Slope of the calibration function.

$p_0$ = -102.54   Intercept of the calibration function.

$rck$ = 44.34   Radar constant.

$rn_m$ = $20\log_{10}$ m. Range normalization term.

$m$ = range cell number, 1 through 120 in increments of 1 and $pcorr$ is a correction factor applied to account for changing noise levels. Thus,

$$pcorr = \frac{(23-lcp)}{sl} \qquad (1b)$$

where

$lcp$ = Maximum value of the last 8 cells of a shot.

A sequence of shots taken at about one second intervals with cell values in dBZ units were summed together and normalized over a 1-minute time period. Each averaged one minute shot was stored sequentially into a rapid access data file. On completion, the file containing the 1-minute average shots was displayed on a computer screen showing the data as a cloud/no cloud image based on a given dBZ threshold. The chosen dBZ threshold "thres" remained constant throughout a given episode but was distributed vertically for each cell as

$$thresh_m = -58.2 + thres + rn_m \qquad (2)$$

where

$m$ and $rn$ are defined in 1a above.

The cloud (gray)/no cloud (white) scene was then scrutinized (rational discussed below) to determine, subjectively, whether the dBZ threshold value chosen was a suitable cloud/no cloud discriminator. If not, a new dBZ threshold was applied and the process repeated. Only when it was decided that a satisfactory cloud/no cloud image was produced was the dichotomous cloud/no cloud data stored for subsequent statistical data processing. It

should be noted that in the dichotomization process precipitation was included in the cloudy situations. This subjective thresholding process was initiated with caution because it could influence the statistics being pursued. For example, if selected thresholds were mostly on the low side, more cloudiness will be allowed whereas higher ones will cause less cloudiness to prevail.

Figure 2 is presented to illustrate the production of an actual cloud/no cloud data file using the threshholding methods described above. Here a file is processed that contains a 7-hour observation episode starting at about 7 a.m. and ending around 2 p.m. on May 10, 1990. (This case is one of the noisiest cases encountered.) The first cloud scene was generated using a threshold value of -50 dBZ, see top of Figure 2. Note that the vertical 1-minute averaged shots of cloudy (gray) and clear (white) pixels are portrayed sequentially in time from left to right forming a rectangular cloud scene. In these scenes, data below about 4,000 feet to the surface were considered too noisy to process and are left blank. The ordinate of the rectangle is linearly scaled, and is labeled to reflect the altitude regions conventionally assigned to cloud layers. Thus, low clouds such as stratus and stratocumulus prevail below 8,000 feet. Medium level clouds such as altostratus and altocumulus are found between 8,000 and 20,000 feet. High clouds such as cirrus and cirrostratus are generally found between 20,000 and 40,000 feet. Super high clouds may prevail at times to as high as 60,000 feet or more. The horizontal axis of the display is labeled by hour (LST). Hours 0-12 are a.m. hours, and 13-24 are p.m. hours.

After scrutinizing the scene shown at the top of Figure 2, it was decided that the -50 dBZ threshold value was too low. The following are the reasons for this decision. First, there appears to be noisy horizontal banding at five consistent height levels. The bands are mostly all the same thickness and it seems unlikely that clouds of that thickness should occur above 40,000 feet. The threshold was then raised to -30 dBZ, and the image in

9

**MAY 10, 1990**
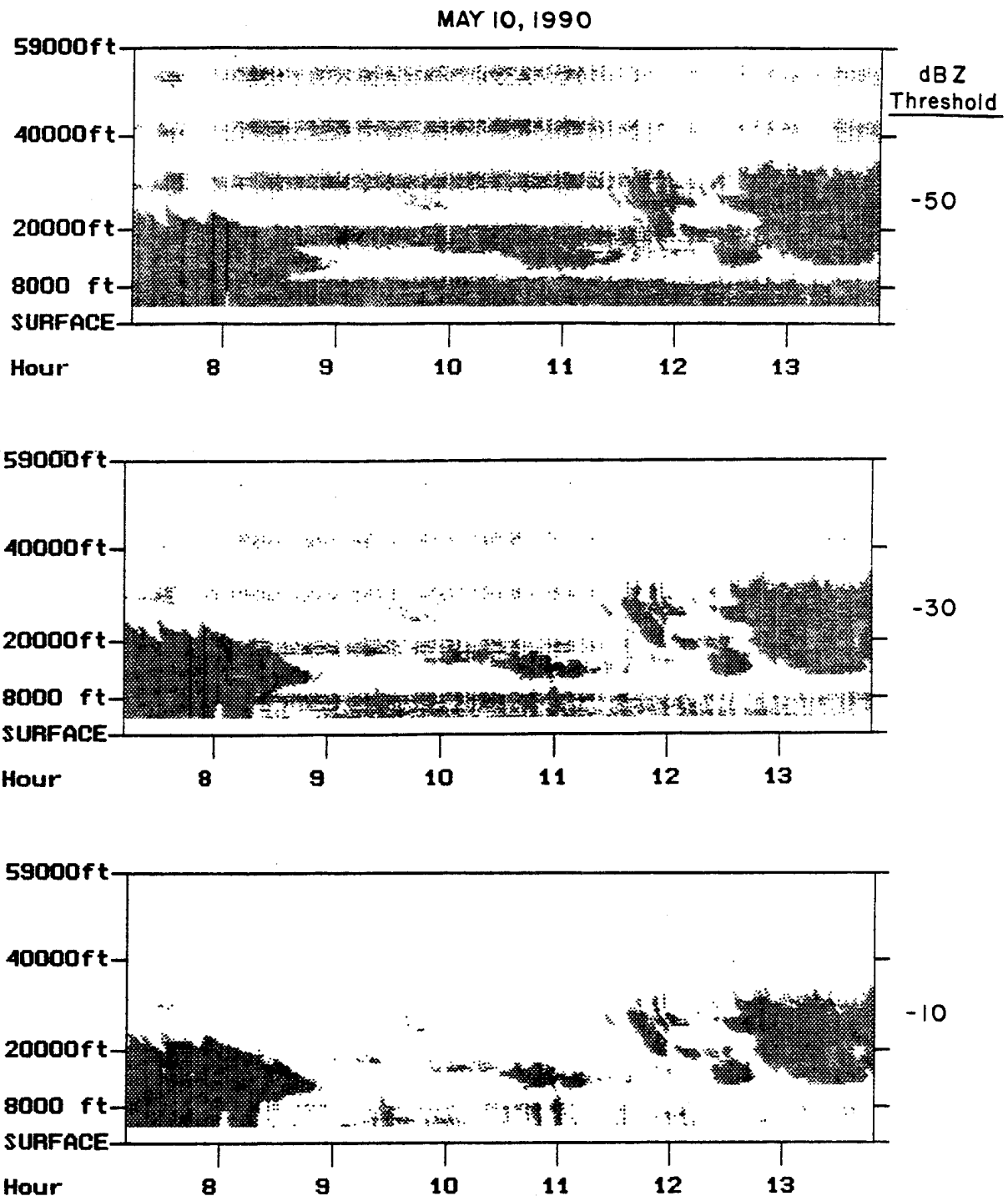


Figure 2. Example Cloud (Gray)/No Cloud (White) Data Image
Generation Using dBZ Thresholding. Initially, a -50 dBZ
threshold was chosen that produced the noisy image
shown at the top. Threshold -30 dBZ, middle, was then
applied showing some improvement of ridding the
apparent noise. Threshold -10 dBZ produced the final
noiseless cloud scene shown at the bottom.

the middle of Figure 2 was produced. The results still show
banding but to a lesser extent. The third try with a threshold
of -10 dBZ produced the apparent noise-free scene shown at the
bottom of the figure. This scene was the final cloud/no cloud
scene stored for statistical processing.

Examples of two other finalized scenes are shown in Figure
3. The scene for February 24, 1992, is typical of clouds in the
winter over New England. There is a consistent region of low
overcast stratus clouds below 8,000 feet which appears for nearly
the entire time period of the episode. Cirrostratus clouds are
shown as a consistent high cloud layer giving way to middle
altostratus cloud types near the end of the observation episode.
This scene was produced using a -30 dBZ threshold. The
observation episode for August 13, 1990, shows a typical summer
type cloud scene. Here it appears that the clear summer evening
sky over the radar beam between 7:00 and 8:30 p.m. was invaded by
a cirrus canopy that was the forerunner of an apparent
thunderstorm. From 11:00 p.m. (hour 23) to about 11:30 p.m., the
clouds at all layers merged together and it appears to have
rained. The dropout of high clouds at around midnight may be
real or the result of a rainfall rate that exceeded 0.75 in./hr.
Heavy rain can attenuate the radar signal enough to cause a
dropout of existing higher clouds. However, for the AN/TPQ-11
radar, "Attenuation by rainfall in general does not constitute a
serious problem in detecting cloud tops unless the rainfall rate
exceeds 0.75 in./hr." (United Aircraft Corporate Systems Center,
1964).

## 3.2 Cloud Layer Statistics and Analysis

Using the data extraction techniques described above, an
entire data bank of digitized cloud/no cloud scenes stratified by
year, month, day, hour, and minute for winter and summer months
was assembled for subsequent processing of cloud layer
statistics. Our definition of a cloud layer does not refer to
the traditional low, middle, and high cloud layers. Instead we
define a cloud layer to be the minimum pulse length that can be

11

FEBRUARY 24, 1992
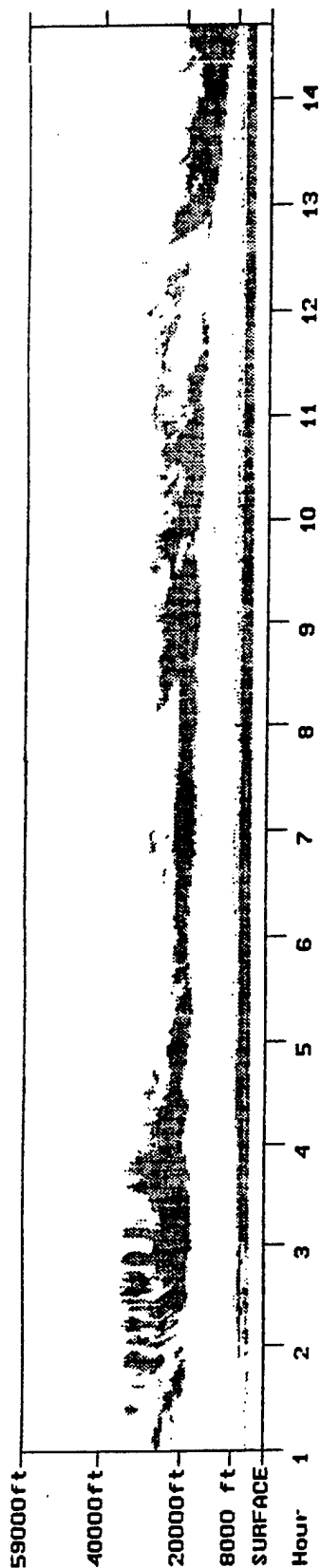


AUGUST 13, 1990
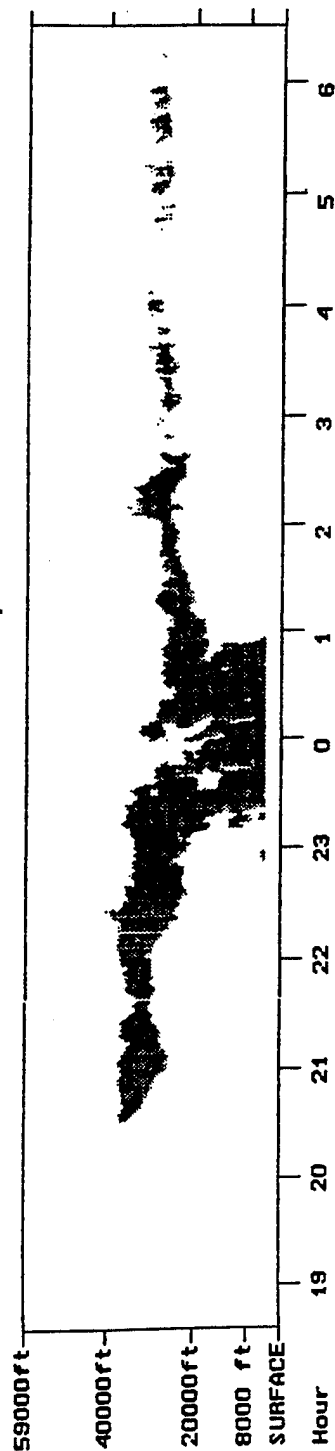


Figure 3. Sample Cloud/No Cloud Scenes Generated From the 35-GHz Radar Data Collected Over Sudbury, MA. Clouds (gray) shown for the February case are persistent high, middle, and low stratoform clouds typical over New England in the winter. The August case portrays the advancement of a thunderstorm that apparently occurred over the radar beam around midnight.

12

resolved consistently. The 150-meter pulse resolution was the lowest resolution element considered in this study. For the small fraction of data that had 75-meter pulse resolution, an average echo intensity between adjacent cells can be used to provide a consistent 150-meter resolution. Because of very noisy echo intensities frequently received at lower levels of the atmosphere, we did not compile statistics below the tenth cell or 1,350 meters (4,428 feet).

Two types of statistics are used to define the cloud layer statistics. The first is the probability that a certain cloud layer condition exists and the second measures the joint occurrences of cloud conditions in two or more cells. In this report correlation statistics are derived using tetrachoric correlations.

### 3.2.1 Tetrachoric Correlation

The word correlation has several meanings. The most common are:

1. An empirical relationship.
2. A measure of dependency in linear regression.
3. The ellipticity parameter in the bivariate (and multivariate) normal distribution.

When data are joint, normally distributed and linear regression is used to obtain an empirical relationship these definitions are equivalent. Many tests in regression **assume** a normal distribution.

Cloud or no cloud measurements are binary and thus are not normally distributed. Suppose we hypothesize that cloud/no cloud results from a continuous variable that has been dichotomized (separated into two parts above and below a threshold). For (simplified) example, if liquid water content is above 1 part per 1,000 volume, there is a cloud, otherwise no cloud. The continuous variable that has been dichotomized is known as an underlying variable. Is it possible to calculate the ellipticity parameter correlation between two underlying variables if we have only the resultant binary data?

13

Karl Pearson worked on this problem at the turn of the century and developed tetrachoric correlation. Earlier, he had refined the correlation formula between continuous variables, and his formula is sometimes called the Pearson Product Moment (PPM) correlation. This is the formula that is used in elementary statistics courses. Note that there are a host of correlation formulas that fit definition 1 above, but they do not fit definition 3. The PPM correlation (given that the variables are normally distributed) and tetrachoric correlation (for dichotomized variables) are designed to estimate the ellipticity parameter.

Why use tetrachoric correlation with cloud/no cloud?

a) Simulated gaussian fields are dichotomized to generate cloud scenes. The basic parameter of the structure function of a gaussian field is the normal ellipticity parameter, which is given by tetrachoric correlation.

b) To calculate joint or conditional probabilities (durations or spatial) using the normal distribution.

c) The tetrachoric correlation is more conservative in the meteorological sense, that is, it varies less at different locations and times.

d) Tetrachoric correlation is robust with respect to outliers and dirty data.

e) Tetrachoric is not adversely affected by a change in threshold. This is a very desirable attribute when dealing with cloud discrimination algorithms when threshold is uncertain.

The tetrachoric correlation is defined as the correlation in a bivariate normal distribution that would be produced if the continuous normal variables observed were reduced to binary variables by the continuous variable being above or below a given threshold. These binary variables can be displayed in a 2 x 2 contingency table. In Table 2, the letters A, B, C, and D are representative of the number of cases in each group.

Table 2. Contingency Table

|        | Below | Above |
| ------ | ----- | ----- |
| Below  | A     | B     |
| Above  | C     | D     |

The following is a simplified example of tetrachoric correlation.

Suppose cloudy or clear Line-of-Sight (LOS) was determined only by measuring relative humidity along the LOS. Suppose relative humidity along the LOS was normally distributed, and whenever the lines averaged relative humidity exceeded a threshold, a cloudy LOS would occur. Now, if all that can be observed is cloudy or clear, can we calculate the correlation between line weighted relative humidity for separate lines if the original continuous variables are joint normally distributed? Tetrachoric correlation does exactly that.

Many approximations of the tetrachoric correlation have appeared over the past. For example, Panofsky and Brier (1965) give the formula for the tetrachoric correlation approximation ($\rho$) as:

$$\rho = \sin\left[\frac{\pi}{2} \frac{\sqrt{AD} - \sqrt{BC}}{\sqrt{AD} + \sqrt{BC}}\right] \tag{3}$$

The equation was derived from the first term of a Taylor series. It is accurate when both variables have been dichotomized at the median. However, larger errors (> 20 percent) can occur where the variables have been dichotomized near the extremes. Additional terms were added in an algorithm by A. Boehm of Hughes STX Corporation, which yields a highly accurate estimate of correlation. This algorithm was used to compute the correlation statistics in this study. The FORTRAN version of it can be found in Smyth et al., (1991).

### 3.2.2 Probabilities

Probability values were computed by simply tallying the number of times a particular radar cell was judged to be cloudy and dividing the final tally by the total number of times the cell was encountered.

### 3.2.2.1 Data Sampling

Before we discuss the derived statistics in the sections that follow, a few things should be noted about the data sample sizes used in developing the statistics. As mentioned in Section 2.2, TPQ11 data collection was limited due in part to budget problems with the purchasing of magnetrons, resolution changes, and damaged data tapes. Table 3 below was assembled to show, in detail, the amount of data that was actually captured in the winter and summer cases presented here versus what the sample sizes could potentially have been without any anomalies.

Table 3.   Potential vs. Actual Radar Data Sample Sizes

| Season | POTENTIAL | | | | ACTUAL | | |
| | Year | Mon | Days | Min's | Year | Min's | % Data Capture |
|--------|----------|------|------|---------|----------|--------|--------|
| Winter | 90,91 | Dec | 62 | 89,280 | 91 | 11,139 | 12.48 |
| | 91,92 | Jan | 62 | 89,280 | 92 | 21,673 | 24.28 |
| | 91,92 | Feb | 57 | 82,080 | 92 | 30,849 | 37.58 |
| Total | | | | 260,640 | Total | 63,661 | 24.42 |
| Summer | 90,91,92 | June | 90 | 129,600 | 90,91,92 | 13,537 | 10.29 |
| | 90,91,92 | July | 79 | 113,760 | 90,92 | 15,925 | 13.99 |
| | 90,91 | Aug | 62 | 89,280 | 90 | 14,729 | 16.50 |
| Total | | | | 332,640 | Total | 44,191 | 13.28 |

For example, for the winter season, consider the two months December 1990 and December 1991. With no downtimes or other anomalies, the potential period of record could have led to a sample size of 89,280 minutes (62 days x 1,440 minutes/day). What actually occurred was that 11,139 minutes of data were captured in December 1991. By dividing the actual amount of sampling minutes by the potential amount multiplied by 100, leads to the percent of data capture, which in the December case is shown to be 12.48 percent. Summing the minute columns for the winter months of December, January, and February and dividing the actual by the potential total number of minutes multiplied by 100 leads to 24.42 percent data capture for the entire winter season. These data capture rates should be remembered when interpreting the derived statistics shown below.

### 3.2.3 Monthly & Seasonal Probability of Clouds Aloft

Figure 4 shows curves of monthly probabilities of clouds aloft as derived from the cloud/no cloud data scenes for the individual winter and summer months. In order to generate one of these curves for a given month, an array p dimensioned as 120 elements long was provided to store values of probabilities of cloudy conditions along the vertical radar beam. The probable cloudy conditions were then computed for each cell for the observation episodes encountered in a given month using the set of equations in (4) below.

$$S_{cell} = \sum_{cell\,=\,10}^{120} \sum_{min\,=\,1st}^{end\ of\ episode} cloudy\ cells,$$

$$n_{cell} = \sum_{cell\,=\,10}^{120} \sum_{min\,=\,1st}^{end\ of\ episode} clear\,+\,cloudy\ cells, \qquad (4)$$

$$then\ for\ cell = 10,120\ \ \rho_{cell} = \frac{S_{cell}}{n_{cell}}$$

where

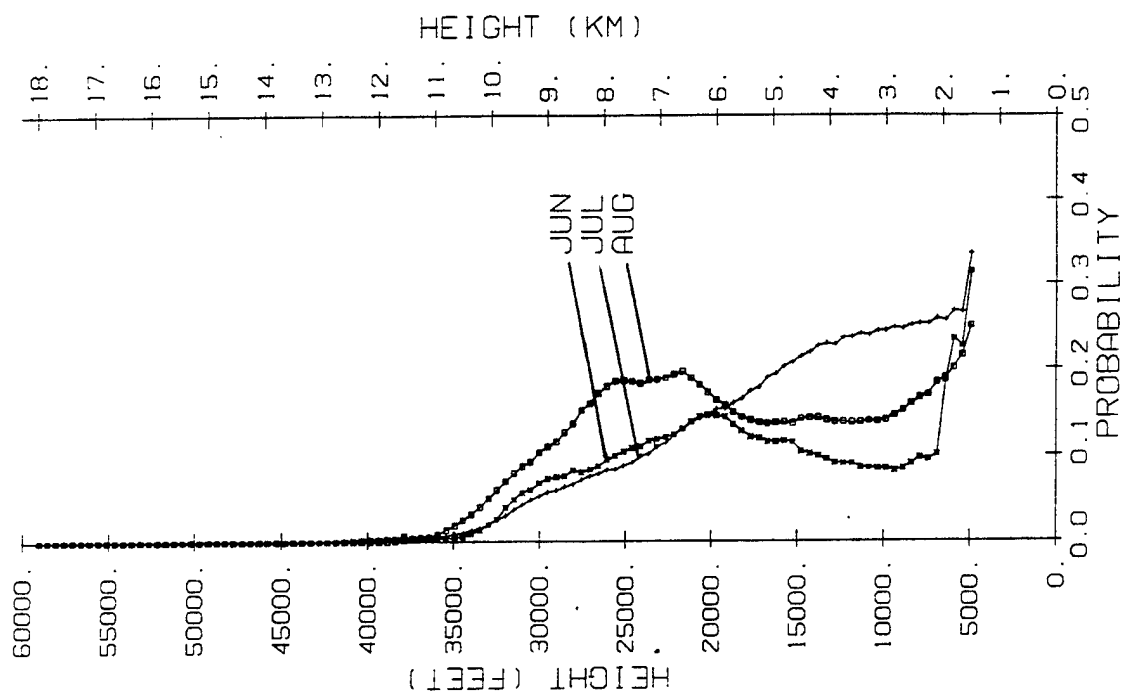$s$ is an array dimensioned 120 elements that is used to store sums of cloudy cell events.

17

Figure 4. Monthly Probability of Clouds Aloft for the Individual Winter (Left) and Summer Months (Right).

*n* is an array dimensioned 120 elements that keeps track of the population of cloudy and clear cells encountered over each episode.

*p* array holds the final probabilities for display. As mentioned before, it was decided that radar echoes from the surface to about 5,000 feet were too noisy for reliable statistics; thus they were not processed. Therefore, processing started with cell number 10 the top of which is 4,920 feet above the transmitter. Processing terminates on cell number 120 the top of which is at a vertical altitude of 59,040 feet.

Figure 5 shows the winter and summer seasonal probabilities of clouds aloft. These curves were generated by summing all of the data from all three months in a season together to form the seasonal probabilities.

All curves show a rather sharp decrease in the probability of cloud cover between 5,000 and 7,000 feet. The individual monthly curves give some insight to the amount of variability that may be expected in probable cloud cover amounts aloft despite the low data sampling rates incurred over the monthly statistics. The seasonal statistics were derived with a larger population and, therefore, may serve as a more reliable indication as to the shape of the curves for cloud cover probabilities aloft. The increase in altitude for probable clouds in the summer case is a reflection of the fact that the troposphere has expanded over New England in the hot summer months. Note also that in the summer season cloud cover probabilities aloft appear fairly constant (.15) from 10,000 feet to about 22,000 feet. Also, note that the probable existence of clouds above 36,000 feet in the summer and about 34,000 feet in the winter is quite small. In order to show these very small probabilities of clouds at higher levels, magnified monthly probabilities of clouds aloft between 35,000 feet and 60,000 feet are portrayed in Figure 6. Note that in the winter months, probable occurrences of clouds range from about .006 at 35,000 feet to 0 at 37,000 feet although some very small probable
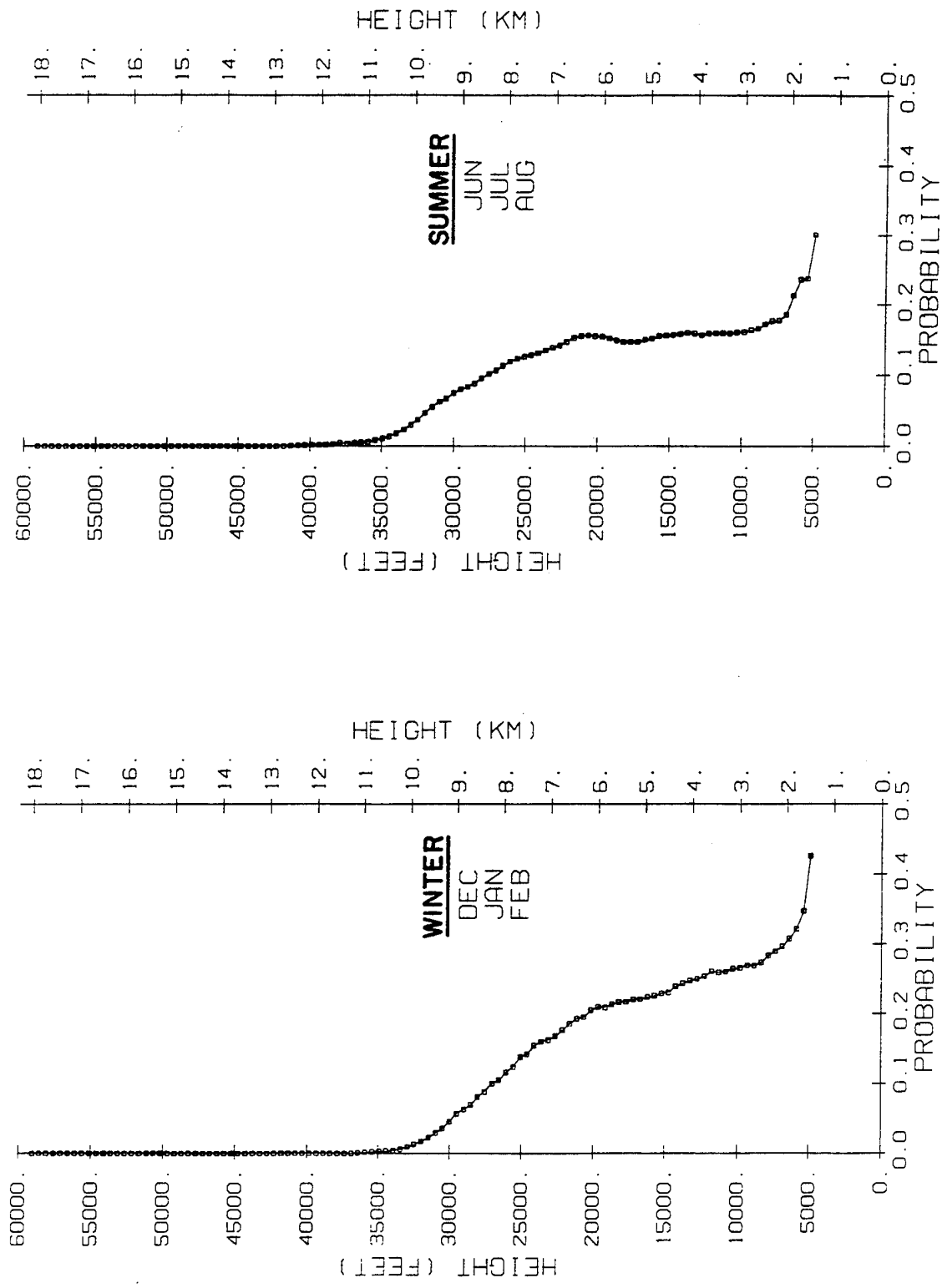
19

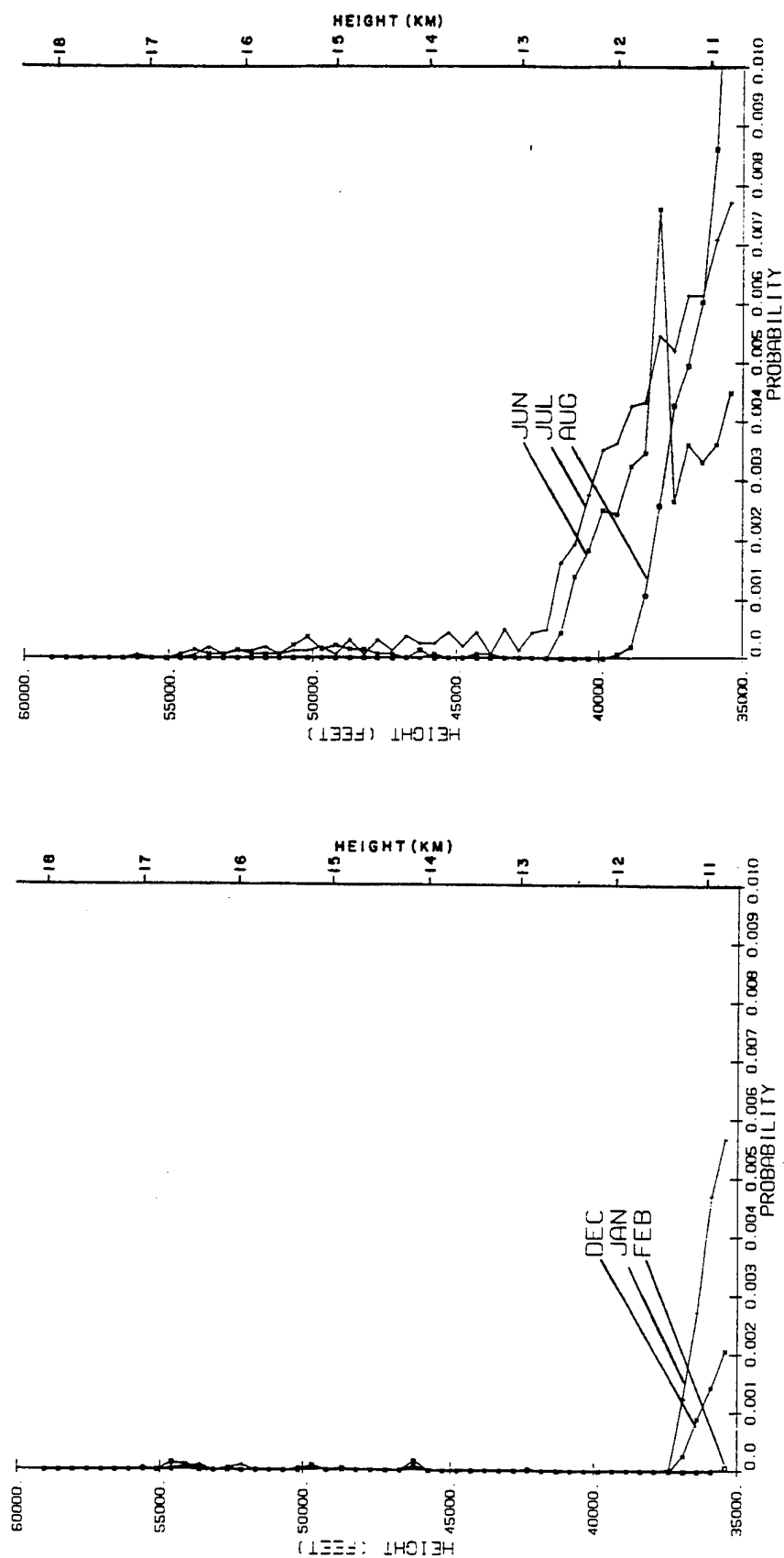Figure 5. Winter (Left) and Summer (Right) Seasonal Probabilities of Clouds Aloft.

Figure 6. Magnified Monthly Probabilities of Clouds Above 35,000 Feet (10.7 KM) for Winter and Summer Months.

occurrences are indicated to as high as 54,000 feet. The curves for the summer months reveal small probabilities of clouds occurring as high as 56,000 feet. (Kantor and Grantham, (1968) show frequency and percent occurrence of radar precipitation echoes to at least 50,000-70,000 feet over the Gulf Coast, central United States and Florida. Figure 7 shows magnified probabilities of clouds above 35,000 feet for the winter and summer seasons. Again, the summer seasonal curve emphasizes the expansion of the troposphere over New England in the summer when comparing vertical extent of probable heights of clouds with those in the winter.

### 3.2.4 Diurnal Cloud Layer Analysis

Figures 8-15 portray monthly and seasonal probabilities of clouds aloft over a diurnal period of 24 hours, hence, a diurnal cloud layer analysis. These statistics were compiled much the same way as those discussed in Section 3.2.3 above. The only difference is that the $p$ array used for storing the probabilities of clouds aloft was expanded to include a second dimension to stratify the results by hour. Thus, the $p$ array was expanded to a two-dimensional array of 73 cells by 24 hours. (Since the curves of probabilities of clouds aloft show very little cloud activity above 36,000 feet, the first dimension of the $p$ array was reduced from 120-73 cells to avoid unnecessary processing). The maximum height processed then will be 73 x 492 feet or 35,916 feet. In fact, the cutoff height of 36,000 feet was adopted in the development of the rest of the statistics displayed in this study because statistical processes on very small occurrences of cloudy conditions above this level become very unstable. For the diurnal cloud analysis the set of equations in (4) were altered to compute the cloud cover probabilities for given episodes as

22
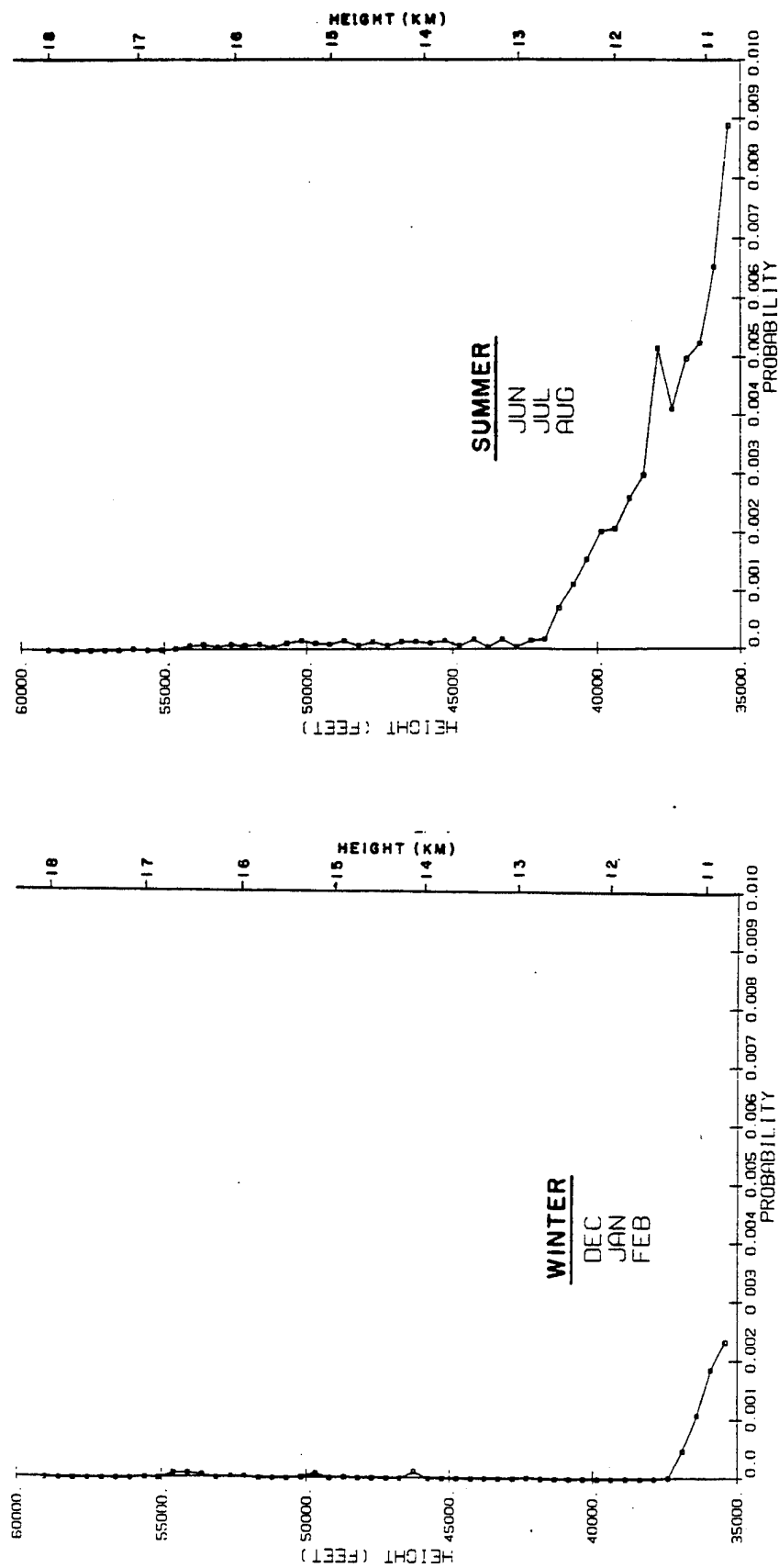
Figure 7. Magnified Seasonal Probabilities of Clouds Above 35,000 Feet (10.7 KM) for Winter and Summer.

# DIURNAL CLOUD LAYER ANALYSIS



Figure 8. Probabilities of Clouds Aloft Over a 24-Hour Period for the Month of December.

# DIURNAL CLOUD LAYER ANALYSIS



Figure 9. Probabilities of Clouds Aloft Over a 24-Hour Period for the Month of January.

# DIURNAL CLOUD LAYER ANALYSIS



Figure 10.     Probabilities of Clouds Aloft Over a 24-Hour
              Period for the Month of February.

26

# DIURNAL CLOUD LAYER ANALYSIS



Figure 11.    Probabilities of Clouds Aloft Over a 24-Hour
             Period for the Winter Season.

27

# DIURNAL CLOUD LAYER ANALYSIS



Figure 12.    Probabilities of Clouds Aloft Over a 24-Hour
              Period for the Month of June.

28

# DIURNAL CLOUD LAYER ANALYSIS



Figure 13.    Probabilities of Clouds Aloft Over a 24-Hour
              Period for the Month of July.
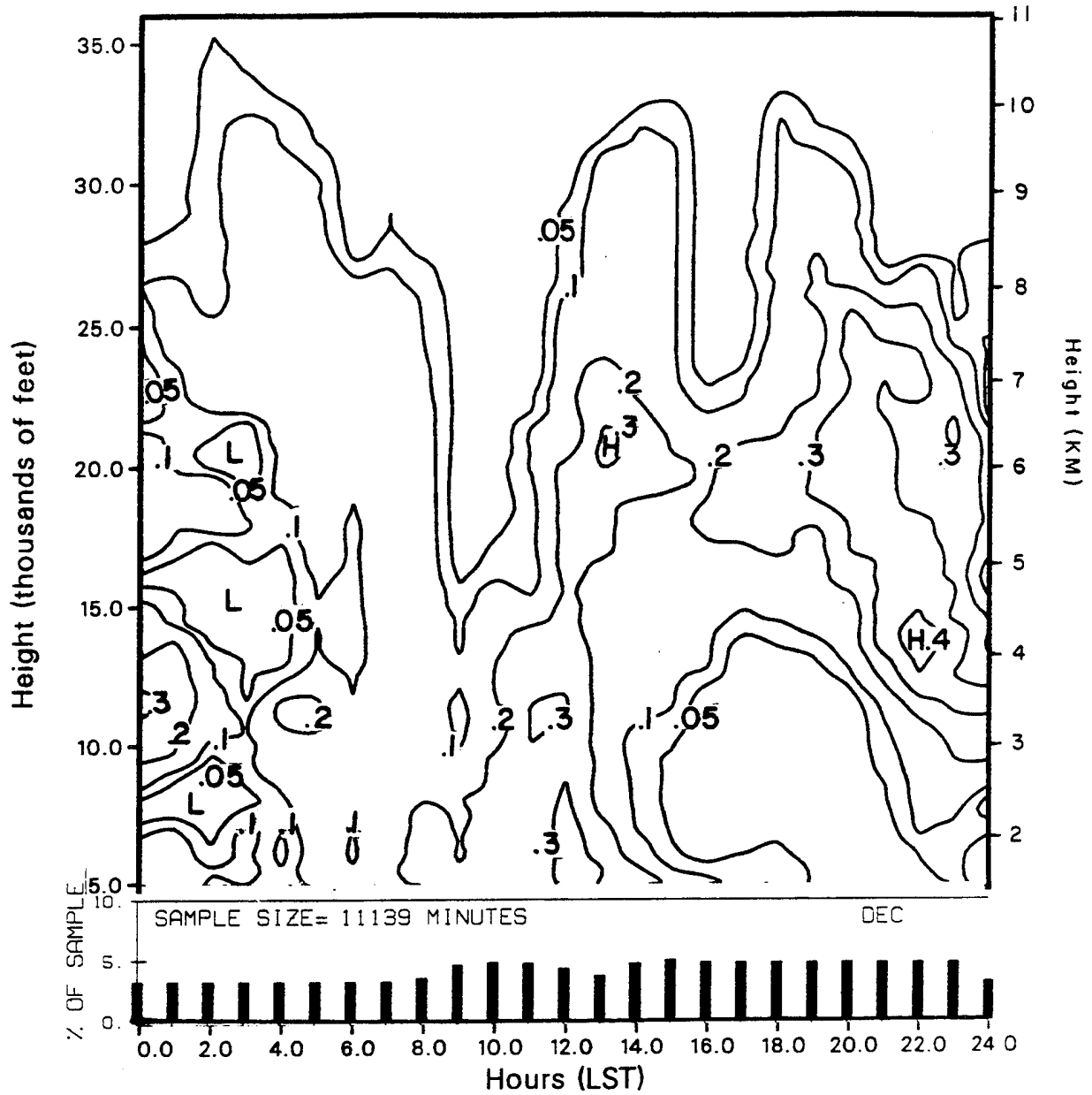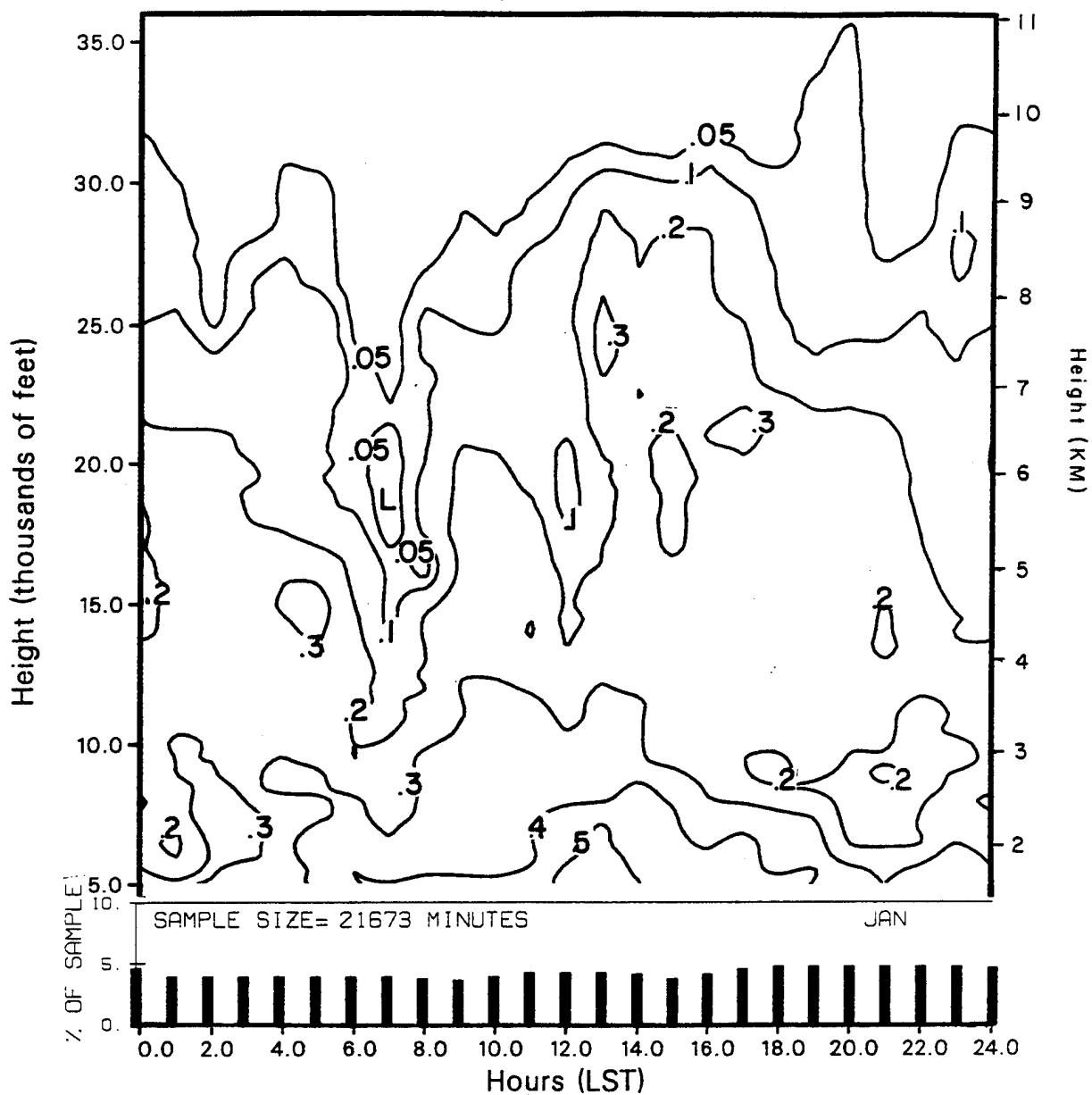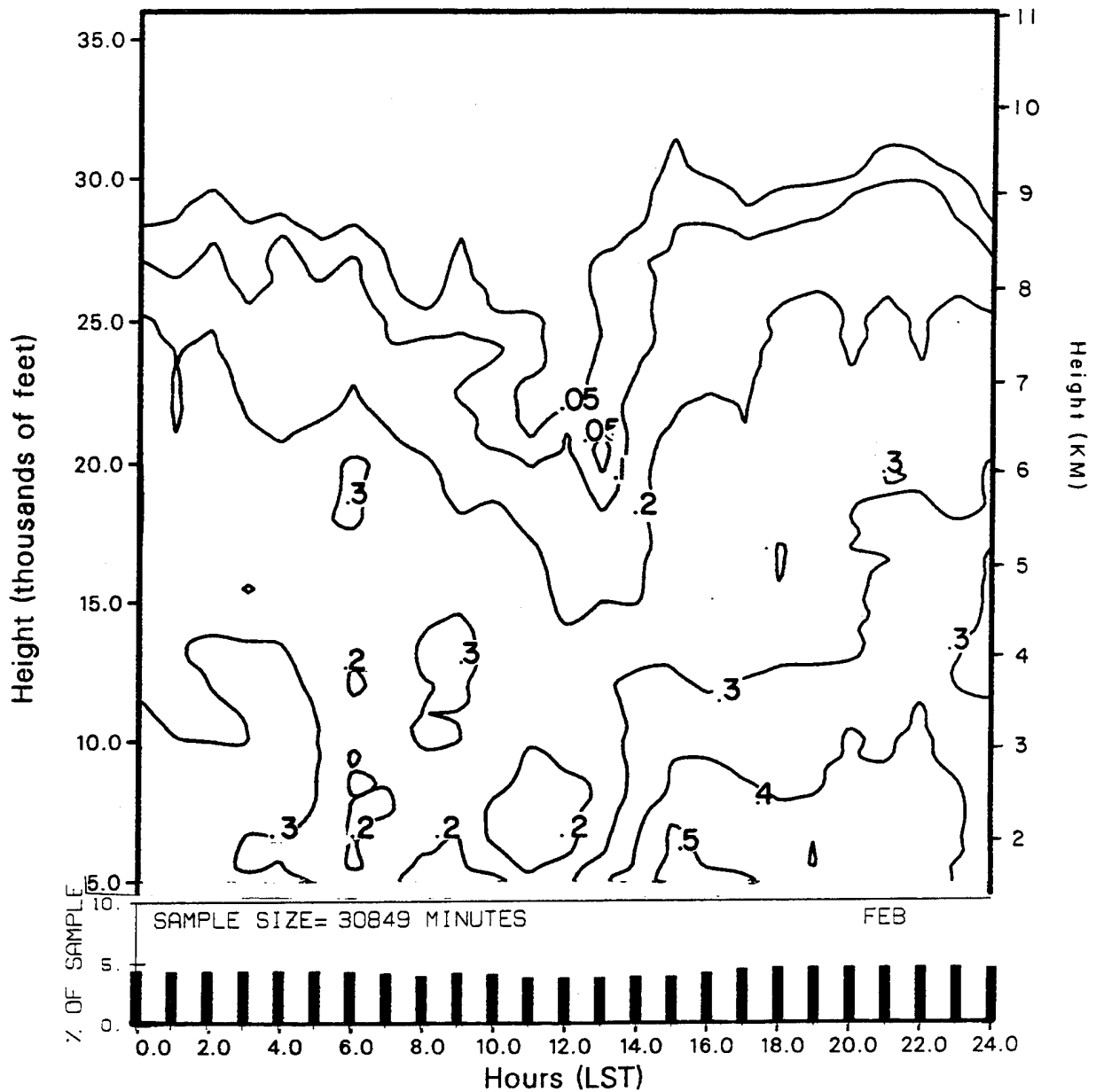
29

# DIURNAL CLOUD LAYER ANALYSIS



Figure 14.  Probabilities of Clouds Aloft Over a 24-Hour Period for the Month of August.
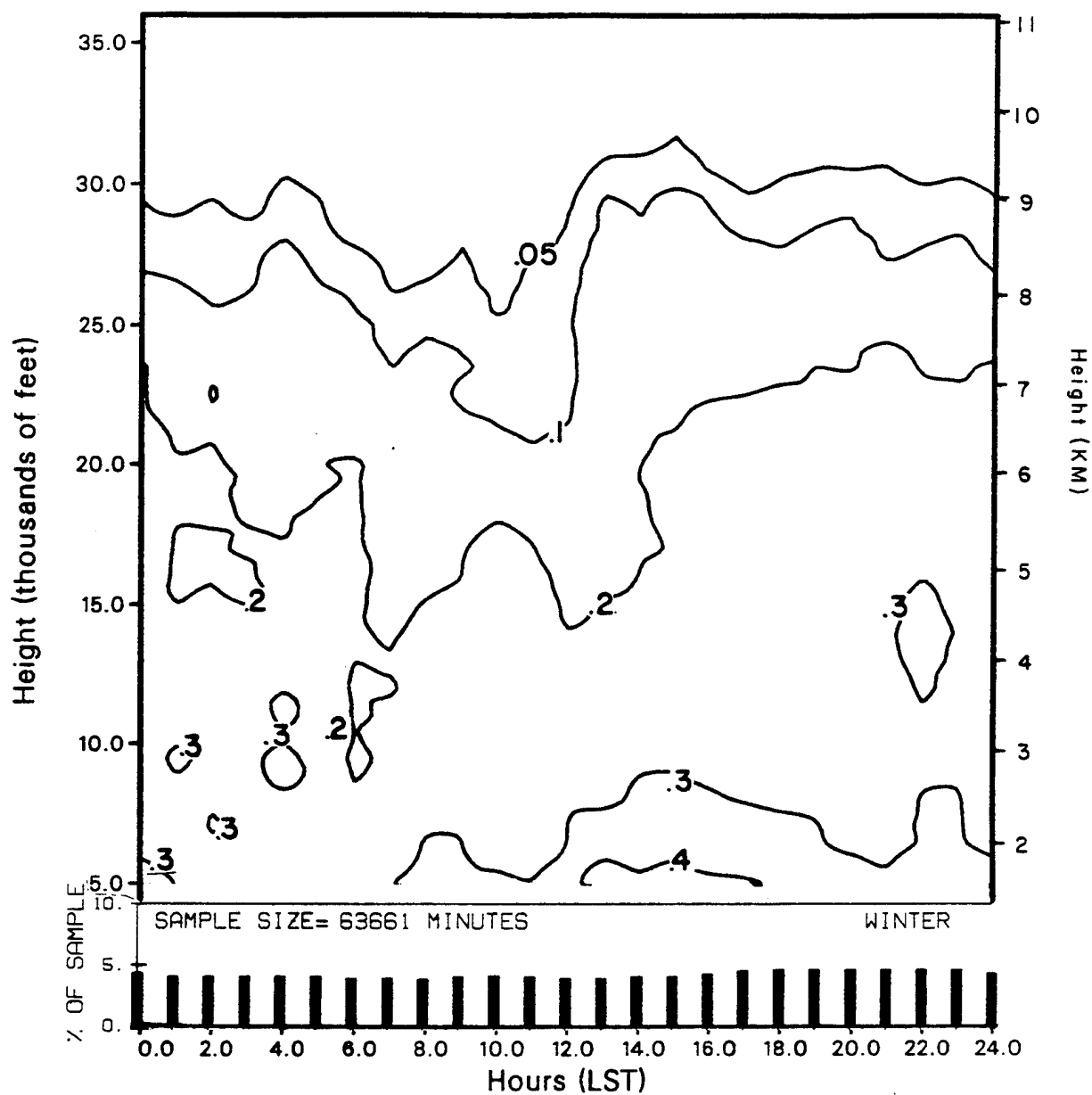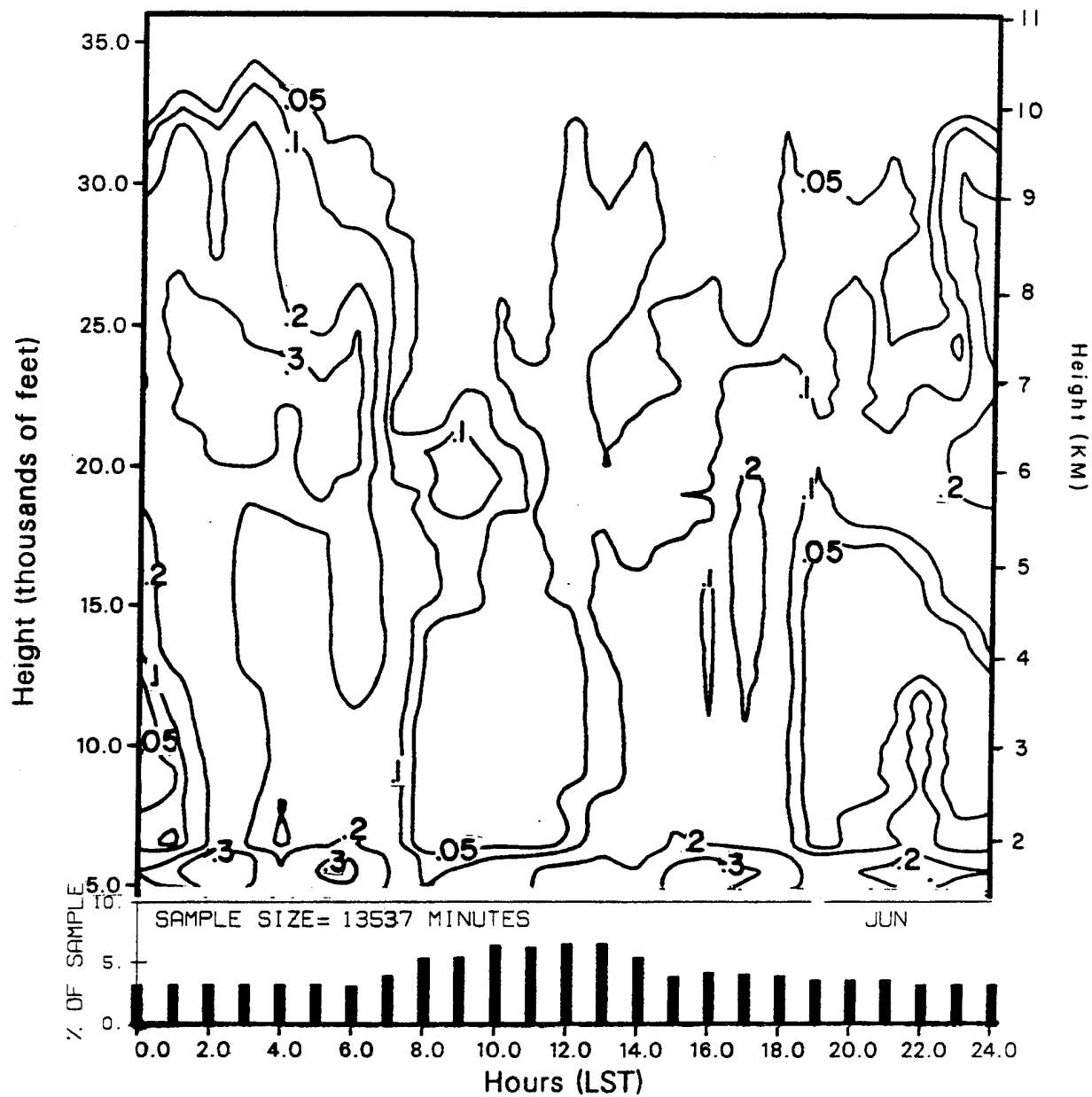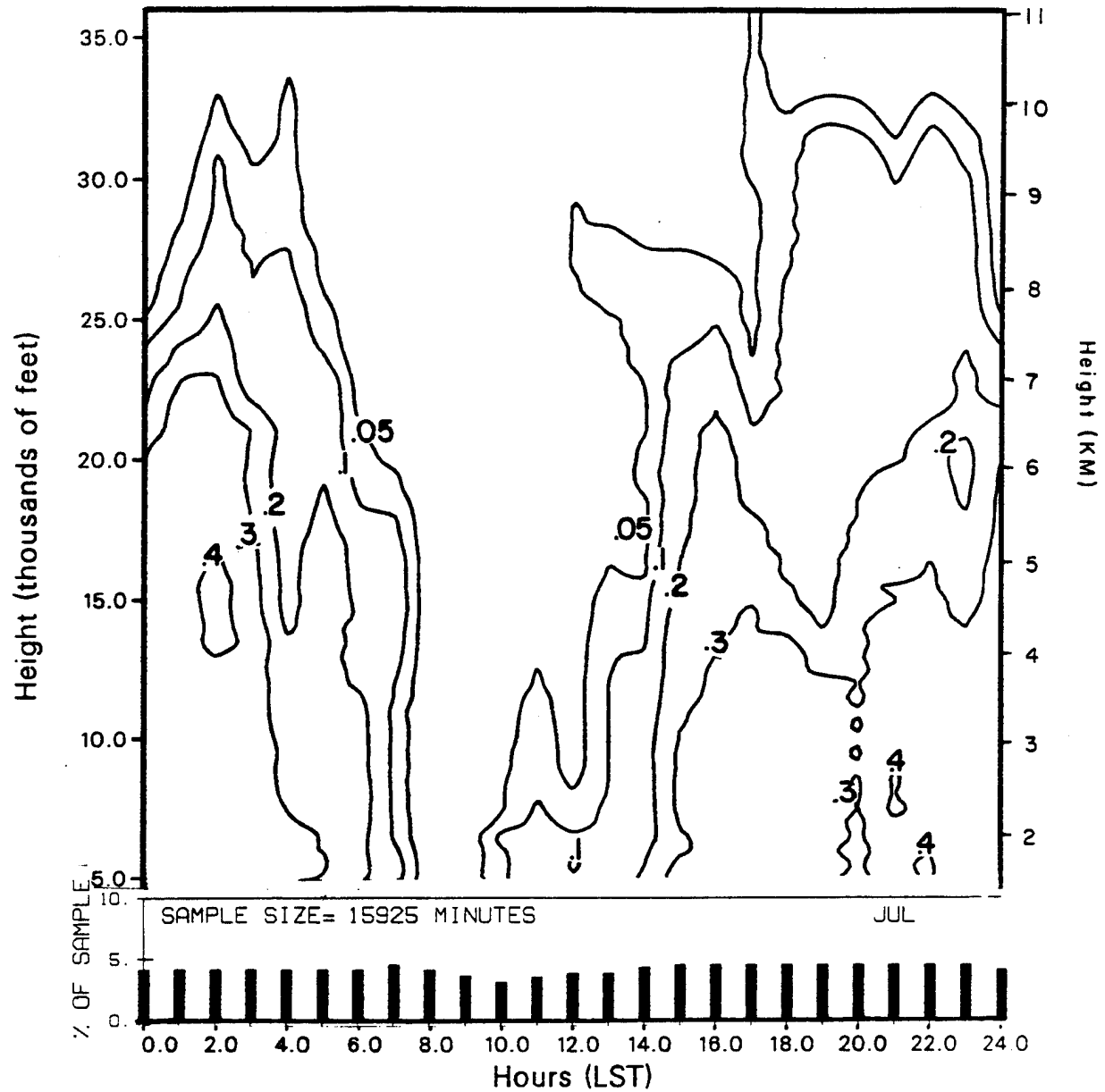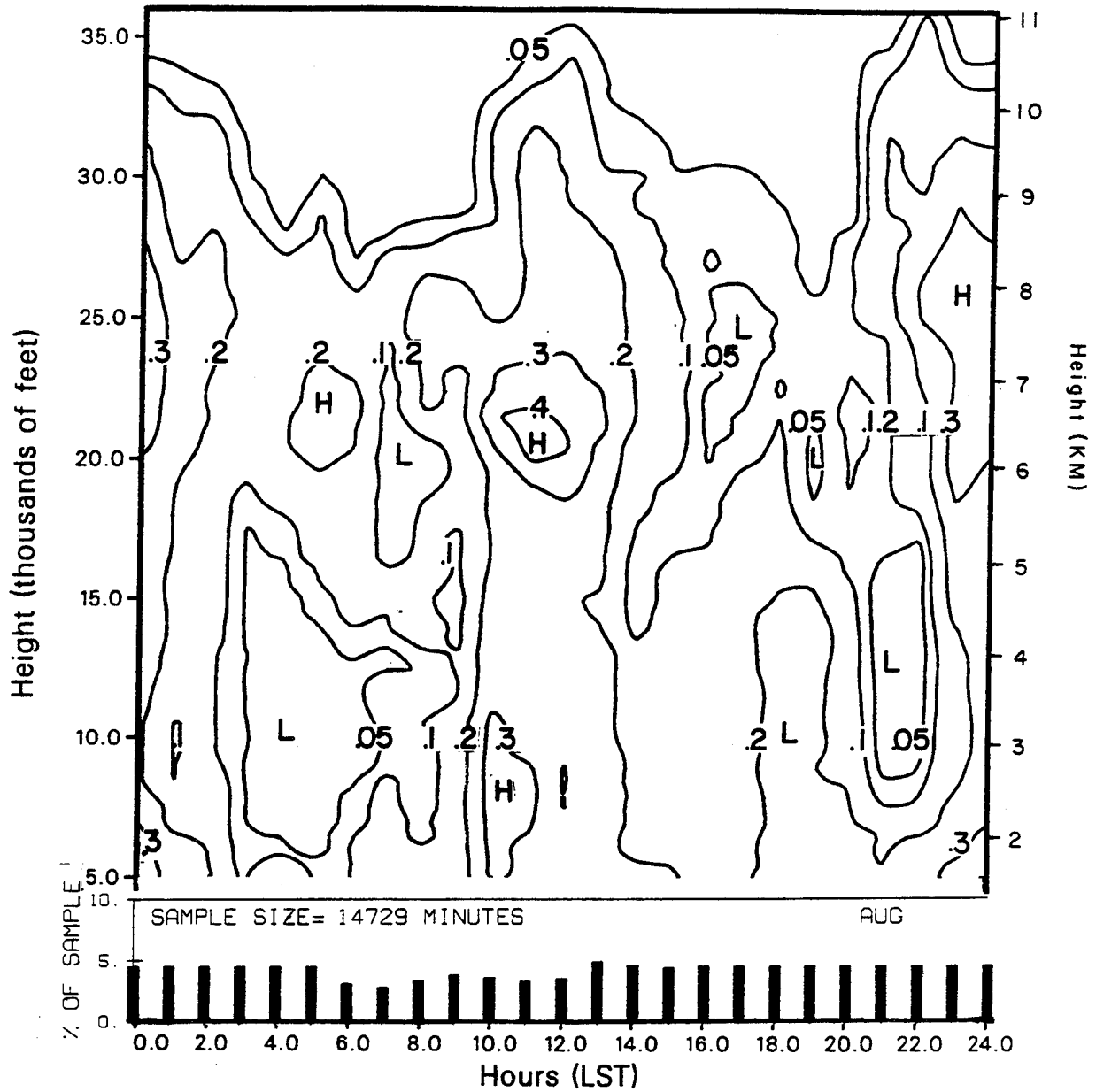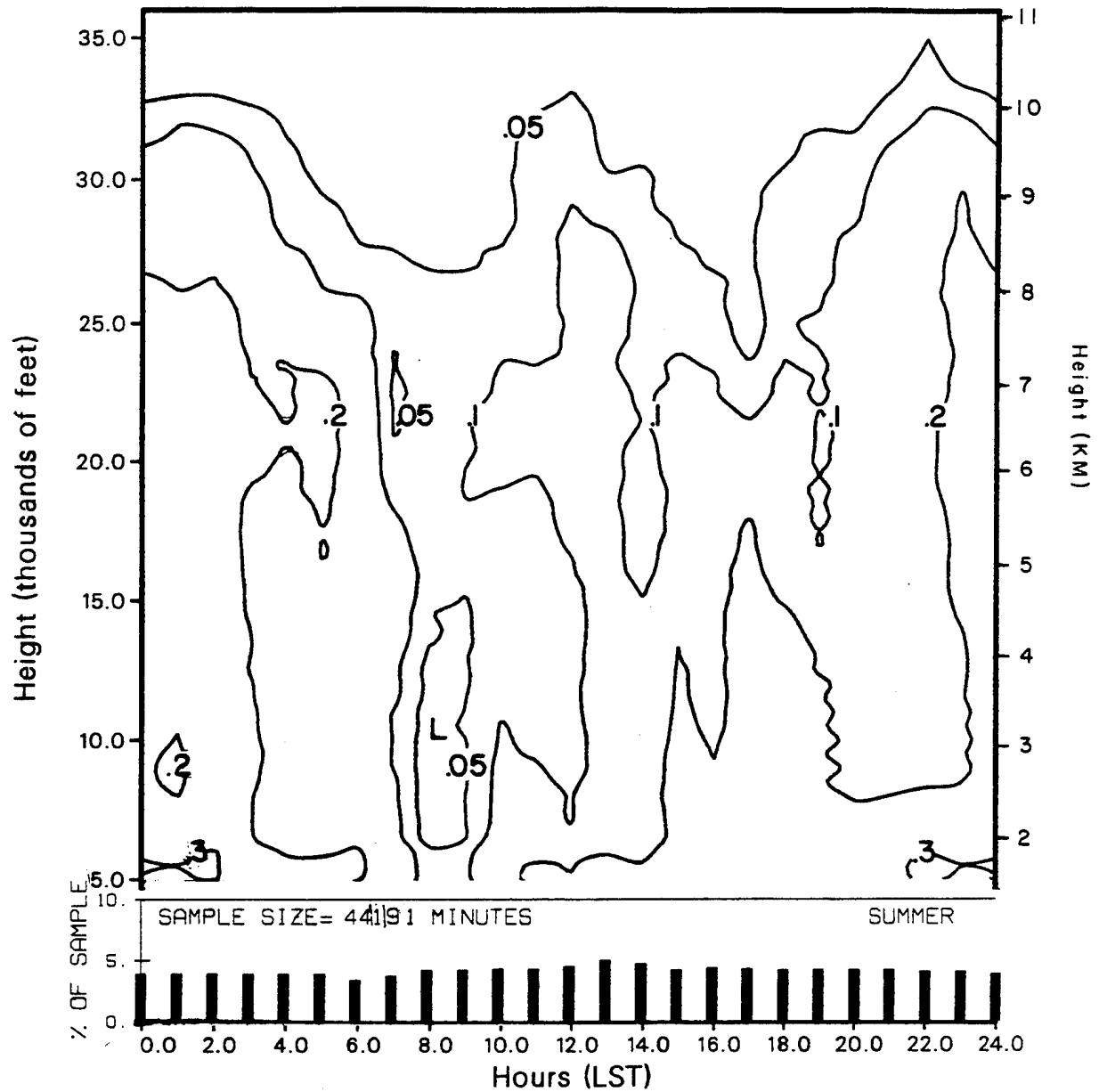
# DIURNAL CLOUD LAYER ANALYSIS



Figure 15.        Probabilities of Clouds Aloft Over a 24-Hour
                 Period for the Summer Season.

31

$$S_{cell,hour} = \sum_{hour=1st}^{last} \sum_{cell=10}^{73} cloudy\ cells,$$

$$n_{cell,hour} = \sum_{hour=last}^{last} \sum_{cell=10}^{73} clear + cloudy\ cells, \qquad (5)$$

$$then\ for\ cell=10,73\ ;\ hour=1st,last$$

$$\rho_{cell,hour} = \frac{S_{cell,hour}}{n_{cell,hour}}$$

where

*s*, *n*, and *p* are two-dimensional arrays that contain the parameters listed in (4) above for 24 hourly bins.

Figures 8-11 show the monthly and seasonal analysis for winter. Figure 8 shows the diurnal cloud layer analysis for the December data ensemble. Since the data are not being analyzed from the surface to 5,000 feet, we take the opportunity to utilize the otherwise empty space at these levels in these figures to display the percent of the sample size used in each of the 24 categories to derive the hourly probabilities of clouds aloft. For example, in processing the December case a total sample size of 11,139 minutes of data were encountered. Of this sample size, only 3.2 percent of it went into the 0 hour category while 4.3 percent of the total sample size was provided for in the noon time analysis. From 5,000 feet to about 36,000 feet the probability values computed over the 24 one-hour categories were contoured to show the diurnal changes in cloud cover probabilities aloft. Note that in the December case, a dramatic decrease in the probability of middle and high clouds (20,000-35,000 feet) occurs between the hours of 8:00 a.m. and noon. Skipping over to the January case, Figure 9, the same phenomenon occurs, only this time between the earlier hours of 6:00 a.m. and 8:30 a.m. Continuing on to Figure 10, the decrease is again apparent between 11:00 a.m. and 1:00 p.m. in the February data ensemble. The winter seasonal diurnal cloud layer analysis displayed in Figure 11 was derived by combining the

three winter months together. Here the decrease in probability of middle and high cloudiness which appears between 6:00 a.m. and 1:00 p.m. has been smoothed out somewhat by the increase in sample size.

Figures 12-15 portray the summer analysis. During this season we again observe an intriguing decrease in middle and high cloudiness during certain hours. However, in some cases it has now extended to low level cloudiness as well. For example, results from the June data analysis, Figure 12, show a decrease in cloud cover probability aloft between the hours of 6:00 a.m. and noon. The decrease is even more prevalent for the July case between 5:00 a.m. and 2:00 p.m. (see Figure 13). Analysis for August, Figure 14, appears rather mixed showing decreases in cloud probabilities aloft between 4:00 a.m. and 8:00 a.m. and again between 7:00 p.m. and 9:00 p.m. The summer diurnal cloud layer analysis, Figure 15, reflects the large decrease in the probability of cloud cover aloft between 6:00 a.m. and noon. Most of these pronounced decreases in probability of cloudiness aloft over the late a.m. and early p.m. hours could be due to sampling error associated with low data sampling sizes. On the other hand, these decreases may be real. That is, since the probability of middle and high clouds are so low to begin with, any natural physical manipulation on these clouds to cause them to dissipate slightly during the late a.m. hours can cause a relatively significant impact on the probability of occurrence. There is also some indications of this decrease in cloud cover at high altitude during the morning hours in Smyth et al., 1991.

### 3.2.5    Probability of Vertical CFLOS & Cloud Layer Correlations Between Two Heights

Figures 16-31 portray graphs of vertical CFLOS & cloud layer correlations between two heights for monthly and seasonal winter and summer cases. The following sections describe the use of these graphs. The algorithms used for deriving these statistics can be found in Sections 4.1 and 4.2.

# PROBABILITY OF VERTICAL CFLOS
## BETWEEN TWO HEIGHTS
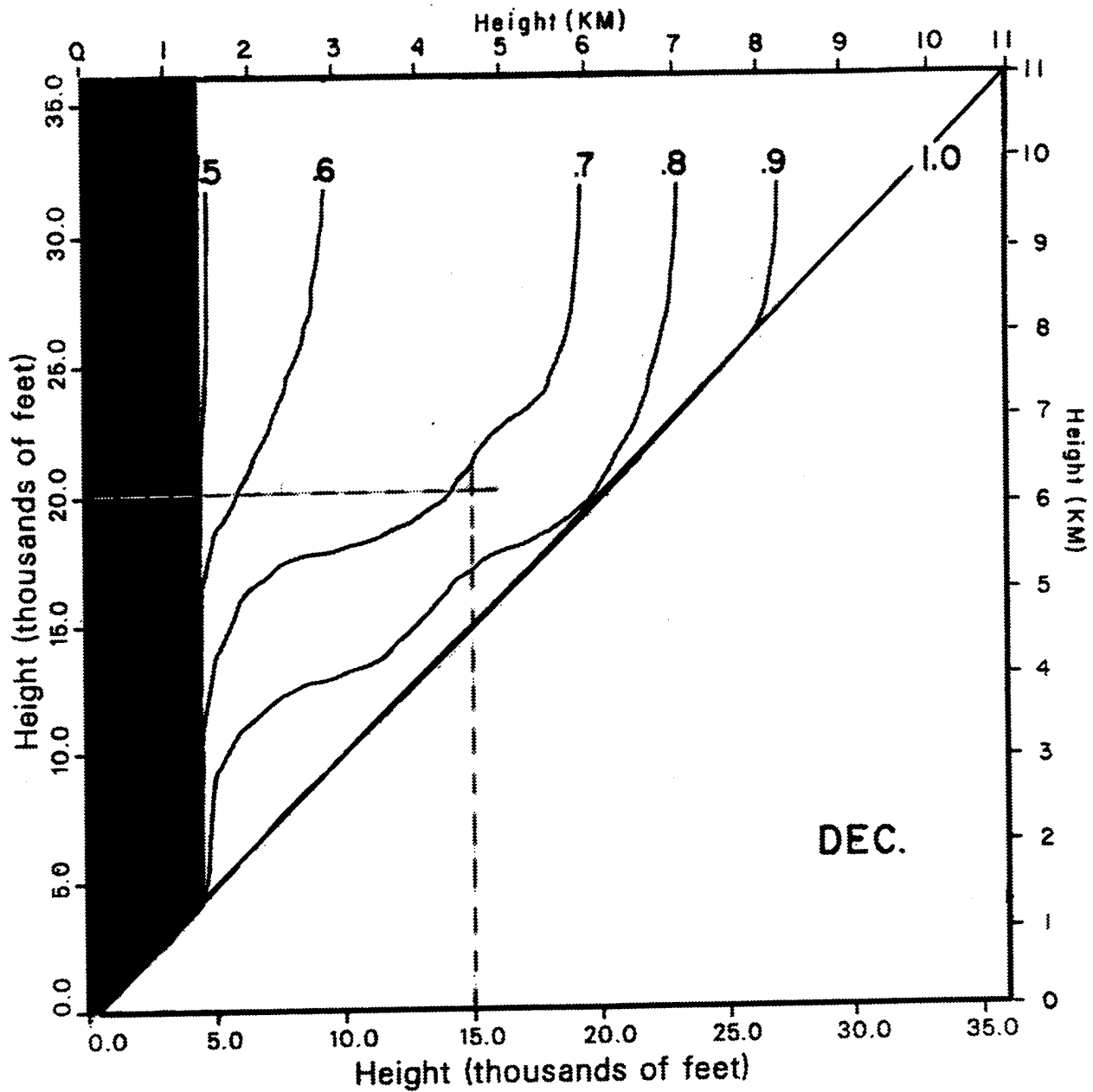


Figure 16.  Probabilities of CFLOS for December. PCFLOS (between 15,000 and 20,000 ft) = 0.72

# CLOUD LAYER CORRELATION
## BETWEEN TWO HEIGHTS



Figure 17.    Cloud Layer Correlation for December.

# PROBABILITY OF VERTICAL CFLOS
## BETWEEN TWO HEIGHTS



Figure 18.    Probabilities of CFLOS for January.

36

# CLOUD LAYER CORRELATION
## BETWEEN TWO HEIGHTS



Figure 19.    Cloud Layer Correlation for January.

# PROBABILITY OF VERTICAL CFLOS
## BETWEEN TWO HEIGHTS



Figure 20.    Probabilities of CFLOS for February.

38

# CLOUD LAYER CORRELATION
## BETWEEN TWO HEIGHTS



Figure 21.    Cloud Layer Correlation for February.

39

# PROBABILITY OF VERTICAL CFLOS
## BETWEEN TWO HEIGHTS



Figure 22.    Probabilities of CFLOS for Winter.

40

# CLOUD LAYER CORRELATION
## BETWEEN TWO HEIGHTS



Figure 23.      Cloud Layer Correlation for Winter.

# PROBABILITY OF VERTICAL CFLOS
## BETWEEN TWO HEIGHTS



Figure 24.     Probabilities of CFLOS for June.

42

# CLOUD LAYER CORRELATION
## BETWEEN TWO HEIGHTS



Figure 25.        Cloud Layer Correlation for June.

# PROBABILITY OF VERTICAL CFLOS
## BETWEEN TWO HEIGHTS



Figure 26.    Probabilities of CFLOS for July.

# CLOUD LAYER CORRELATION
## BETWEEN TWO HEIGHTS


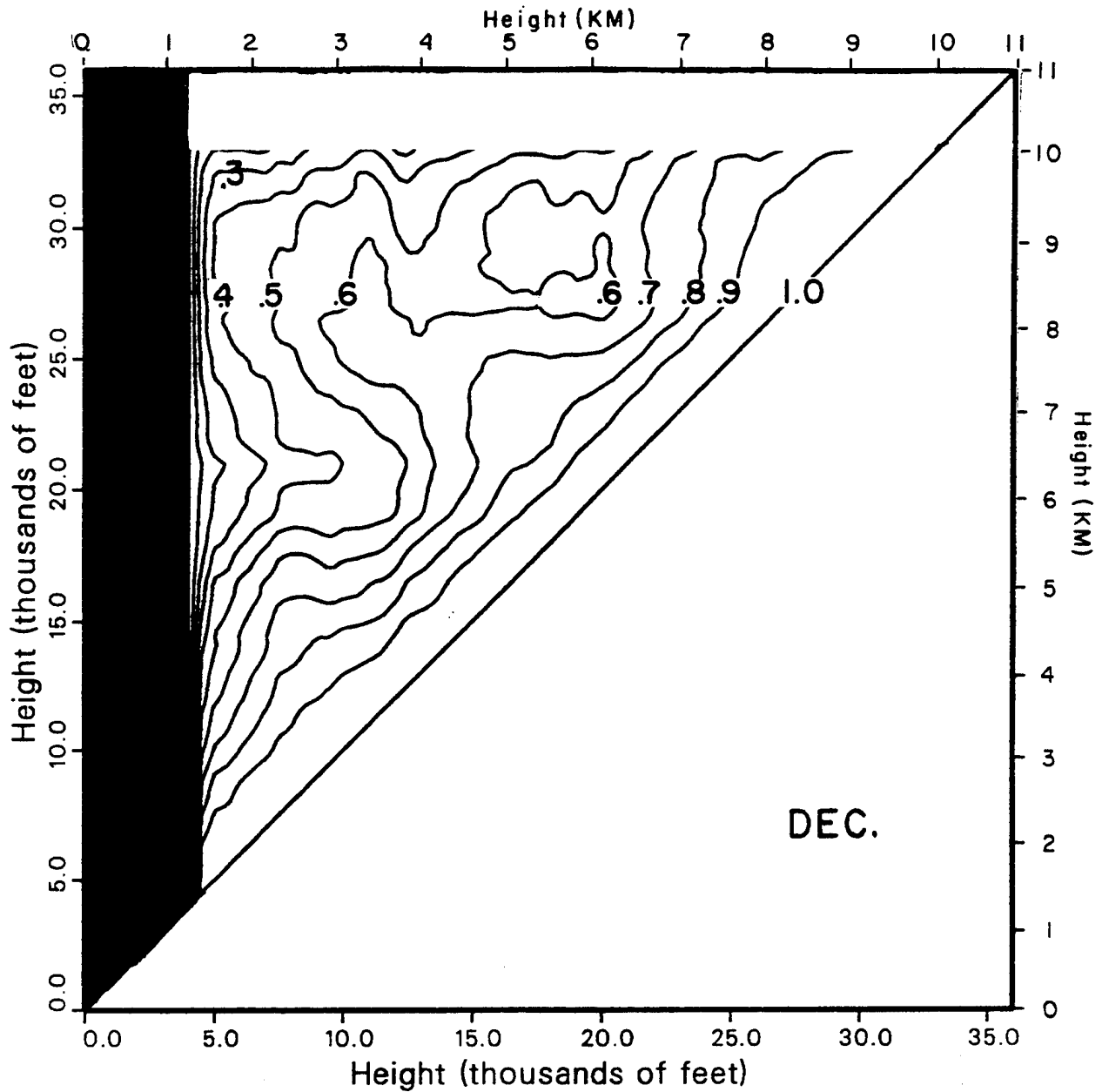
Figure 27.      Cloud Layer Correlation for July.

45

# PROBABILITY OF VERTICAL CFLOS
## BETWEEN TWO HEIGHTS



Figure 28.    Probabilities of CFLOS for August.

46

# CLOUD LAYER CORRELATION
# BETWEEN TWO HEIGHTS
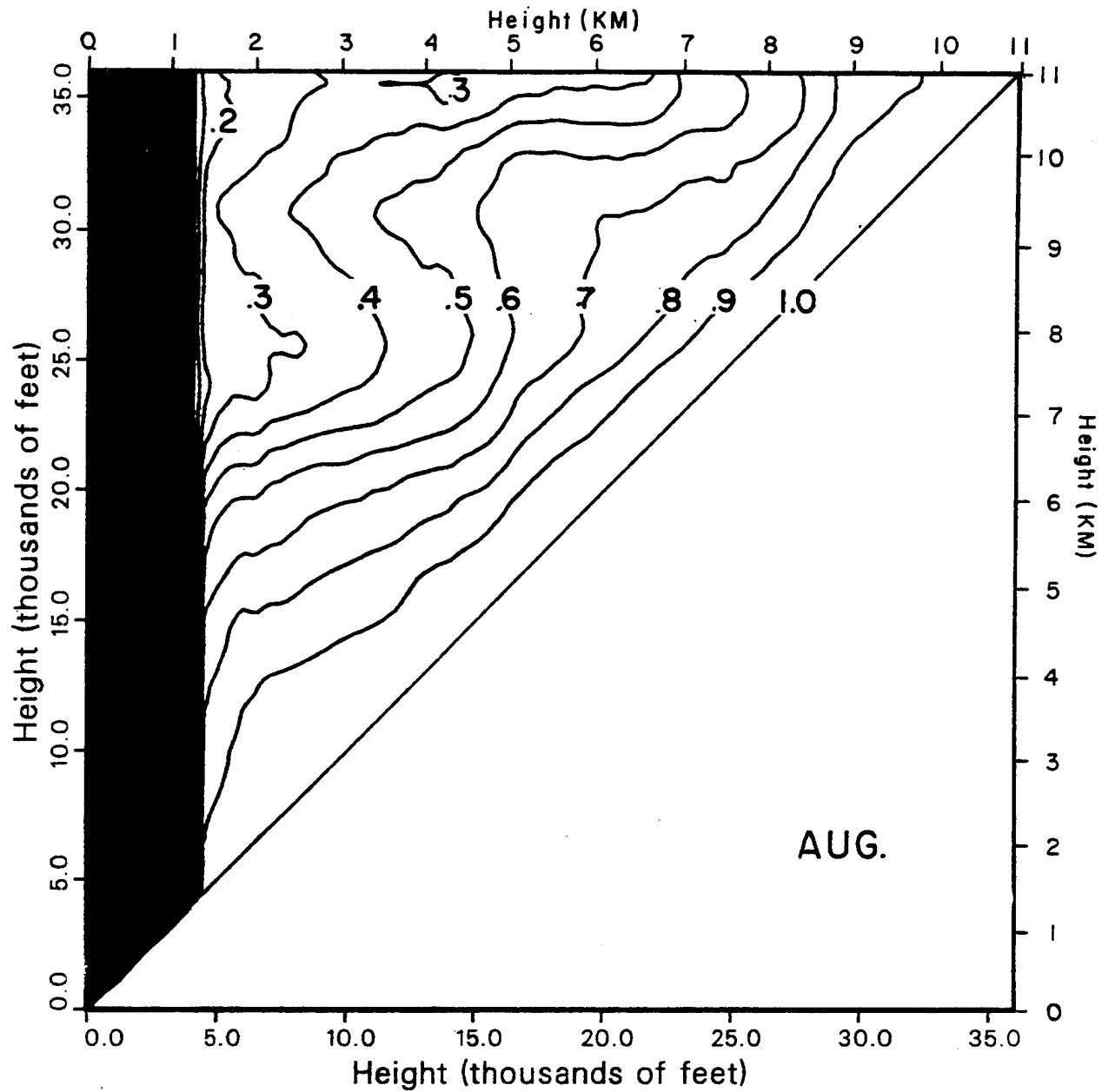


Figure 29.    Cloud Layer Correlation for August.

47

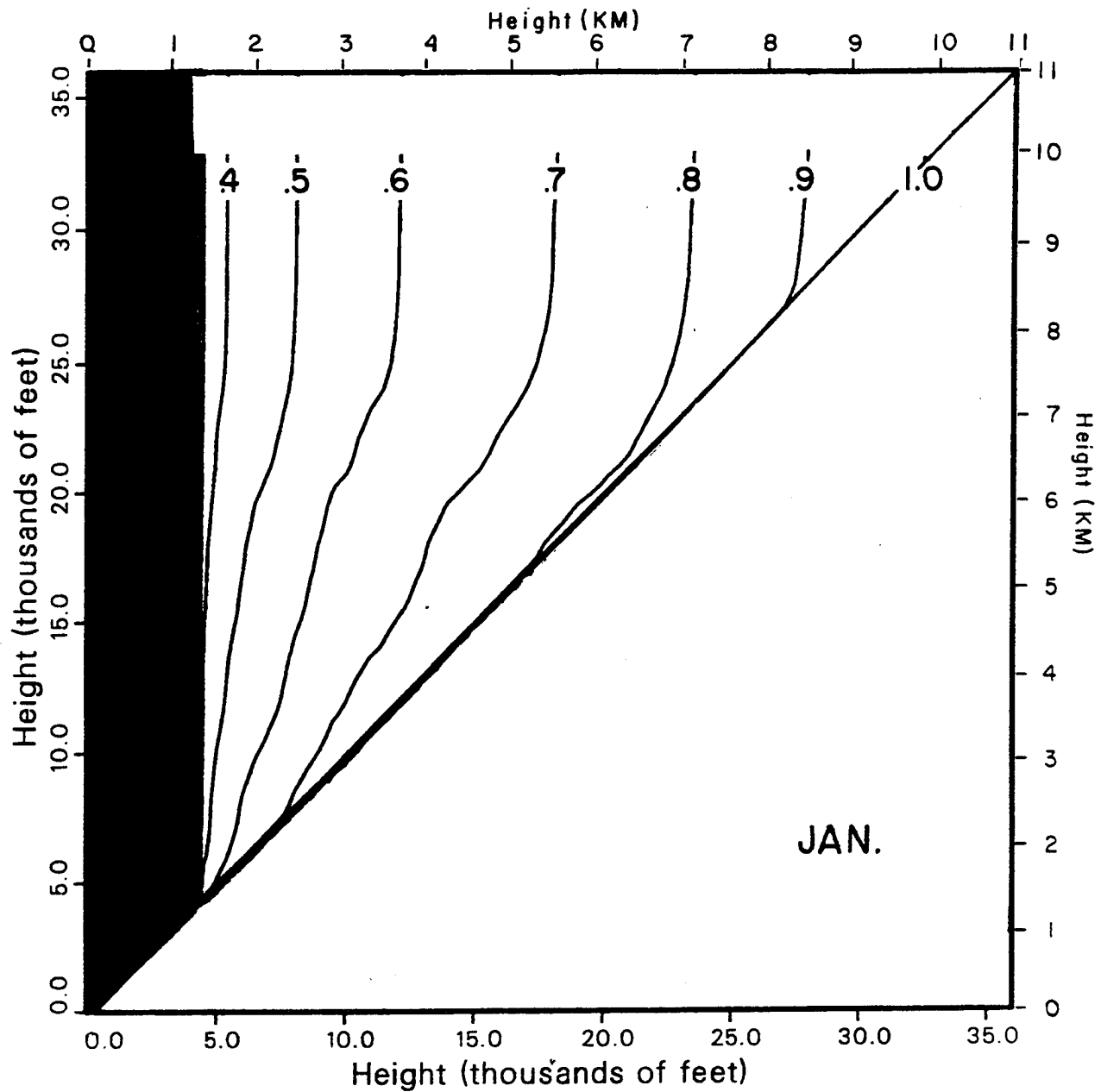# PROBABILITY OF VERTICAL CFLOS
## BETWEEN TWO HEIGHTS
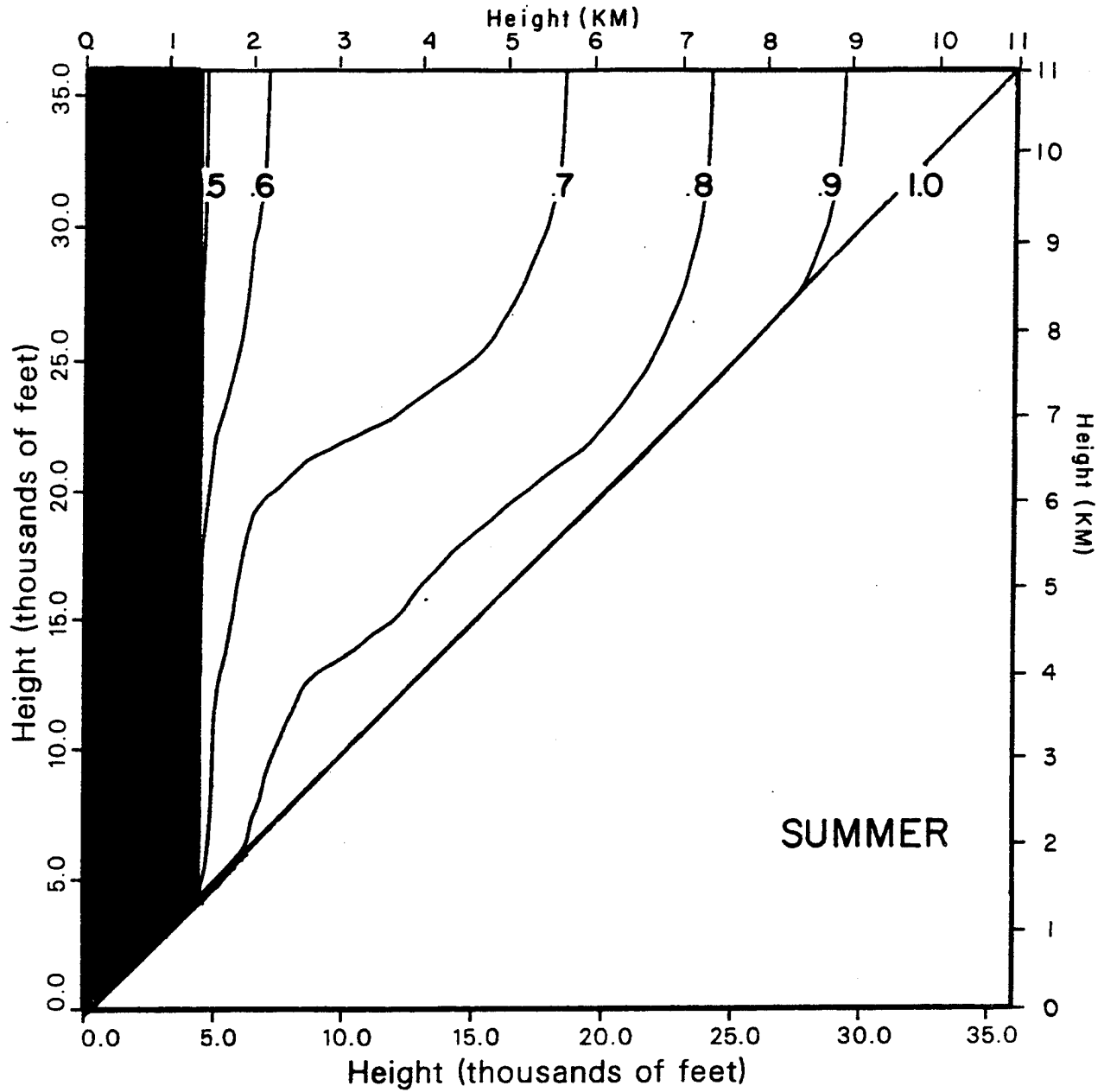


Figure 30.      Probabilities of CFLOS for Summer.
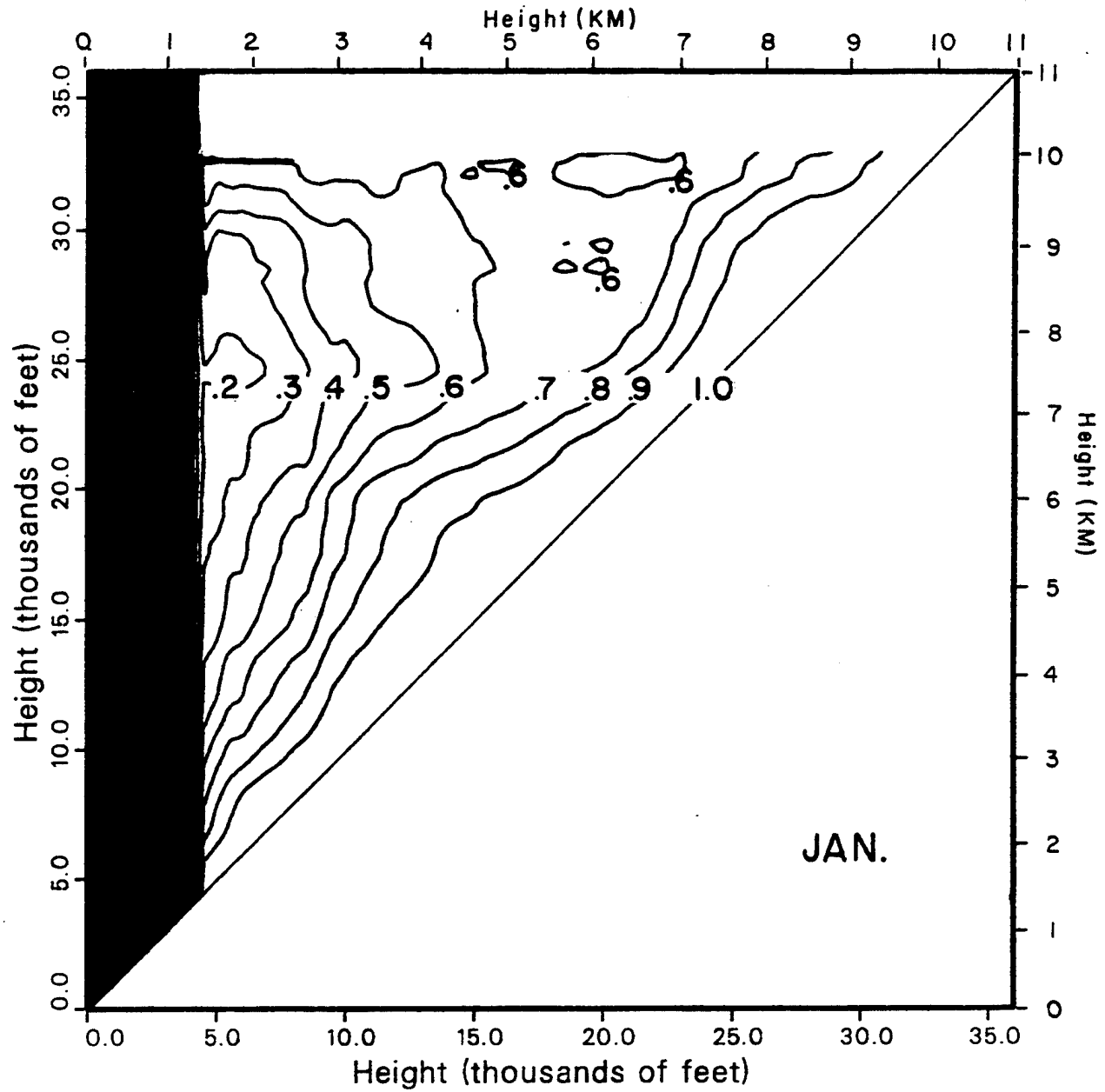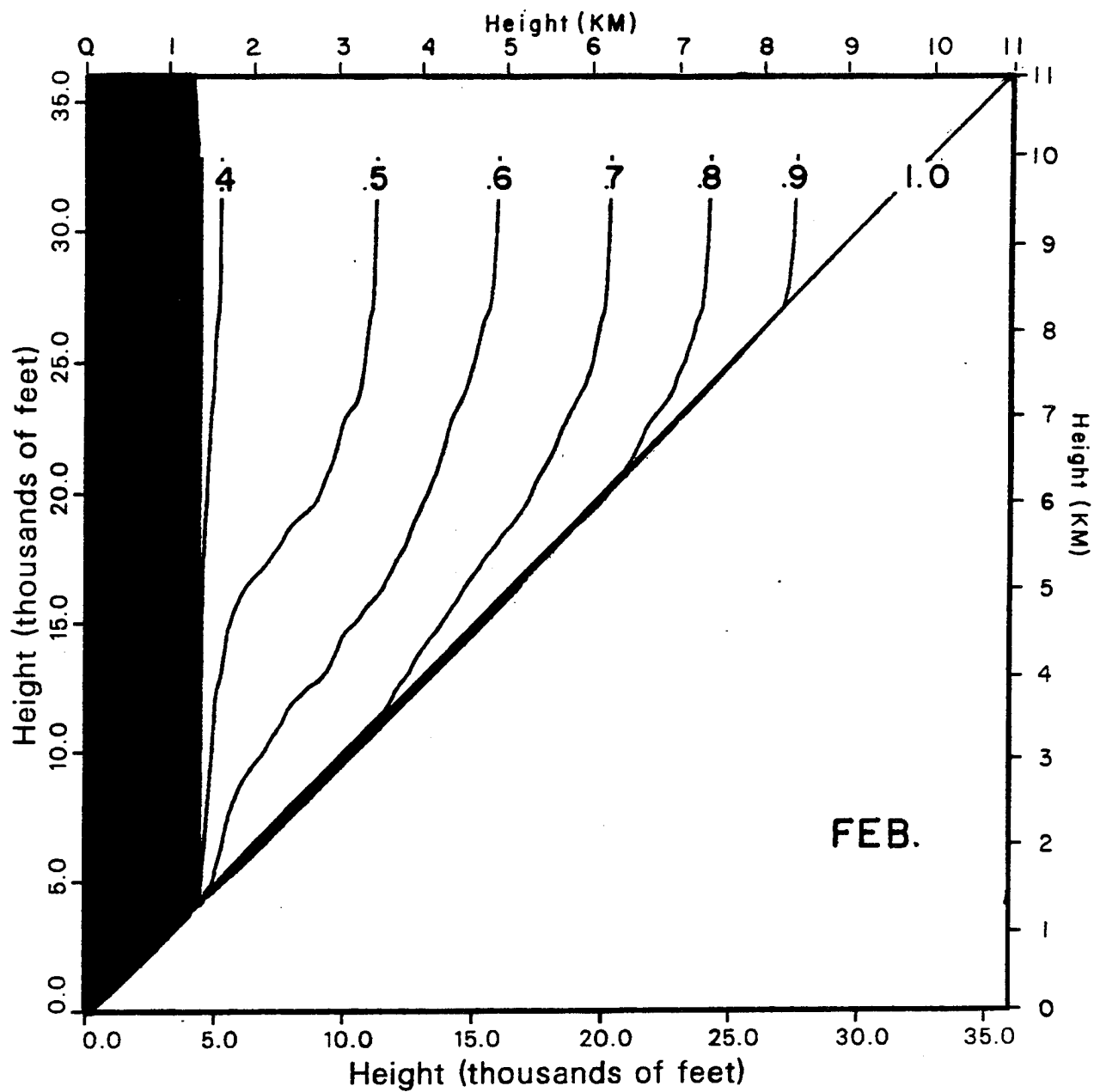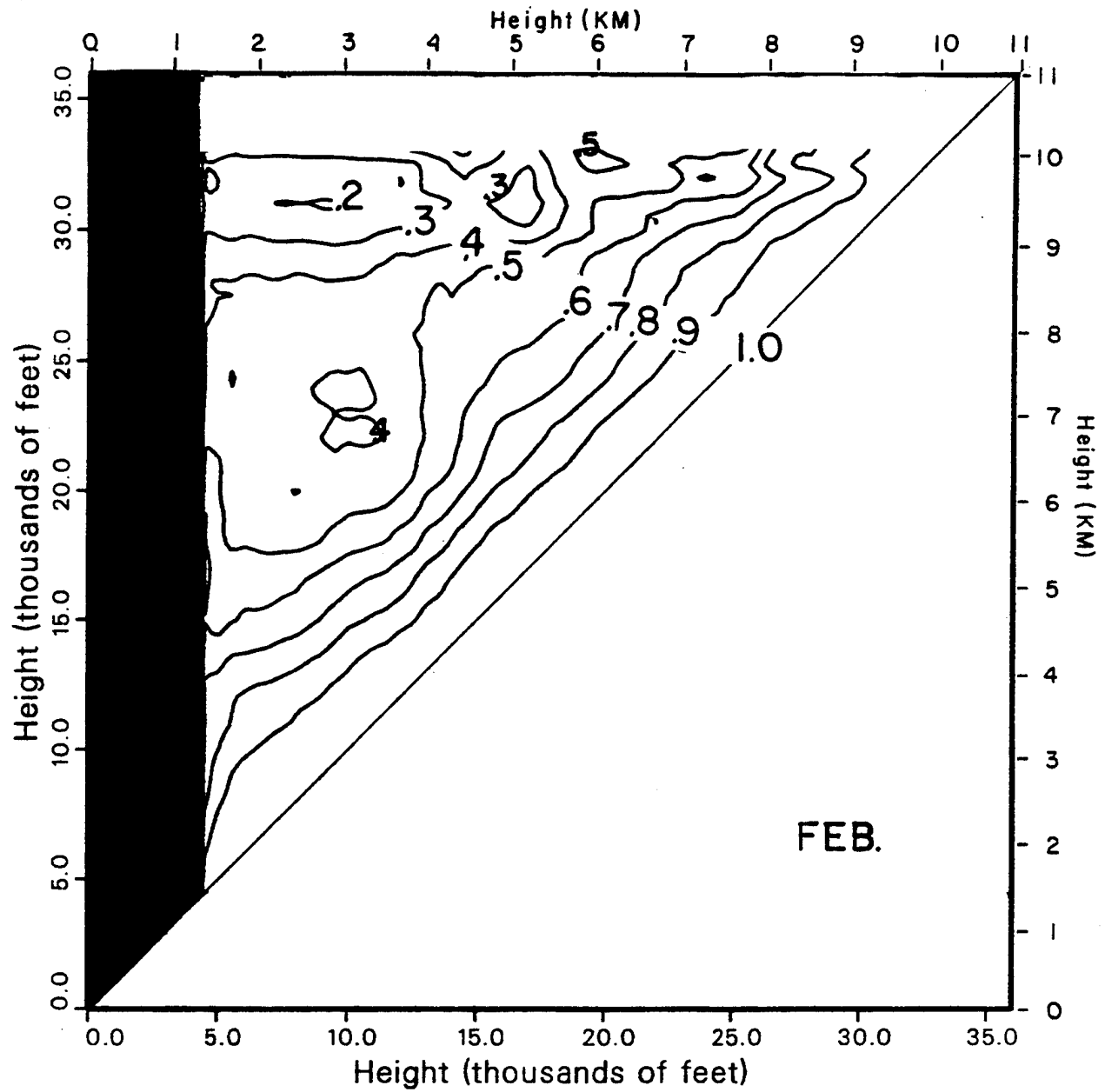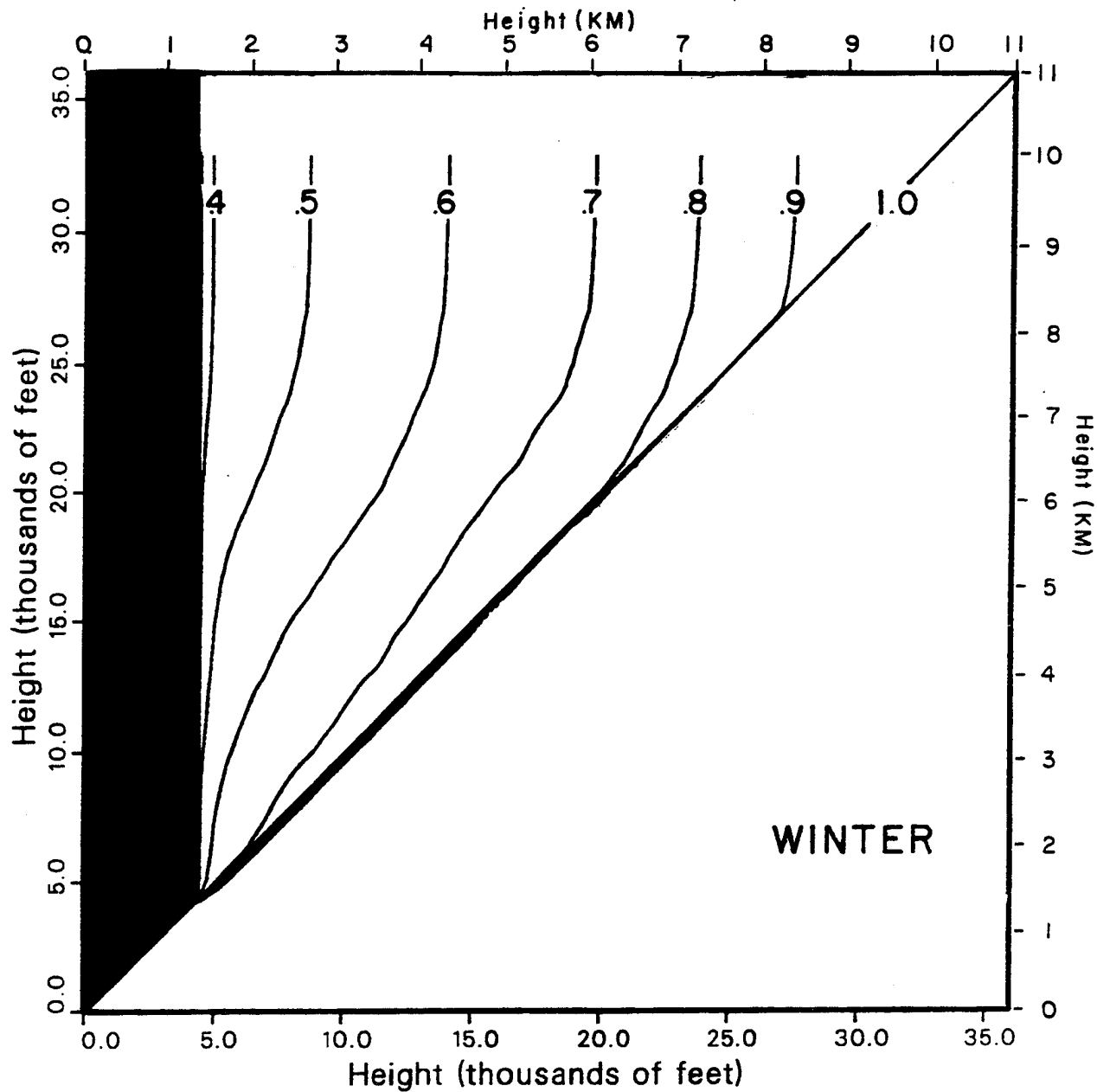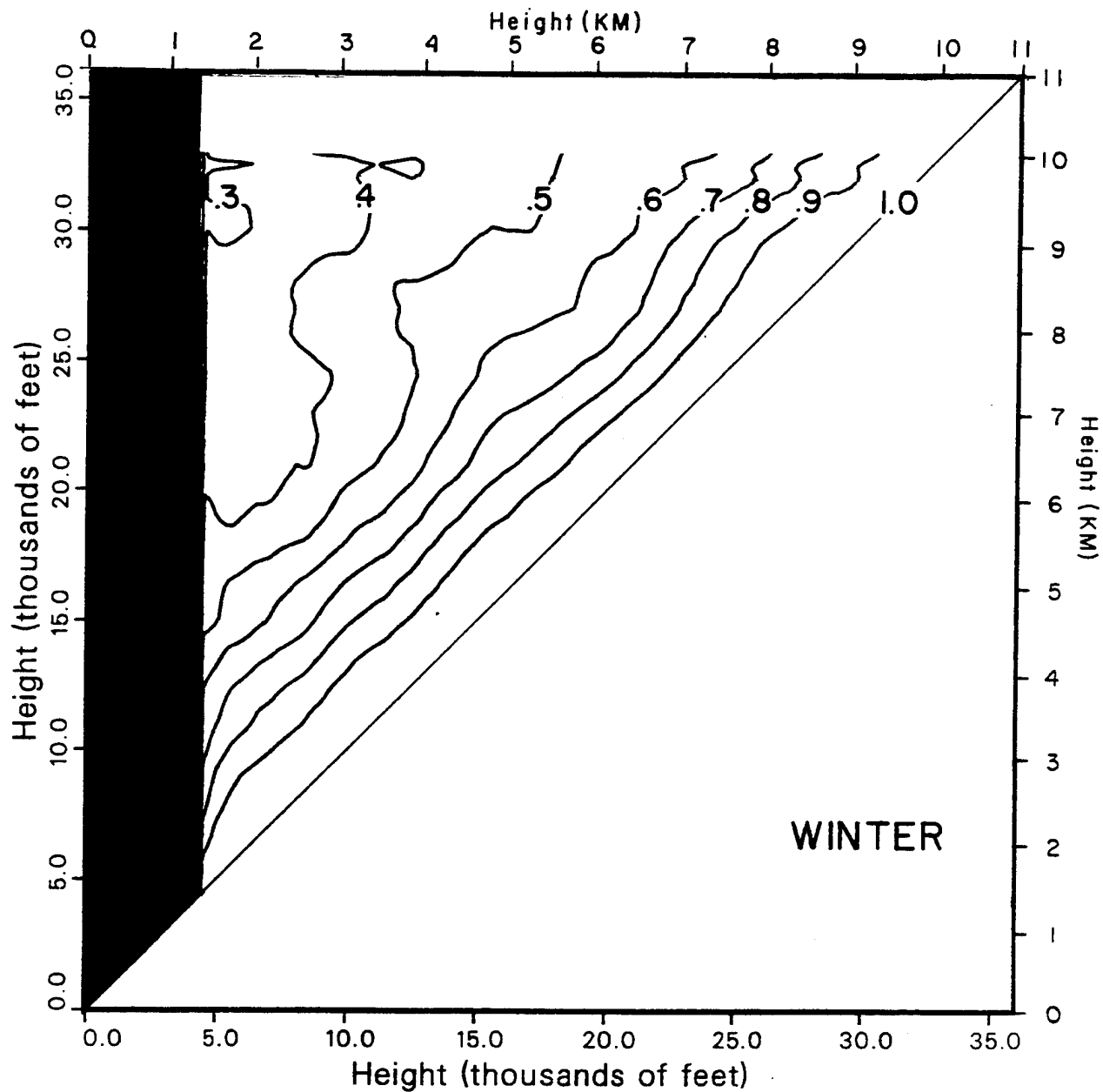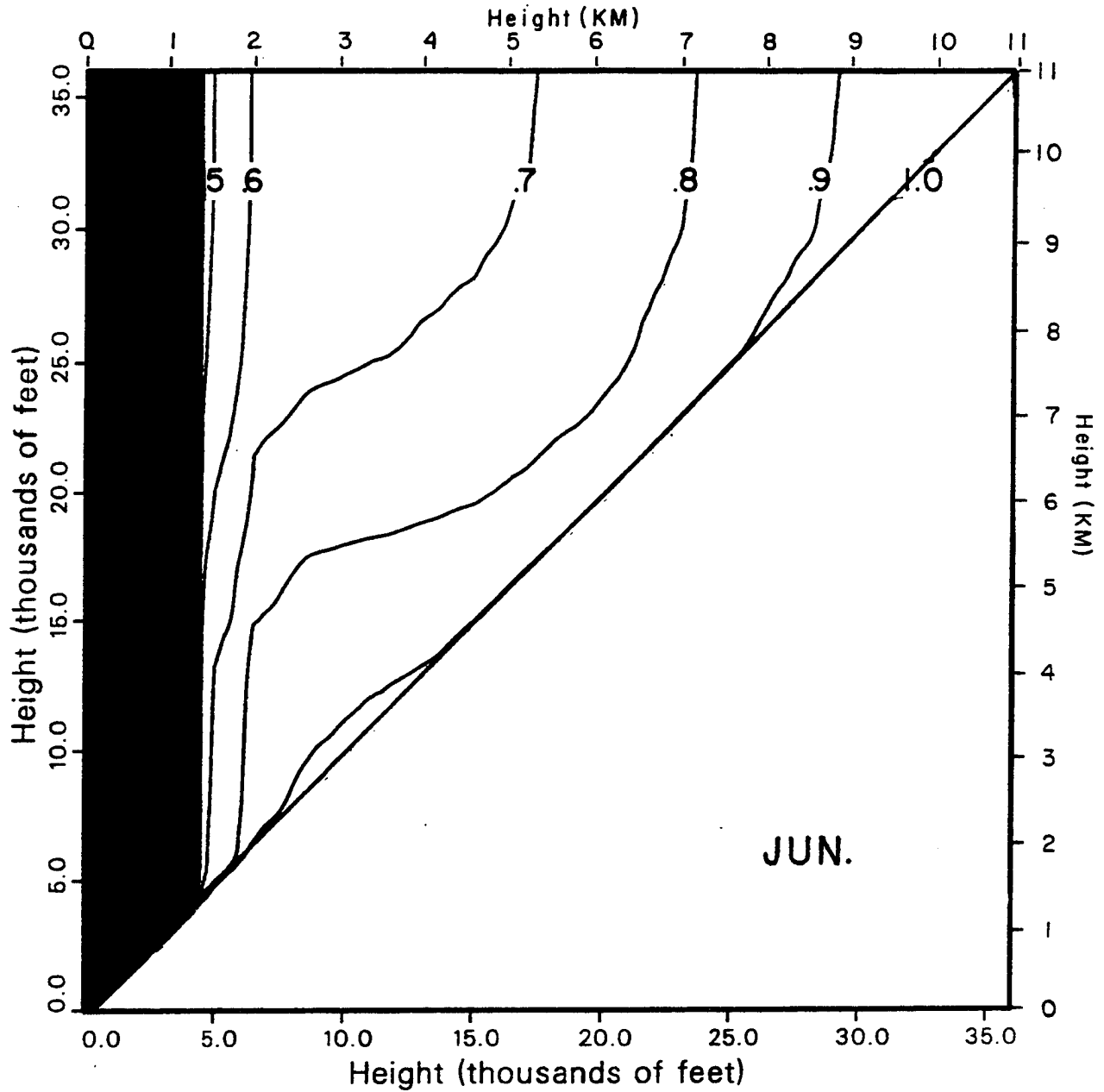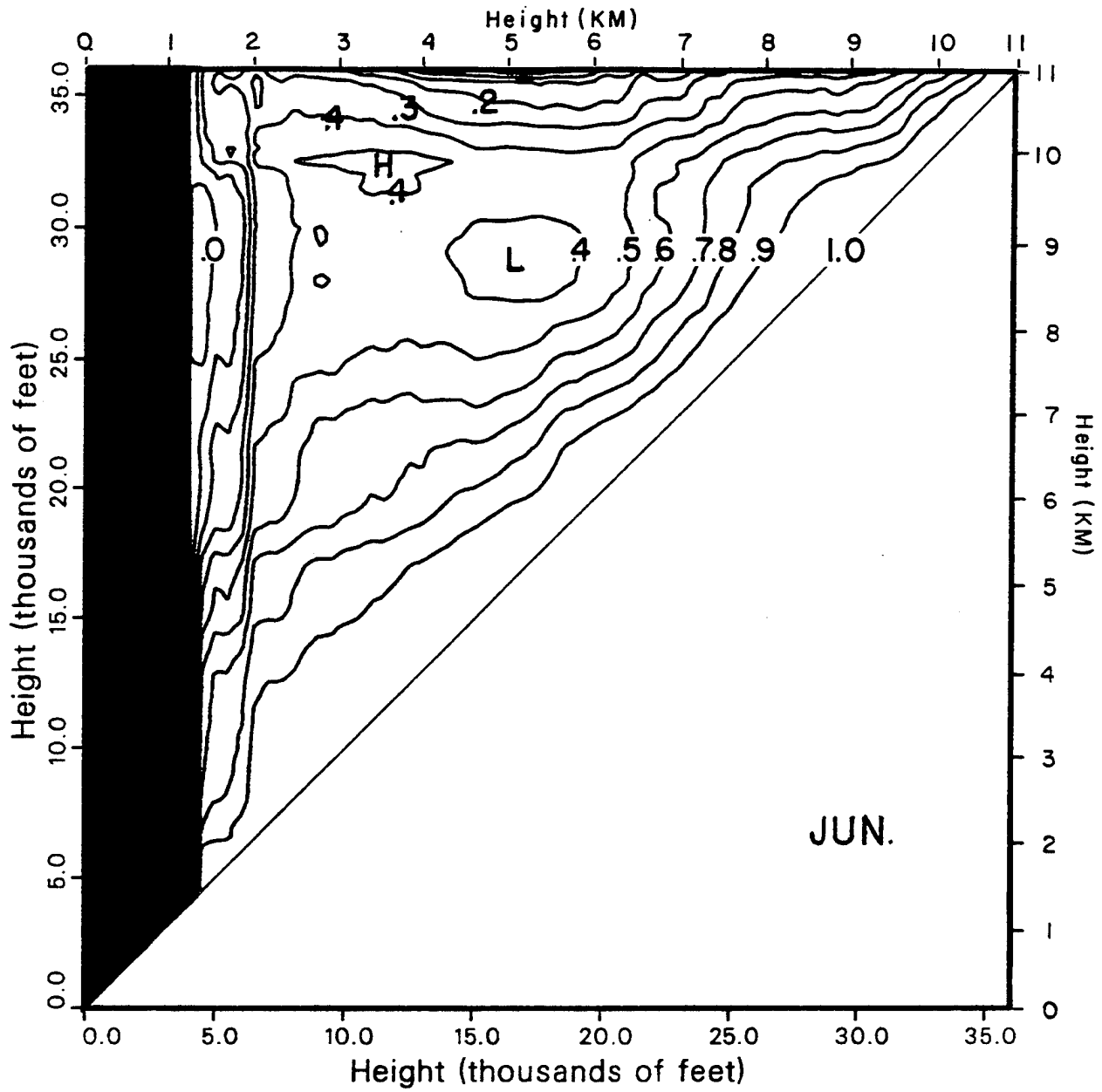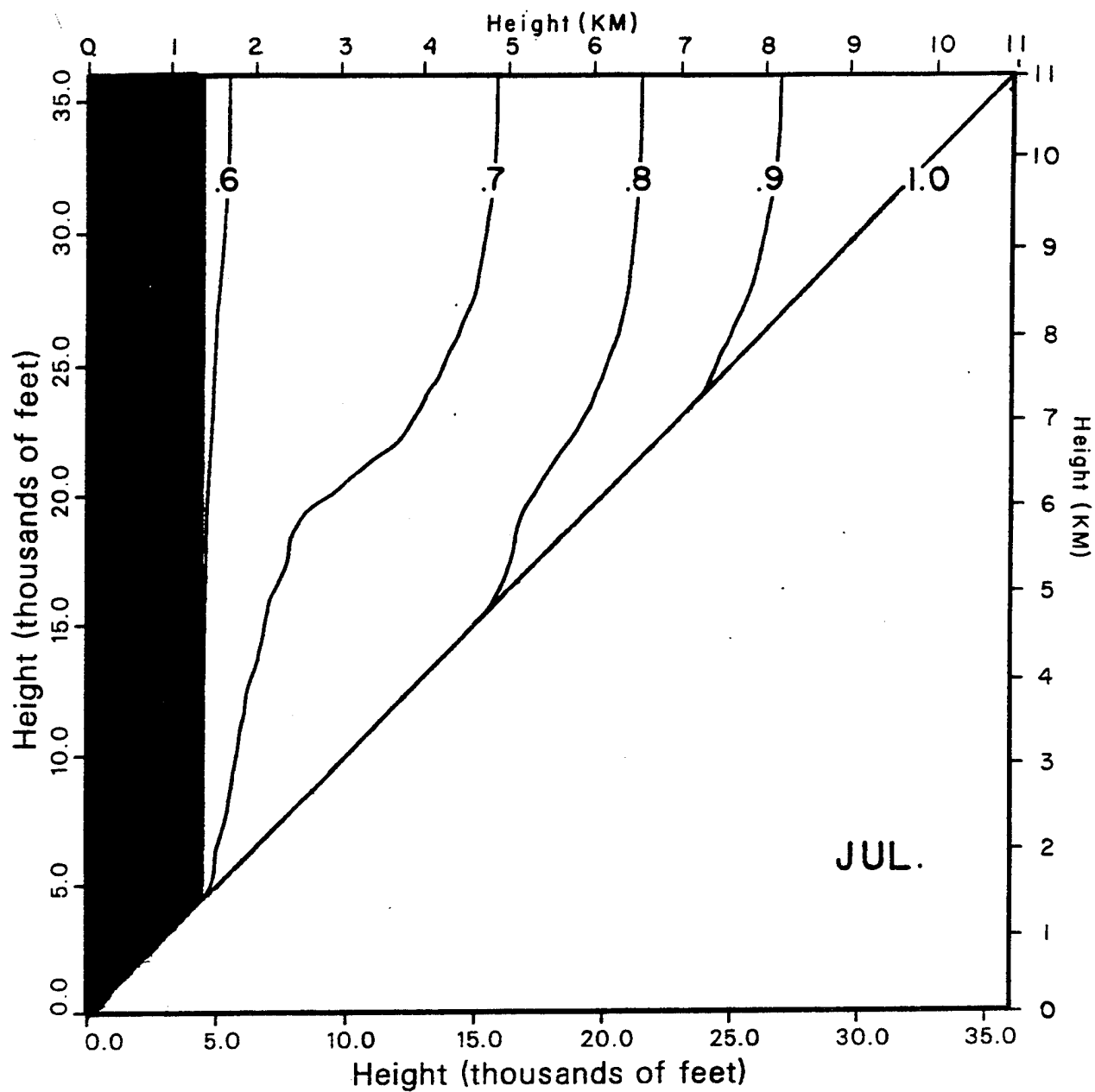
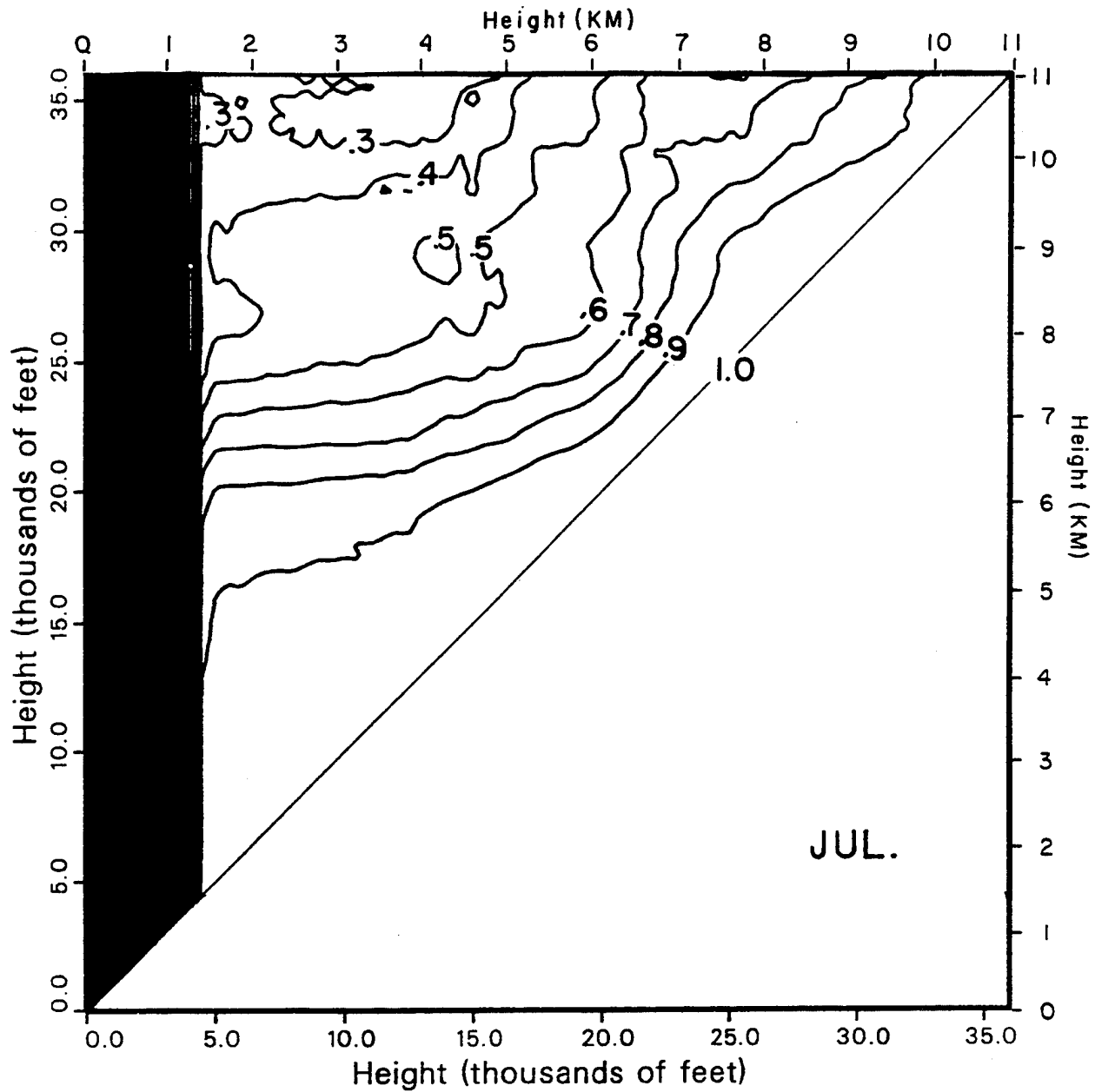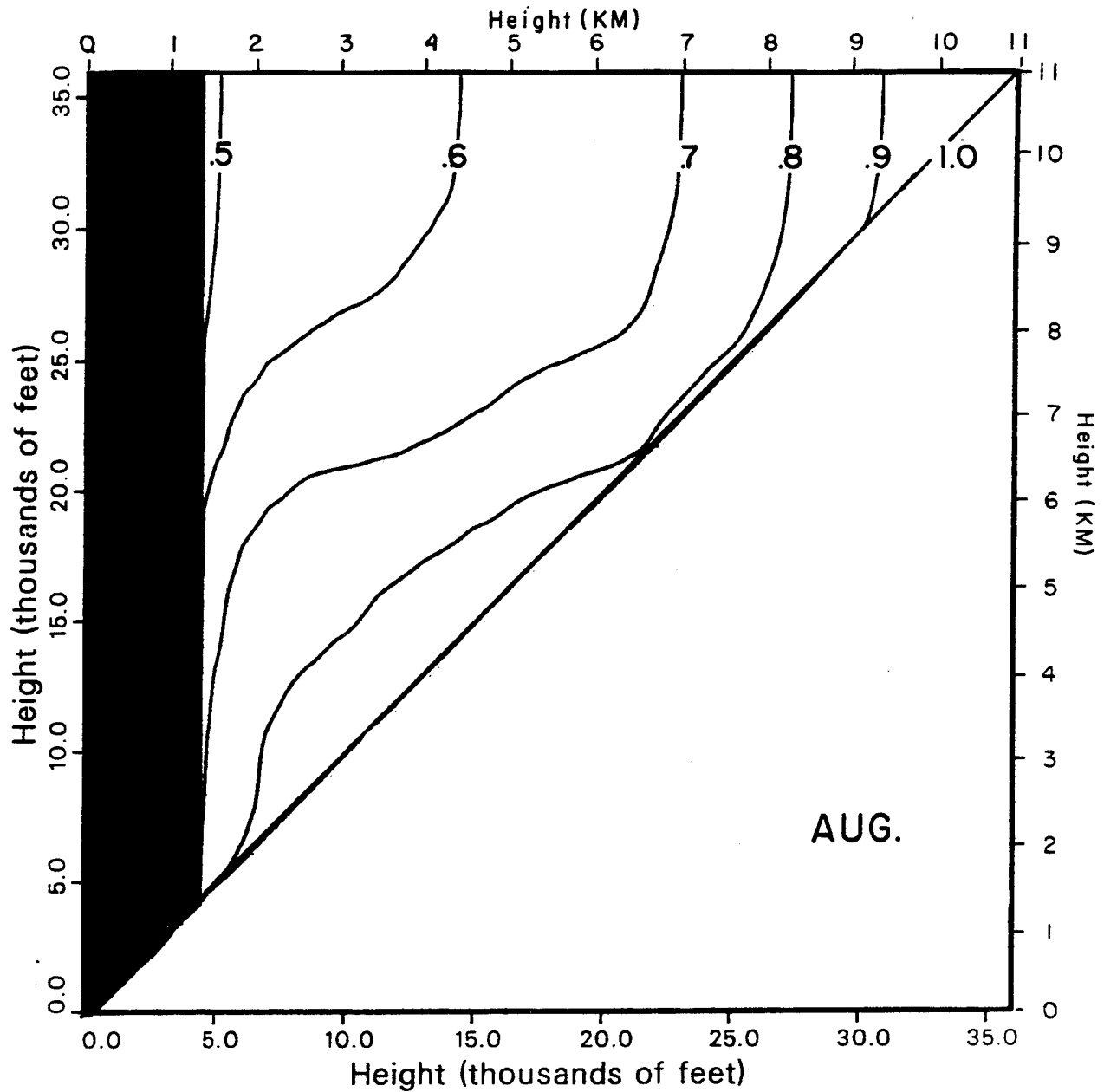# CLOUD LAYER CORRELATION
## BETWEEN TWO HEIGHTS
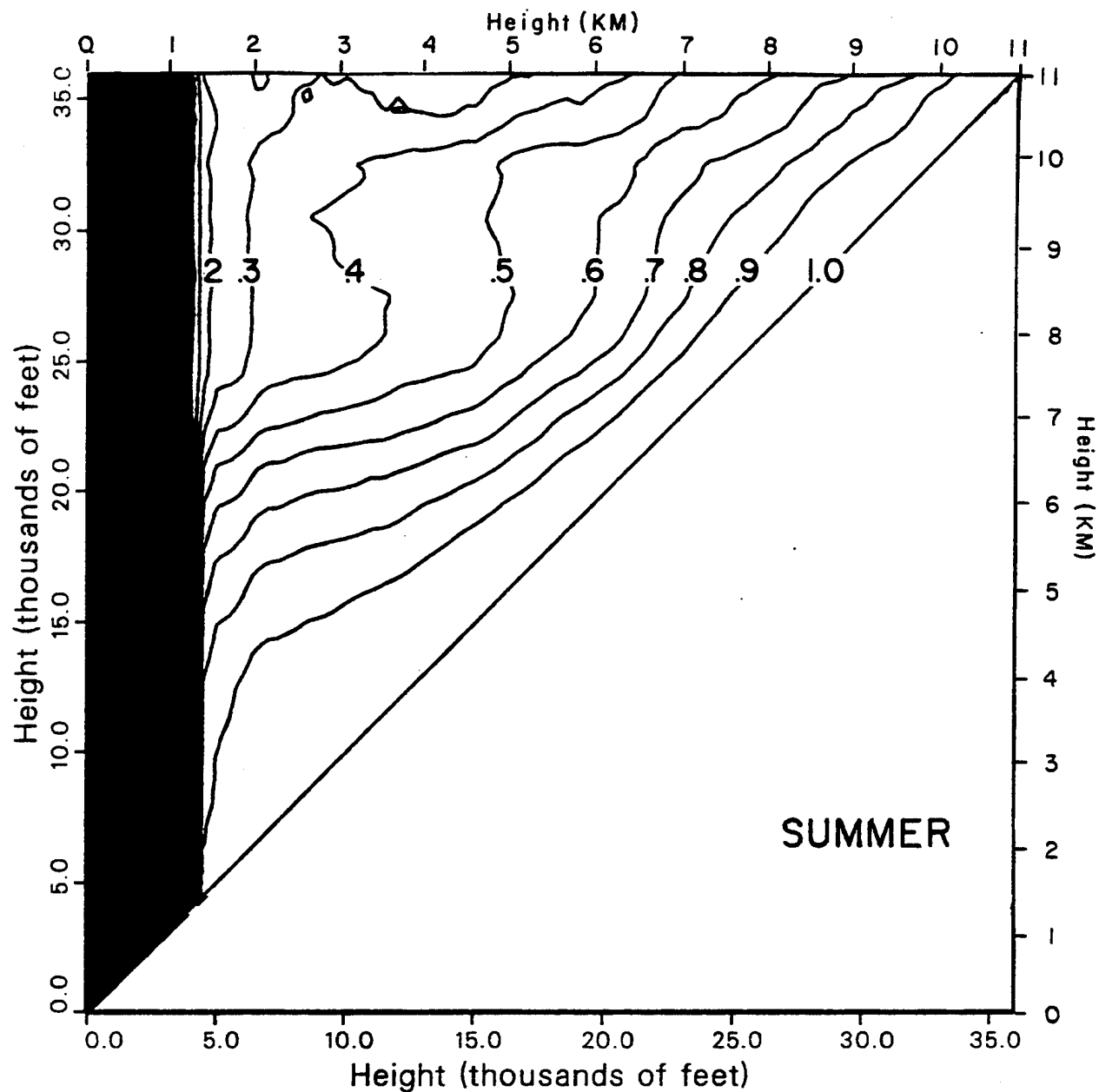


Figure 31.        Cloud Layer Correlation for Summer.

### 3.2.5.1 Graphs of Probability of Vertical CFLOS Between Two Heights

To explain the use of these graphs, we will start with Figure 16, "Probability of Vertical CFLOS Between Two Heights," which was produced using the December data ensemble. Note that both the horizontal and vertical axis are labeled in thousands of feet from 0-35,916 feet. The region between the surface and about 4,920 feet was purposefully blacked out because, as mentioned before, data at these lower heights were too noisy to process. The contours in the upper left section of the graph are lines connecting equal one tenth probability values of vertical CFLOS. For these winter cases only, the area between the 33,000-foot mark and the top of each graph was left blank because of computational problems with deciphering correlation statistics at these rather cloudless levels. The bottom right section is left blank because it otherwise would contain a mirror image of the information content portrayed in the upper left sector.

To determine the probability of vertical CFLOS looking **up** between say 15,000 and 20,000 feet, draw a vertical line from the 15,000-foot tick mark on the horizontal axis to a horizontal line drawn from the 20,000-foot tick mark on the vertical axis. Where these two lines intersect, interpolate between the two contours to determine the probability value. In this case, the probability value was estimated to be 0.72. If you are instead looking **down** from 20,000 to 15,000 feet then proceed up the vertical axis to 20,000 feet and go over horizontally until you are directly over the 15,000 foot mark on the horizontal axis. The same probability of 0.72 emerges at their intersection.

Thus, the probability of CFLOS deduced from radar data is the same looking up as looking down. This need not be the case at those frequencies where scattering into the beam can dominate, for example, in the visible light region of the electromagnetic spectrum.

50

### 3.2.5.2  Graphs of Cloud Layer Correlation Between Two Heights

Figure 17 displays the graph of cloud layer correlation which was derived from the same ensemble of December data used in the case immediately above. This graph is entered in the same manner as that described for Figure 16. Thus, by using the same axis coordinates as in the example above, we get a value of about 0.73 correlation at the line intersections in Figure 17.

### 3.2.6  Serial Correlation of Clouds at Altitude

Figure 32 shows serial (time) correlation of clouds at altitude for the winter and summer seasonal cases separately. These correlations combined with probabilities of clouds aloft can lead to statistics pertaining to cloudy or clear recurrences. These recurrence statistics can be computed by utilizing appropriate subroutines found in program, TETRA, which is published in Smyth et al. 1991.

Equal correlation values of every two tenths are contoured. The left vertical axis of each figure showing the height scale in thousands of feet can also be considered the 1.0 correlation contour. The zero contour is darkened to emphasize the compaction of the contours from winter to summer seasons.

Note that in the winter case, correlation values run fairly high, (upwards of 0.4) in the higher cloud layer regions between about 28,000-33,000 feet for most of the entire 24-hour lag time. This amount of persistent rather high correlation is likely attributed to the typical sky cover found over New England in the winter. That is, in the winter large storms having lots of clouds at high levels can persist over two or three days at a time, eventually giving way to clear conditions that can persist over the same lengthy time period. The summer case, on the other hand, shows correlation values at higher levels of correlations above 0.4 lasting only for about 3 hours or less for levels between 28,000 and 33,000 feet. This decrease is likely the result of summer time convective activity over New England which brings small, sudden, storm outbreaks that last for short periods of time. Note also that high correlation values between 0.6 and
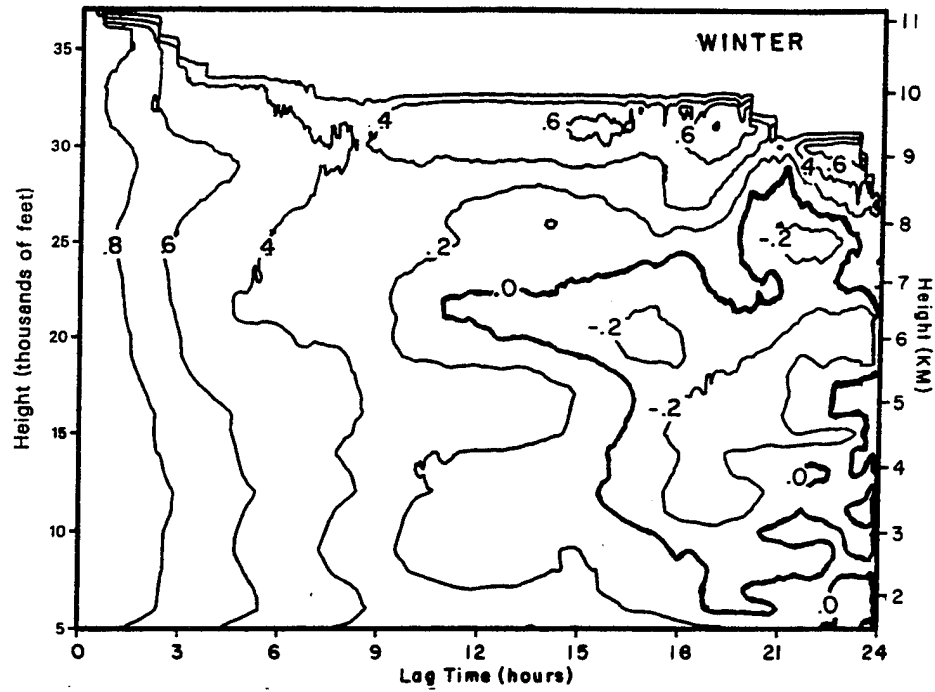
51

# SERIAL CORRELATION OF CLOUDS AT ALTITUDE



# SERIAL CORRELATION OF CLOUDS AT ALTITUDE
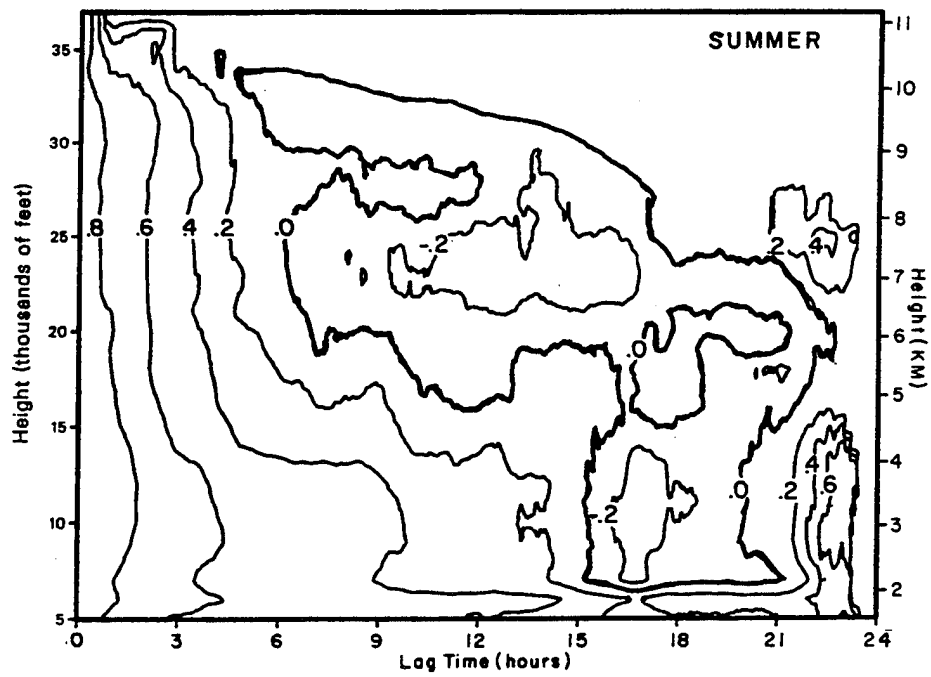


Figure 32.    Serial Correlation of Clouds at Altitude for Winter and Summer Cases.

52

unity have notably shorter lag times at all levels in the summer than in the winter season. This behavior is typical of that found in seasonal **spatial** correlation of sky cover calculated from the center sectors of whole-sky photographs (see Willand, 1990). The high correlation values in the summer case beyond the 21-hour lag time are likely due to lower sample sizes that are typical at these longer lag times.

This statistic can be influenced by the data collection operations of the radar device. That is, a continuous cloudy or clear condition over the beam could be interrupted during a radar shutdown for maintenance or a tape change. When the radar is turned on there is no way of telling how long the initial immediate cloudy or clear event being recorded had been in effect.

### 3.2.7 Probability of Vertical Cloud Thickness

Here we are measuring the geometric thickness of a cloud layer. This is not the optical thickness, which also takes into account the density of water droplets.

Probability of vertical cloud thickness graphs are shown for winter in Figure 33 (a through p) and for summer in Figure 34 (a through p). To explain the use of these graphs, we will start with Figure 33 (a). Because of the 150-meter data resolution element size, each black bar in the figure represents a minimum cloud thickness of 150 meters (492 feet). Therefore, 10 black bars would represent a cloud that is 10 x 150 meters or 1,500 meters thick. These bars extend upward to their value of probability labeled on the vertical axis for clouds having bases between 1,350 and 1,950 meters or 4,428 and 6,396 feet. Thus, if one is interested in knowing the probability of a cloud being 150 meters thick and that the cloud base is between 1,350 and 1,950 meters in the winter, refer to the first black bar in Figure 33 (a) which will show a 0.012 probability. In the same figure, the probability of seeing a cloud 7,500 meters thick is only about 0.0001.
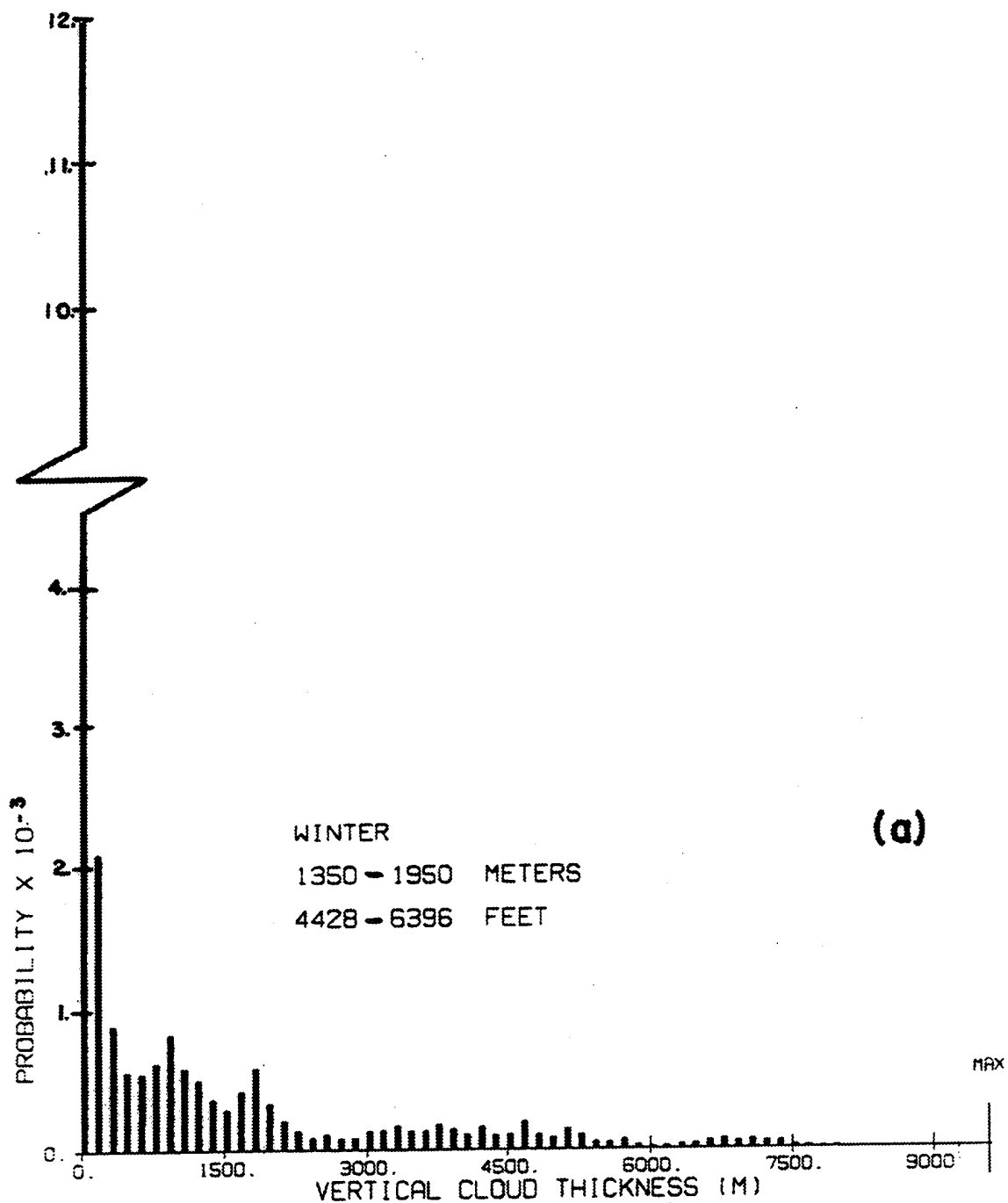
Figure 33.    (a)    Probability of Vertical Cloud Thickness for a
Cloud With Bases Between 1,350 and 1,950
Meters. The maximum possible vertical
thickness is indicated by the line labeled
MAX.

Figure 33.   (b,c,d)   Probabilities of Vertical Cloud
Thicknesses for Clouds With Bases
Between the Indicated Altitudes.

Figure 33.    (e,f,g)    Probabilities of Vertical Cloud
                        Thicknesses for Clouds With Bases
                        Between the Indicated Altitudes.

Figure 33.    (h,i,j)    Probabilities of Vertical Cloud
                        Thicknesses for Clouds With Bases
                        Between the Indicated Altitudes.

WINTER

8550 - 9150 METERS

28044-30012 FEET

**(m)**



WINTER

7950 - 8550 METERS

26076-28044 FEET

**(l)**



WINTER

7350 - 7950 METERS

24108-26076 FEET

**(k)**

Figure 33.　(k,l,m)　Probabilities of Vertical Cloud
Thicknesses for Clouds With Bases
Between the Indicated Altitudes.

58
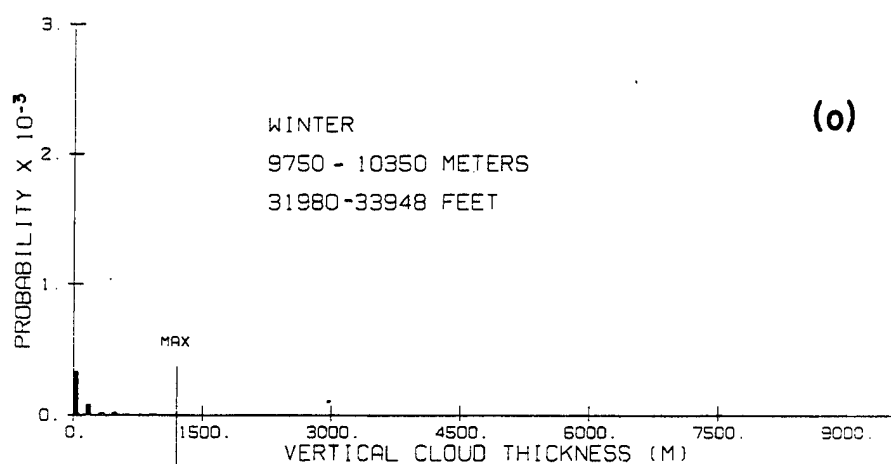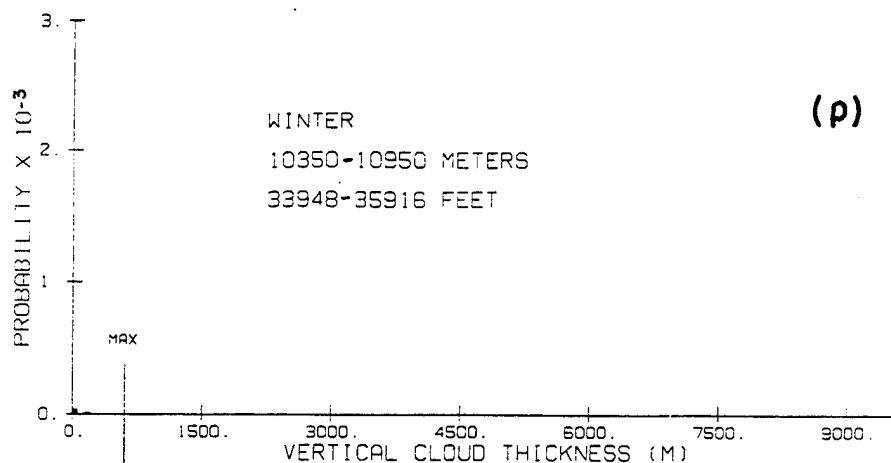
Figure 33.     (n,o,p)     Probabilities of Vertical Cloud
                            Thicknesses for Clouds With Bases
                            Between the Indicated Altitudes.

59
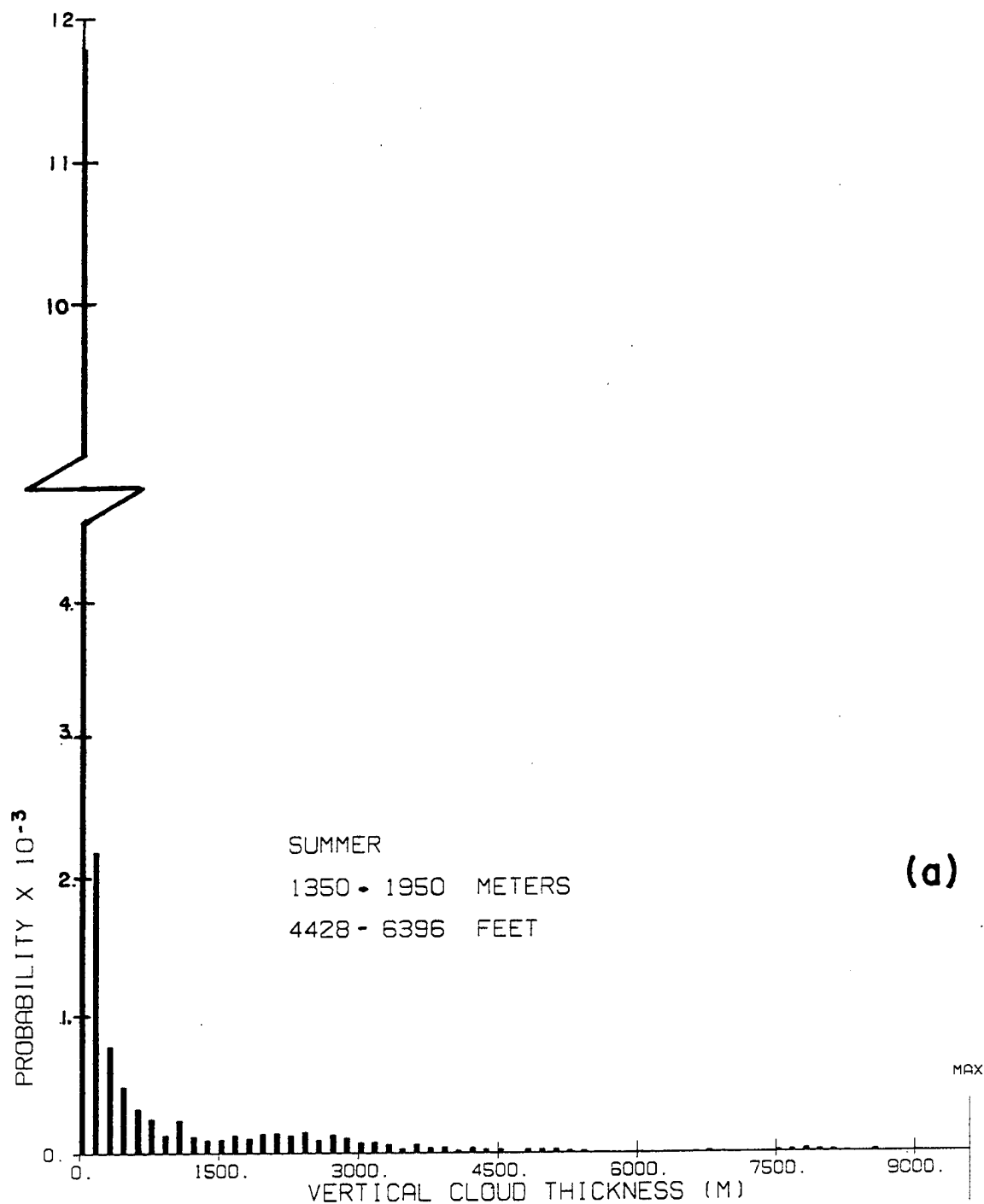
Figure 34.    (a)        Probability of Vertical Cloud Thickness
                        for a Cloud With Bases Between 1,350 and
                        1,950 Meters.  The maximum possible
                        vertical thickness is indicated by the
                        line labeled MAX.

60
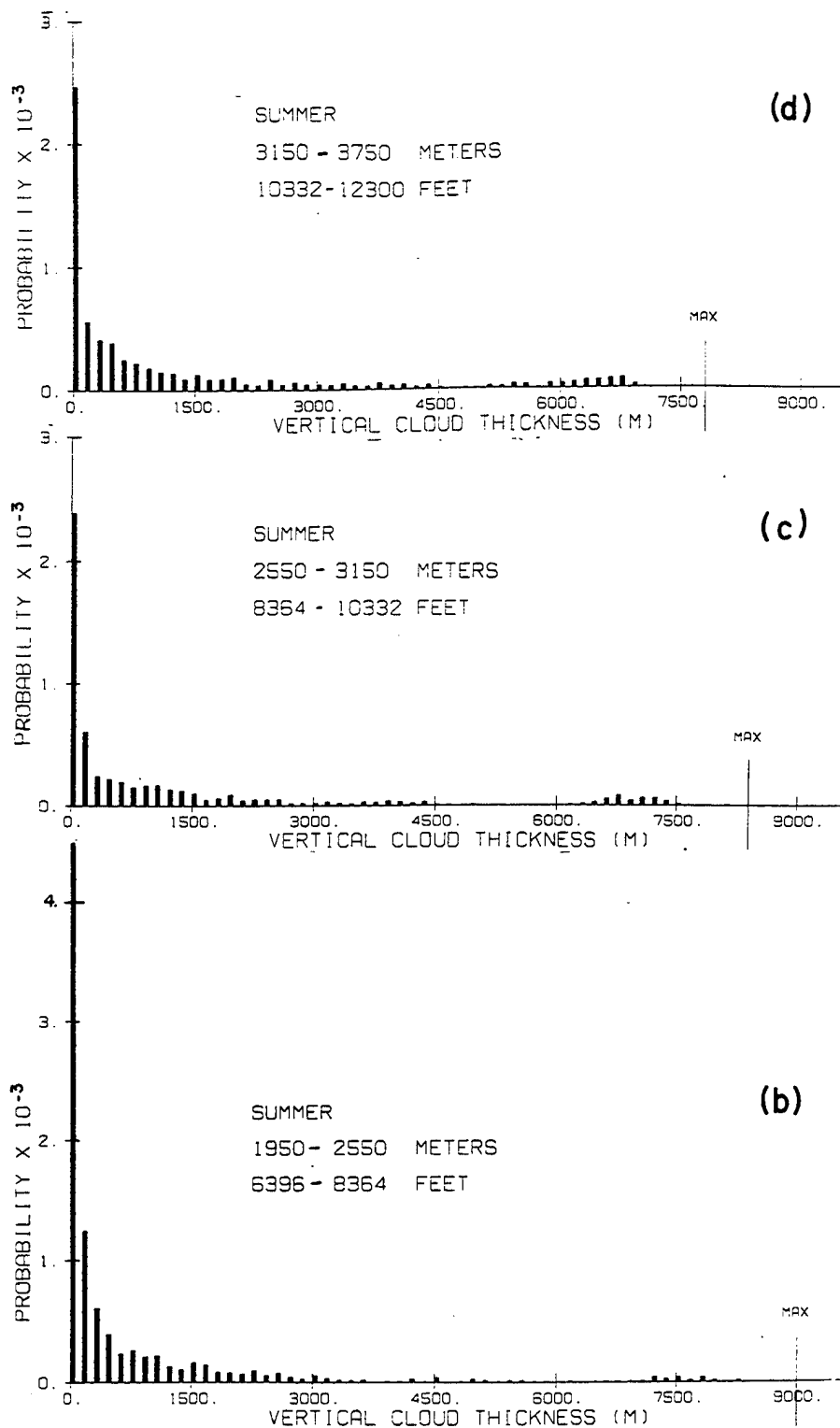
Figure 34.    (b,c,d)    Probabilities of Vertical Cloud
Thicknesses for Clouds With Bases
Between the Indicated Altitudes.

61
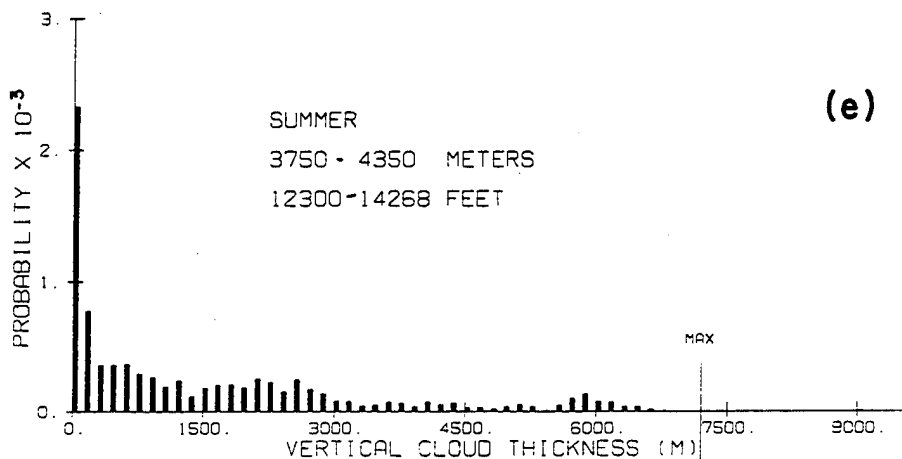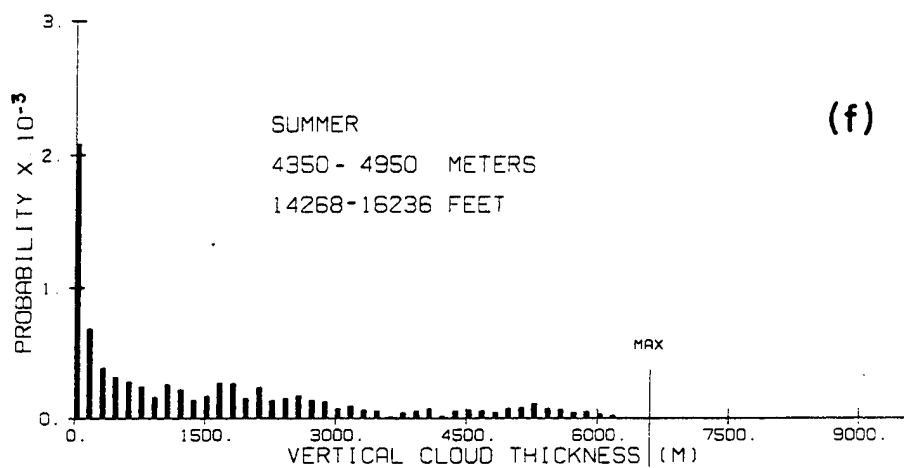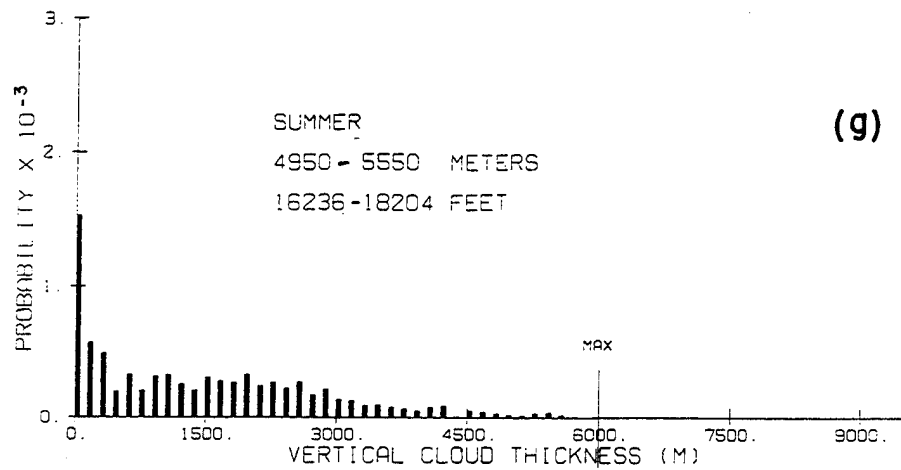
Figure 34.    (e,f,g)    Probabilities of Vertical Cloud
Thicknesses for Clouds With Bases
Between the Indicated Altitudes.
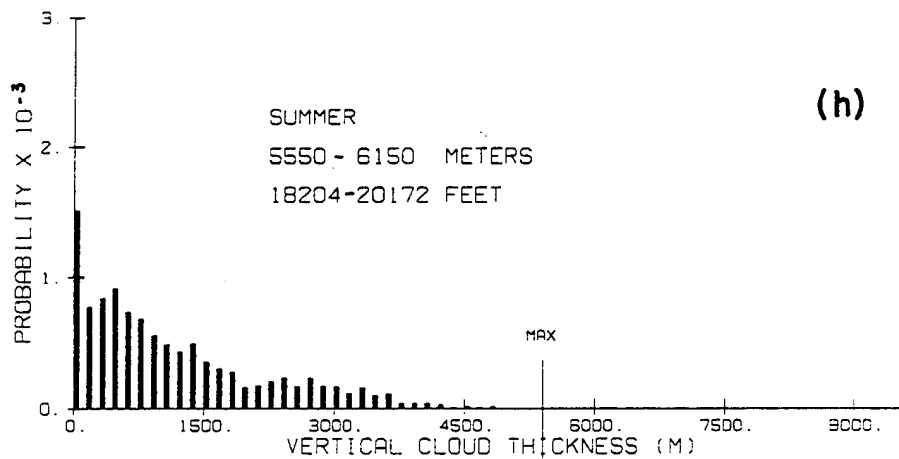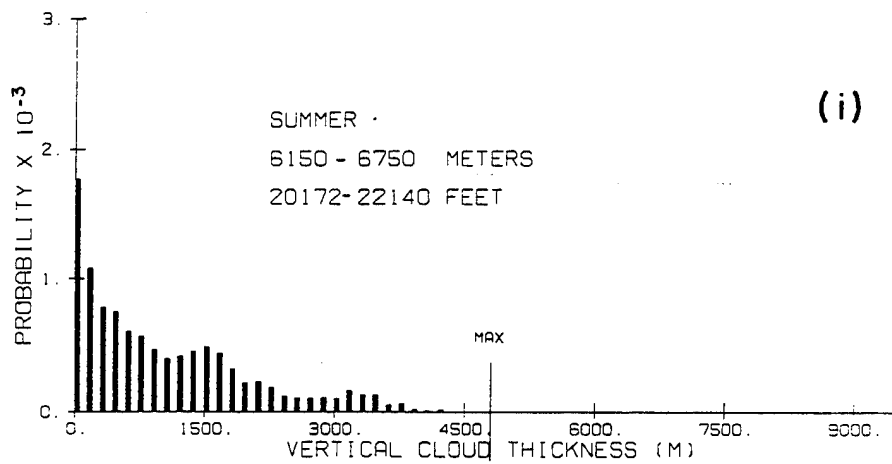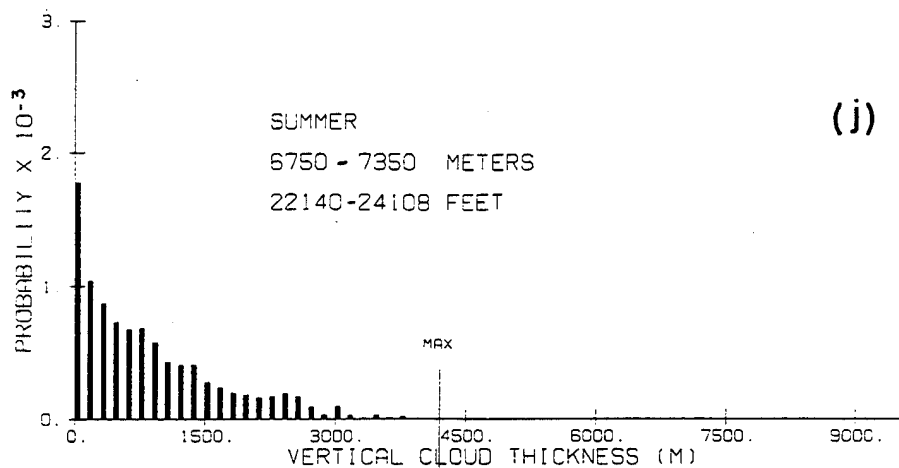
Figure 34.    (h,i,j)    Probabilities of Vertical Cloud
                         Thicknesses for Clouds With Bases
                         Between the indicated Altitudes.
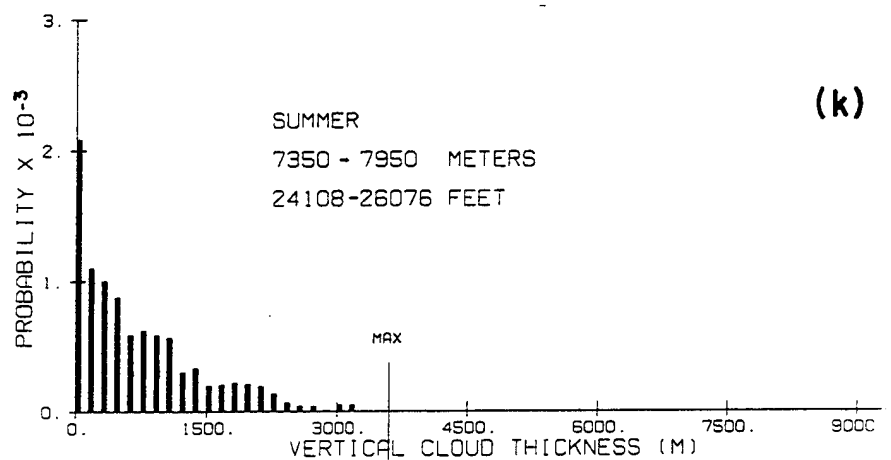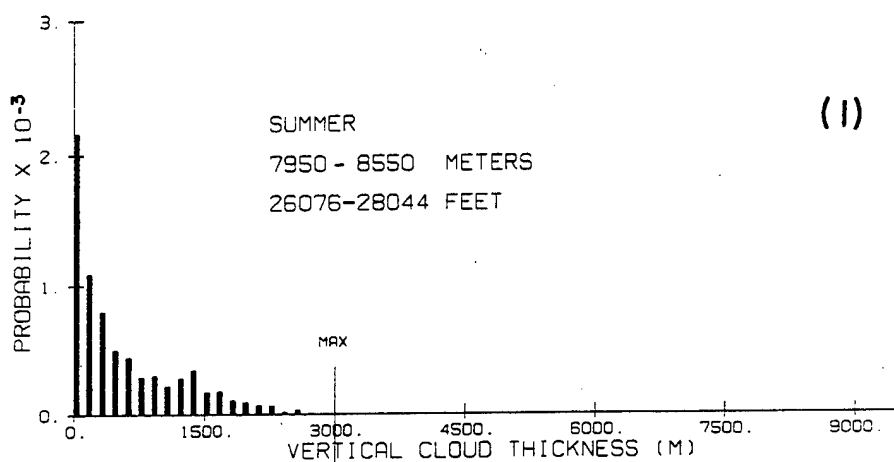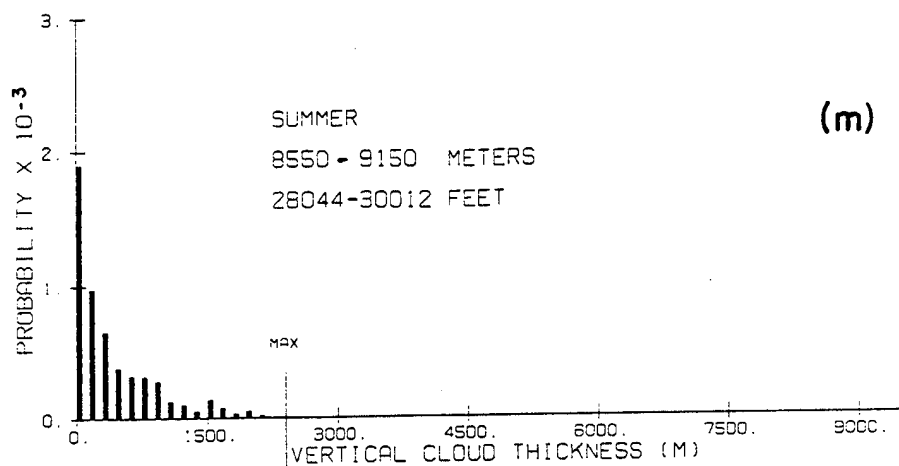
Figure 34.      (k,l,m)      Probabilities of Vertical Cloud
                             Thicknesses for Clouds With Bases
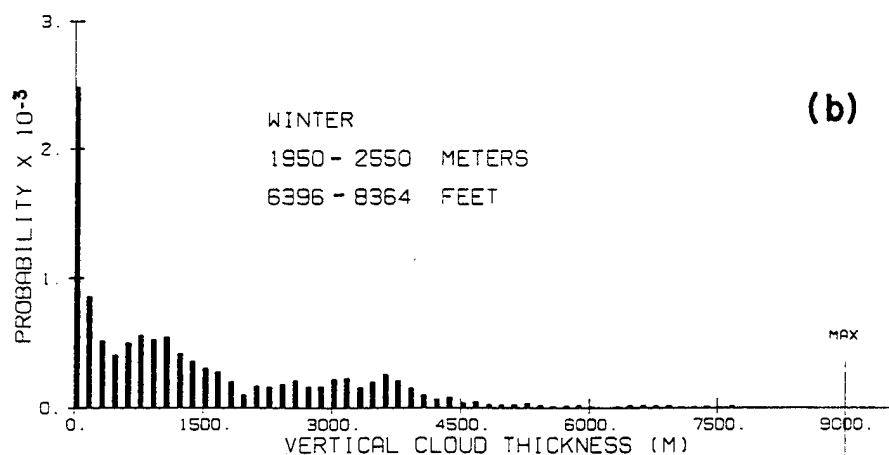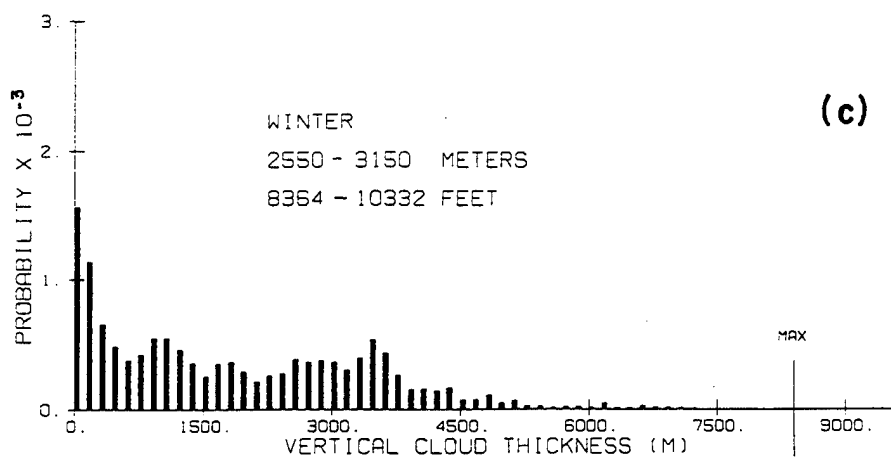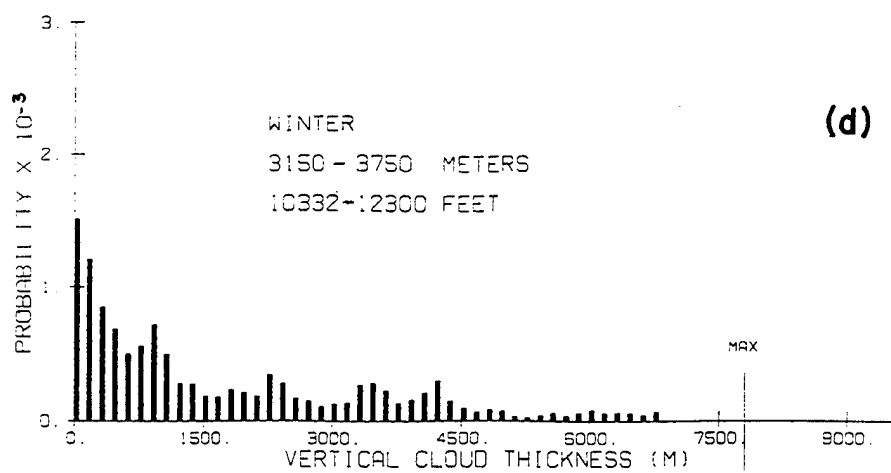                             Between the Indicated Altitudes.
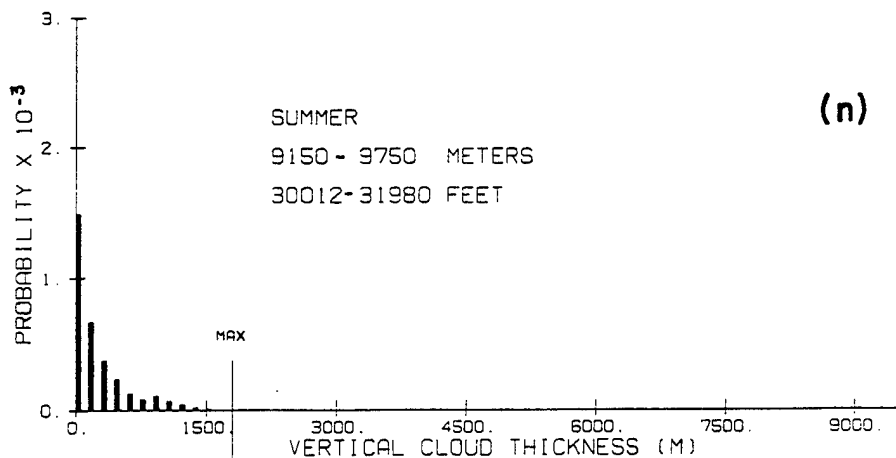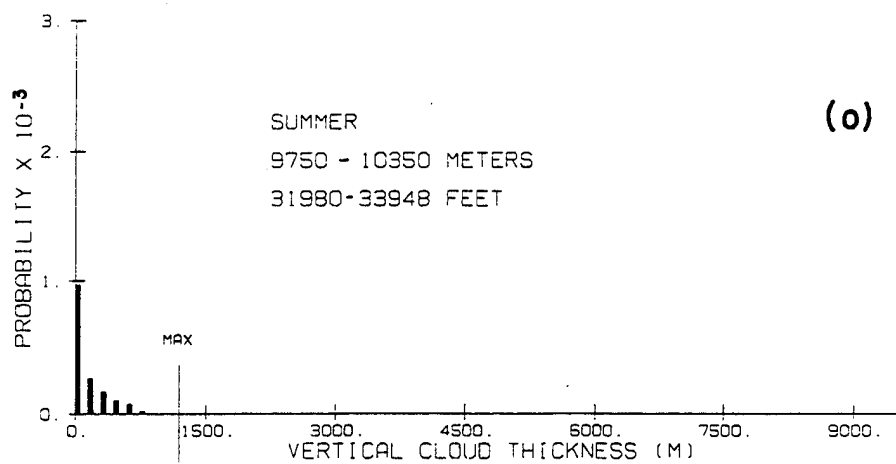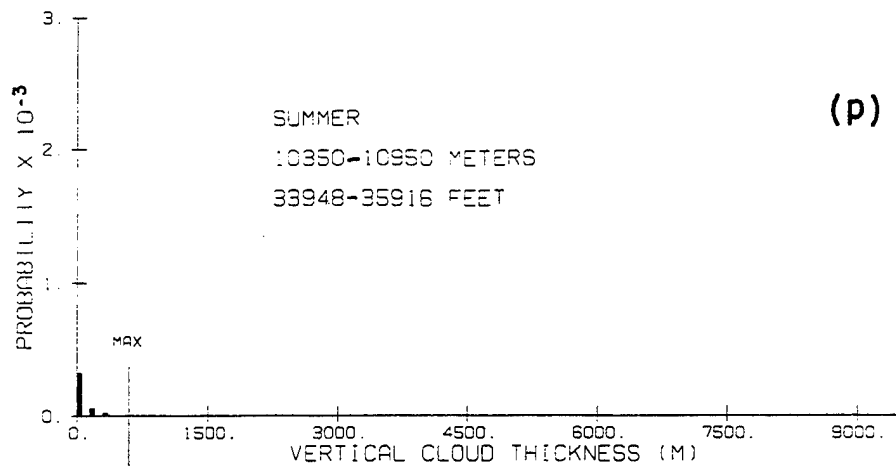
Figure 34.    (n,o,p)    Probabilities of Vertical Cloud
Thicknesses for Clouds With Bases
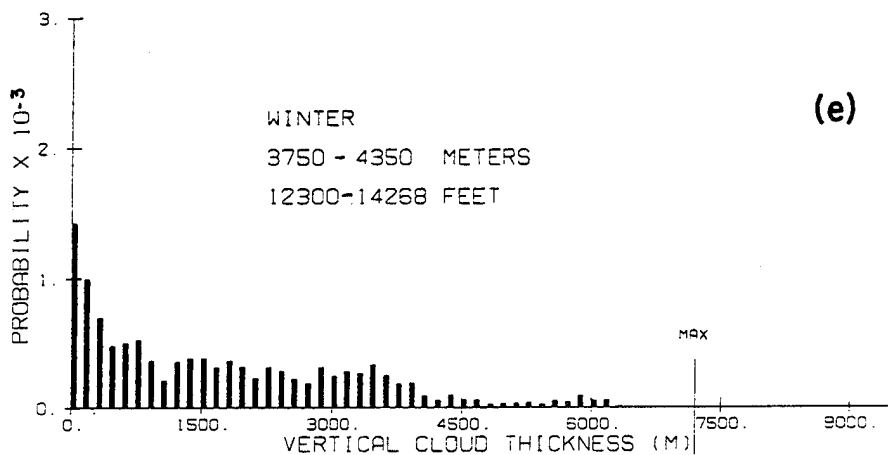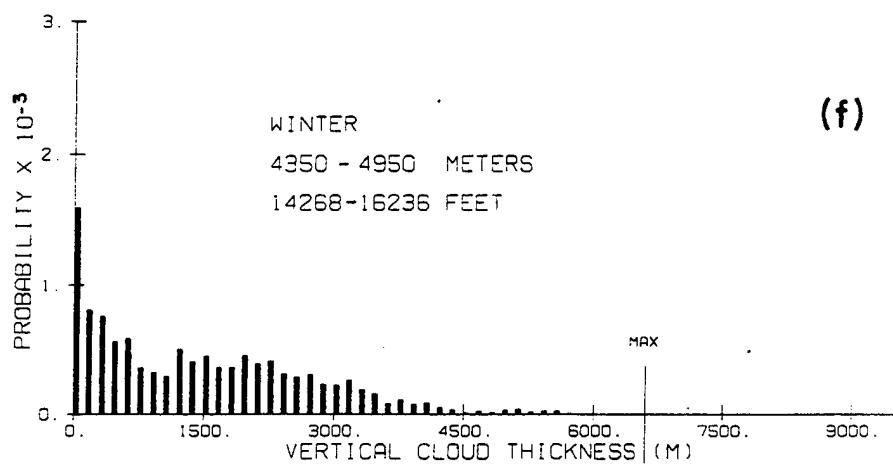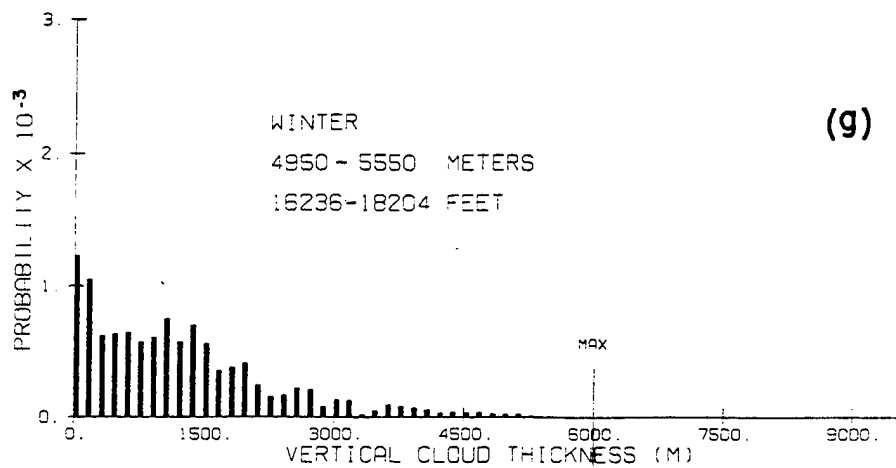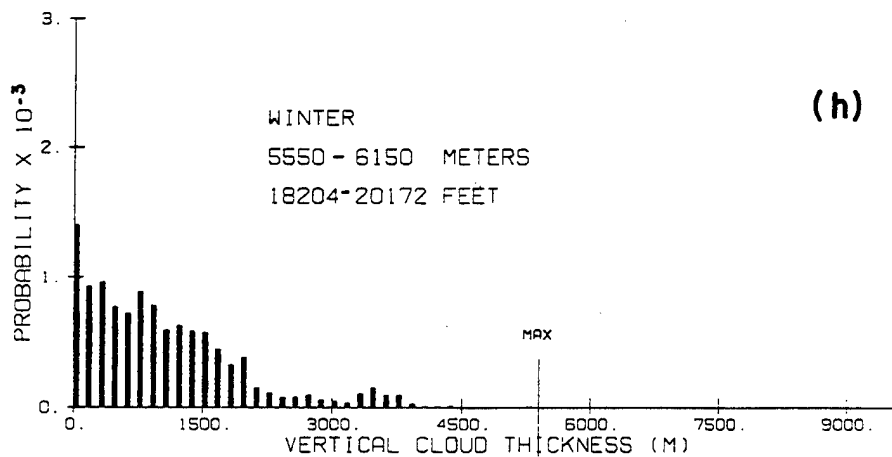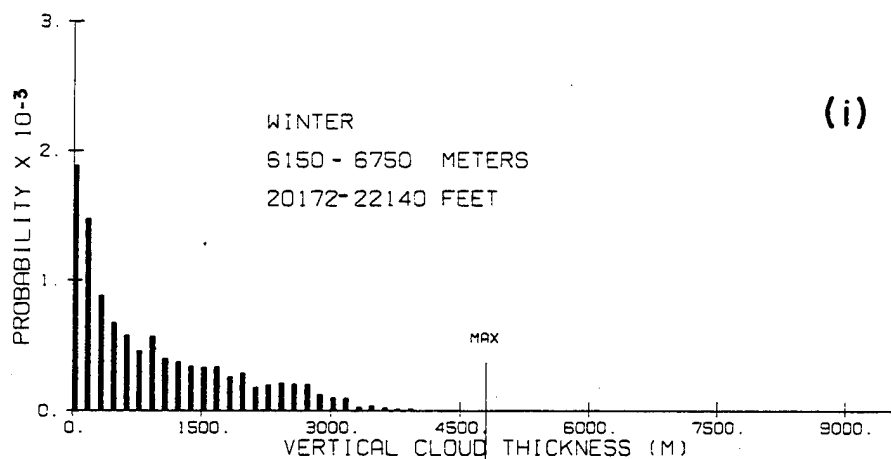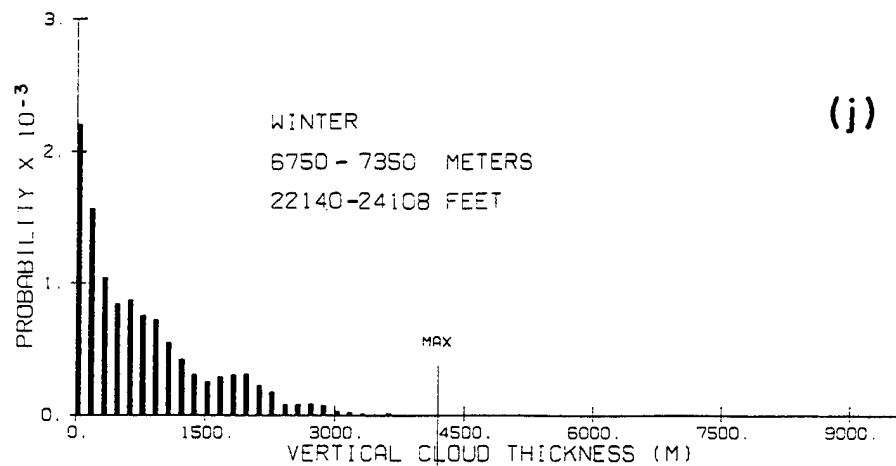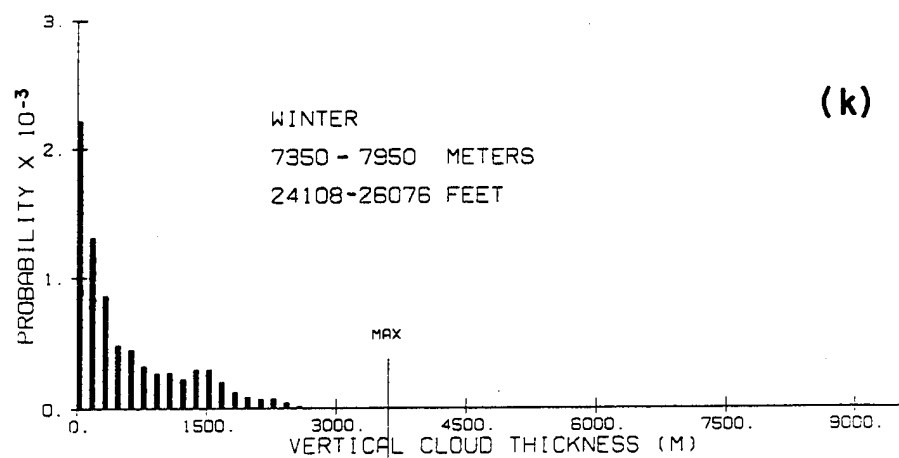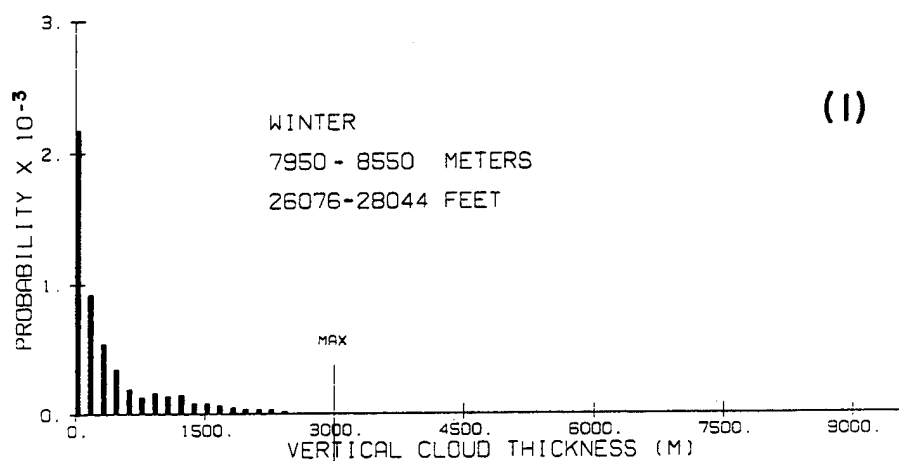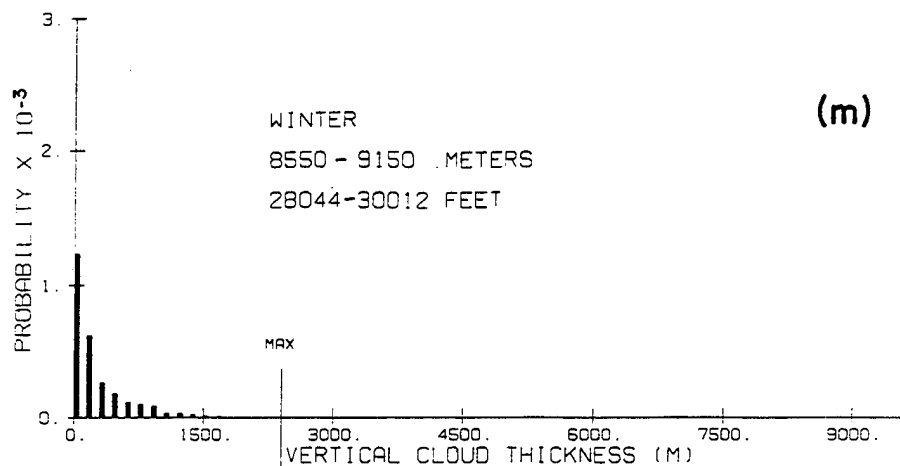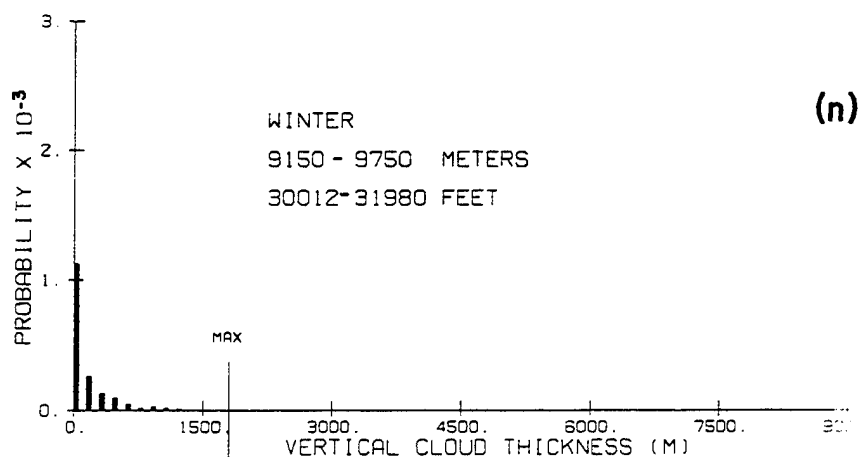Between the Indicated Altitudes.

65

The maximum possible cloud thickness in the figure is 9,600 meters (10,950 meters minus the lowest height of 1,350 meters). This thickness is marked on the horizontal axis as a vertical line labeled MAX. The remaining figures, three to a page, show probabilities of cloud thicknesses for clouds originating between the indicated altitudes using 600-meter increments up to 10,950 meters.

Note that these are probability densities using a 150-meter resolution. Other resolutions would give different densities. For example, a 75-meter resolution would have densities half as large on the average.

### 3.2.8  Probability of Cloudy or Clear Run Lengths

A run is an uninterrupted sequence of the same kind of condition e.g., 1 hour of cloudy. This statistic shows the probability of how long a continuous time period of either a cloudy or a clear condition over the radar beam will last. Program TPQRUN was set up to tabulate the number of continuous running clear or cloudy 1-minute shots that occurred in a sequence of observation episodes for winter and summer cases. The criterion for each clear case was that no cloudy cells were found along a given shot between 4,428 and 36,000 feet. Otherwise, it was deemed a cloudy case. Graphs of the probabilities of cloudy or clear run lengths for the winter season are shown in Figures 35 and 36, respectively. Figures 37 and 38 show graphs for the summer season.

Figure 35 (a) shows the probability of a run length greater than or equal to the specified run length shown in minutes along the horizontal axis for cloudy conditions in the winter months of December, January, and February. Figure 35 (b) is a continuation of Figure 35 (a). Here the vertical axis in (b) is magnified to show in more detail the probability of run lengths greater than or equal to run lengths found on the horizontal axis at a lesser resolution of 1-24 hours. The actual numbers used for deriving the statistic are shown in the sentence found above each graph. Note that cloudy run lengths in the winter, Figure 35 (b),

66

CLOUDY CONDITIONS ONLY
DEC
JAN
FEB

PROBABILITY OF A RUN >= SPECIFIED RUN LENGTHS
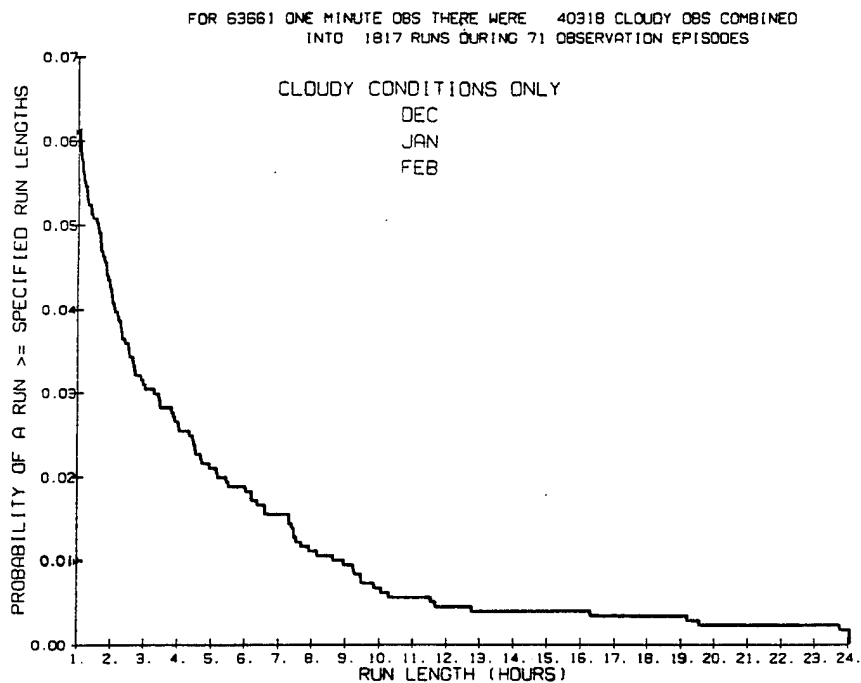
RUN LENGTH (HOURS)

**Figure 35.     (b)   Continuation of Probable Cloudy Run Lengths Greater Than or Equal to Specified Run Lengths From 1-24 Hours.**

PROBABILITY OF A RUN >= SPECIFIED RUN LENGTHS
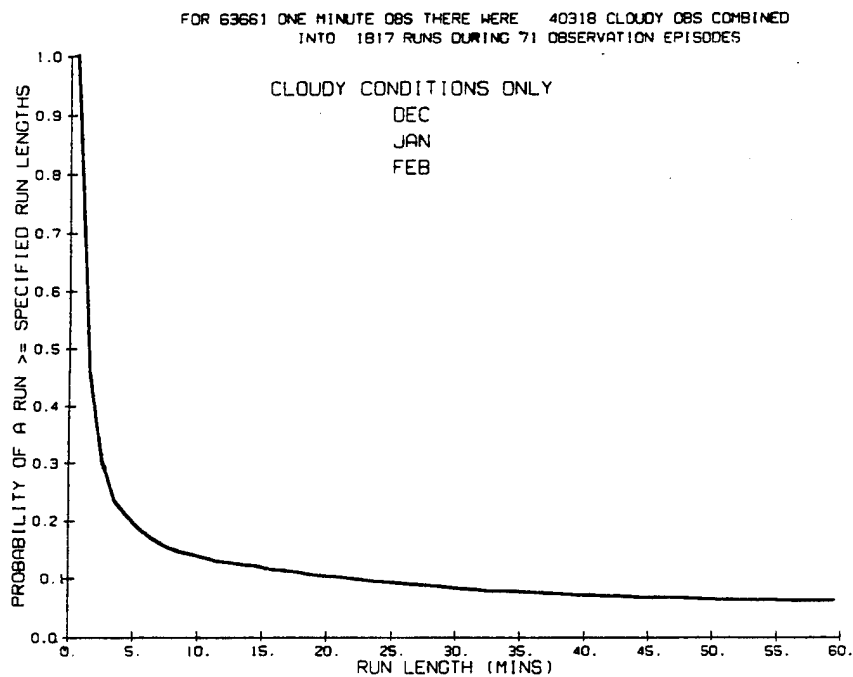
RUN LENGTH (MINS)

**Figure 35.     (a)   Probability of a Cloudy Run Length Greater Than or Equal to Specified Run Lengths in Minutes up to One Hour for Winter Months.**

67

CLEAR   CONDITIONS ONLY
DEC
JAN
FEB
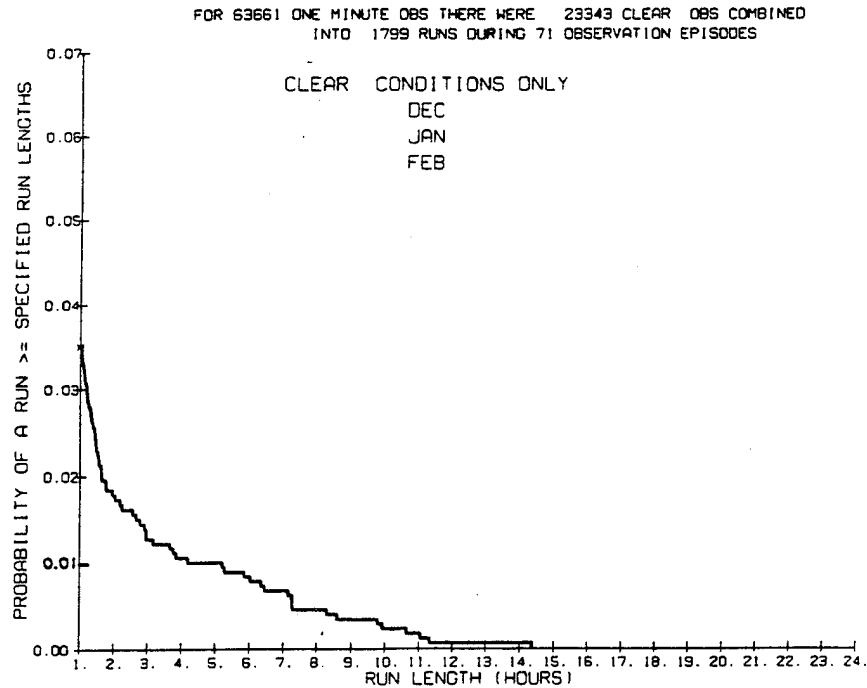


Figure 36.     (b)   Continuation of Probable Clear Run Lengths
Greater Than or Equal to Specified Run
Lengths From 1-24 Hours.

CLEAR   CONDITIONS ONLY
DEC
JAN
FEB
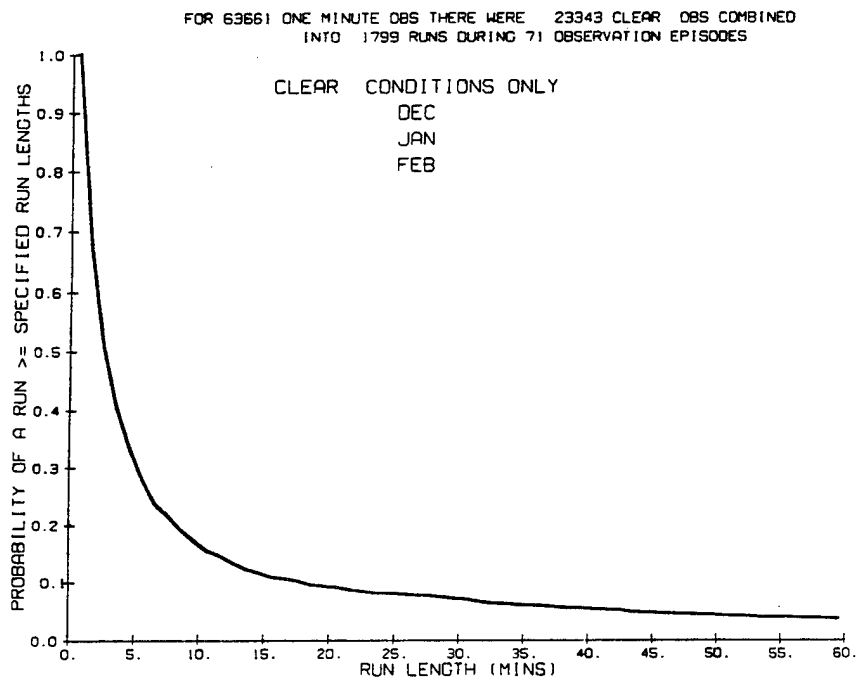


Figure 36.     (a)   Probability of a Clear Run Length Greater
Than or Equal to Specified Run Lengths in
Minutes up to One Hour for Winter Months.

CLOUDY CONDITIONS ONLY
JUN
JUL
AUG
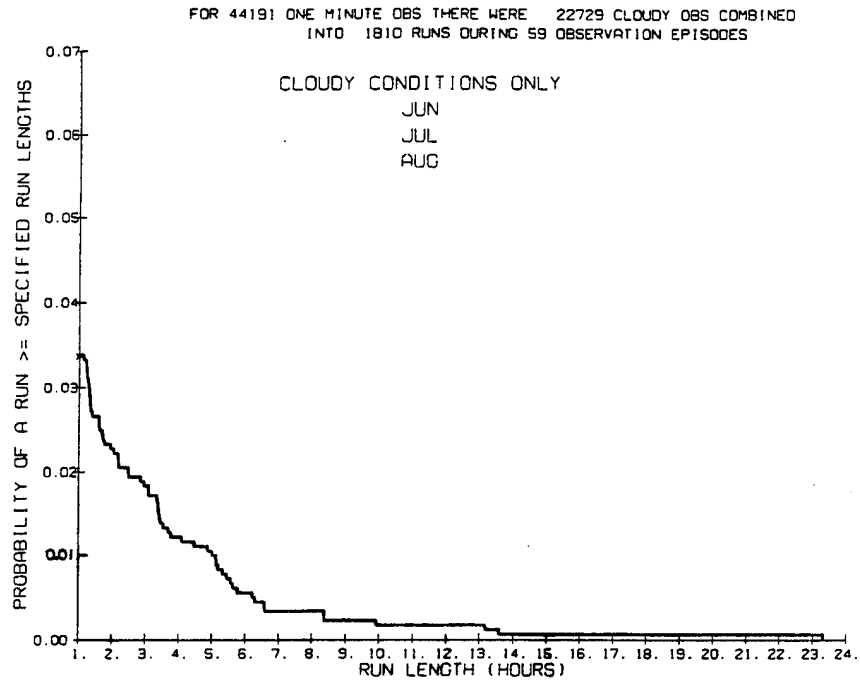
Figure 37.    (b)    Continuation of Probable Cloudy Run Lengths Greater Than or Equal to Specified Run Lengths From 1-24 Hours.

FOR 44191 ONE MINUTE OBS THERE WERE   22729 CLOUDY OBS COMBINED
INTO   1810 RUNS DURING 59 OBSERVATION EPISODES

CLOUDY CONDITIONS ONLY
JUN
JUL
AUG
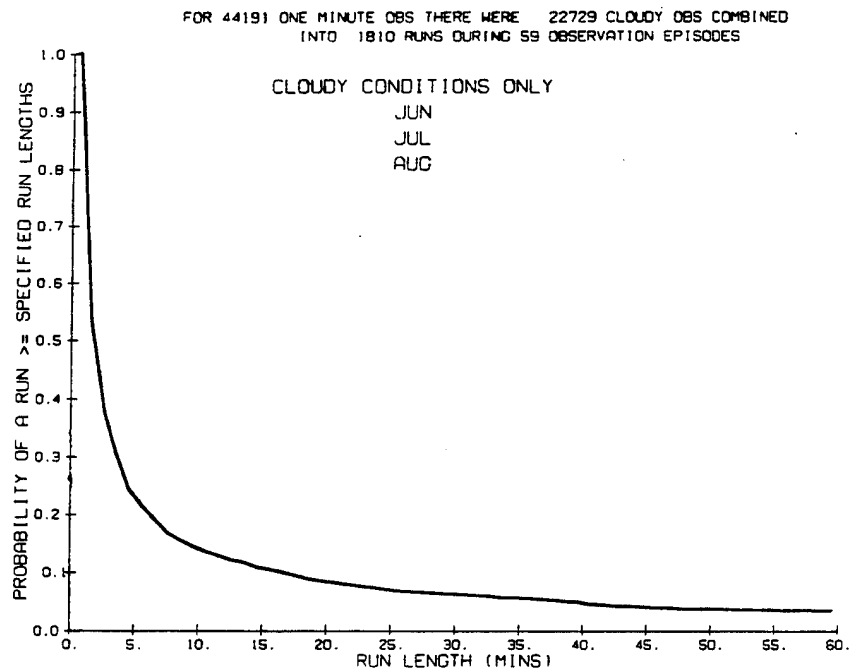
Figure 37.    (a)    Probability of a Cloudy Run Length Greater Than or Equal to Specified Run Lengths in Minutes Up to One Hour for Summer Months.

CLEAR CONDITIONS ONLY
JUN
JUL
AUG

RUN LENGTH (HOURS)

PROBABILITY OF A RUN >= SPECIFIED RUN LENGTHS
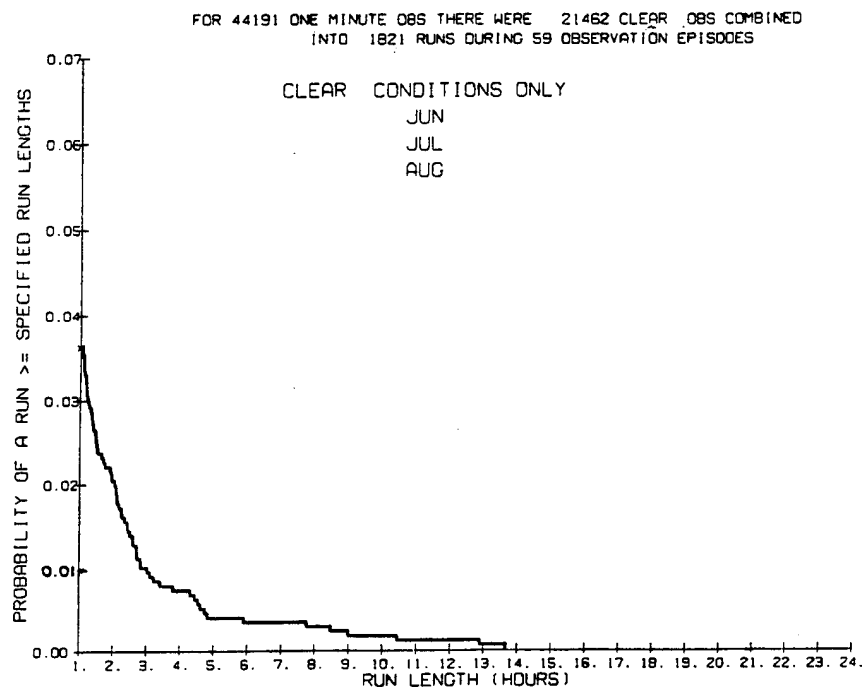
Figure 38. (b) Continuation of Probable Clear Run Lengths Greater Than or Equal to Specified Run Lengths From 1-24 Hours.

FOR 44191 ONE MINUTE OBS THERE WERE 21462 CLEAR OBS COMBINED
INTO 1821 RUNS DURING 59 OBSERVATION EPISODES

CLEAR CONDITIONS ONLY
JUN
JUL
AUG

RUN LENGTH (MINS)

PROBABILITY OF A RUN >= SPECIFIED RUN LENGTHS
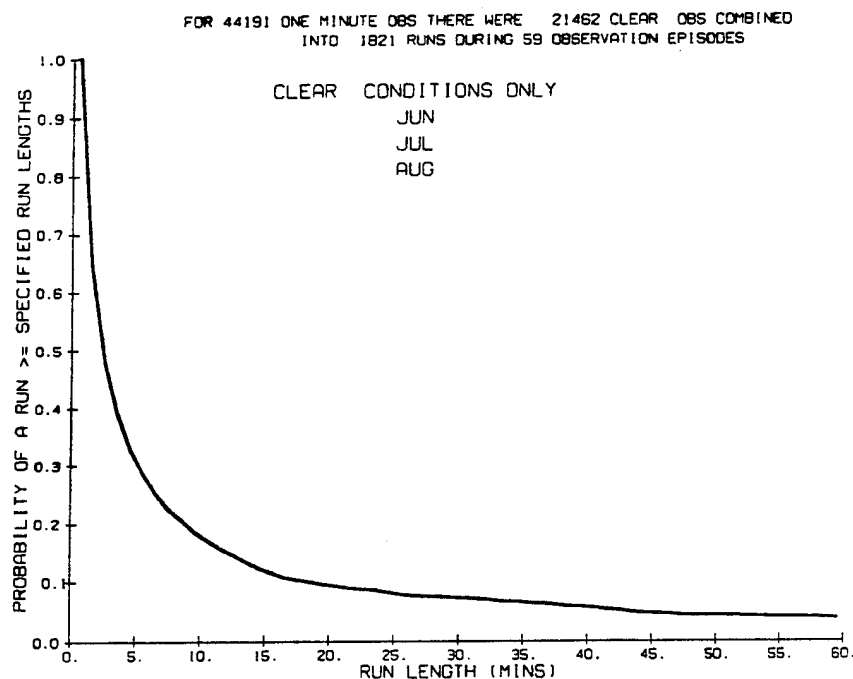
Figure 38. (a) Probability of a Clear Run Length Greater Than or Equal to Specified Run Lengths in Minutes up to One Hour for Summer Months.

70

occurred as long as 24-hours or more. (Because of a data processing cutoff point of 24-hours, graphs were terminated at the 24-hour run length.) Clear run lengths in the winter occurred for only a maximum of 14.3 hours, Figure 36 (b). In the summer, cloudy run lengths occurred up to 23.3 hours, Figure 37 (b), while clear runs occurred up to only 13.7 hours, Figure 38 (b).

The same problem exists with deriving this statistic as that with deriving the serial correlation of clouds at altitude in Section 3.2.6. That is, duration of cloudy or clear events are lost during radar operations when shutdown and turn-on events take place. Ways to eliminate the problem are to keep the radar on indefinitely or eliminate first and last events within each observation episode. Eliminating first and last events was not used here because of lack of data. Thus, these statistics have a small bias toward being too short.

### 3.2.8.1 To Convert Runs to Persistence Probability

Again, we define a run as an uninterrupted sequence of the same condition, e.g., 1 hour of cloudy. A run begins when the condition starts and ends when the condition changes. This definition can apply to a continuous measurement or to discrete measurements at a fixed time interval or in this case an average over one minute. However, run statistics, e.g., average length, will differ depending on the length of the time interval. Runs can be converted to persistence probability where persistence probability is the probability that a condition will remain uninterrupted for a given length of time **given that the condition is occurring initially**. The initial time often will be in the middle of a run. The TPQRUN program computed the number of runs for 1 minute intervals up to 24-hours (see Section 4.5). A single count was made of all runs longer than 24-hours without regard to their length. This lack of information on the longer runs precludes the direct method of counting. However, the following formula starts with the shortest run and works up.

71

where

$$P_k = 1 - \frac{kN}{C} - \frac{1}{C} \sum_{j=1}^{k} (j - k) \, N_j \qquad (6)$$

$P_k$ is the persistence probability that the same condition
will continue uninterrupted for at least k time steps,
$N$ is the total number of runs of the condition of all
lengths,

$N_j$ is the number of runs of length j, and

$C$ is the total number of occurrences of the condition.
Note that $N$ is synonymous with the variable, kount, and $C$ is
synonymous with the variable, iclcd, both of which are defined in
Section 4.5. $N_j$'s are obtainable through data files stored on a
single diskette, again see Section 4.5.

## 4.0 ALGORITHMS FOR DETERMINING THE CLOUD LAYER STATISTICS

This section is devoted to documenting the algorithms used
in determining the cloud layer statistics shown in this report.
A mixture of FORTRAN code and conventional array subscripting may
be best for detailed descriptions of the algorithms used.
Descriptions of algorithms for deriving the probabilities of
clouds aloft and the diurnal cloud layer analysis have already
been discussed in Sections 3.2.3 and 3.2.4. We will, therefore,
start with describing the algorithm for determining probability
of vertical CFLOS between two heights.

### 4.1 Algorithm for Determining Probability of Vertical CFLOS Between Two Heights

The probabilities of vertical CFLOS between two heights were
determined by first defining an array (s) dimensioned 73 x 73
elements for summations of CFLOS events and a second array (p)
dimensioned as 73 elements to provide storage for population
counts. The (p) and (s) arrays were set to zeroes and then for
each one-minute averaged radar data shot being processed for a
given case, a loop was entered to sum the CFLOS events
encountered into the s and p arrays as follows:

```
            DO i = 10,73
            p_i = p_i + 1
                DO j = i,73
                    IF(SHOT_j .NE. CLEAR) GO TO **
                    s_{i,j}=s_{i,j} + 1
                ENDDO
        ** ENDDO.
```

At the completion of all cases processed, an array called, prob, dimensioned 73 x 73 was filled with resulting CFLOS probabilities by dividing all summations in the s array by the population values in the p array. The probability array was then sent to a contouring routine to produce the graphs of probability of vertical CFLOS between heights.

## 4.2 Algorithm for Determining Cloud Layer Correlation Between Two Heights

The cloud layer correlation graphs were derived in the following manner. First, a four-dimensional array was configured to store summations of cloudy or not conditions occurring at a given height with those that are cloudy or not at some other height. For discussion, we will dimension and call this array $ibox_{2,2,73,73}$ (see Section 3.2.4 for explanation of why cells 74 through 120 were omitted). The 2 x 2 portion of the array defines space for contingency tables of dichotomous events of cloudy or not conditions for tetrachoric probability computations. The 73 x 73 portion defines space for storing these events at specified heights. For each one minute averaged radar shot being processed for a given episode, a loop was entered to sum the conditional cloud cover events into the ibox array in the following manner:

```
        DO i = 10,73
        given = CLEAR
        if(shot_i .ne. CLEAR) given = CLOUDY
            DO j = i,73
                condition = CLEAR
                if(shot_j .ne. CLEAR) condition = CLOUDY
```

73

$$ibox_{given,condition,i,j} = ibox_{given,condition,i,j} + 1$$

ENDDO

ENDDO.

An array "corr" dimensioned 73 x 73 was used to store the final resulting correlations in the manner described below,

```
DO i = 10,73
      DO j = 10,73
      a = ibox_{1,1,i,j}
      b = ibox_{2,1,i,j}
      c = ibox_{1,2,i,j}
      d = ibox_{2,2,i,j}
      if(a.or.b.or.c.or.d .lt. 11) then
            corr_{i,j} = BLANK ; Not enough data.
        else
            corr_{i,j} = tetra(a,b,c,d)
      endif
      ENDDO
      ENDDO.
```

where

"tetra" is a function for deriving tetrachoric correlation.

When all cases for a given month or season were processed, the array corr was sent to a contouring routine to produce the contours of equal one tenth correlation values between 0 and 1.0.

## 4.3 Algorithm for determining Serial Correlation of Clouds at Altitude

Two computer programs, TPQTEM and TPQTETR, were assembled to produce serial correlation of clouds at altitude. The first program TPQTEM, was a preprocessing program used to sum dichotomous cloud events at given levels of the atmosphere. In the program, a two-dimensional array named and dimensioned as $it_{1440,74}$, was utilized to store up to 1,440 minutes (24 hours) of cloud/no cloud data for 74 cells. For each case encountered for a given month, the cloud/no cloud values in the cells along a

74

given shot were distributed into the it array. This data transfer was made so that the first cloud/no cloud value at a given height, regardless of its time of day, was distributed into the first element of the it array. On completion of the distribution of all the data for a single case, a summation of dichotomous events took place using a four-dimensional array called $ibox_{2,2,1440,74}$. This summation process is documented in detail below.

```
      DO i=10,74
        DO m=1,minutes - 1
        given = it_{m,i}
        j = m + 1
        k = 0
          DO mm = j,minutes
            k = k + 1
            cond = it_{mm,i}
            ibox_{given,cond,k,i} = ibox_{given,cond,k,i} + 1
          ENDDO
        ENDDO
      ENDDO
    where
```

minutes = the total number of minutes of a given episode and

i = 10,74. (Processes cells from 4,920-36,408 feet. After processing all cases for a given month the ibox array was stored for subsequent processing using program TPQTETR. For the record, these files were named tpqdec.sav, tpqjan.sav, tpqfeb.sav, tpqjun.sav, tpqjul.sav, and tpqaug.sav.

The second program, TPQTETR, utilized the ibox information retained in the .sav files by the above process to compute the final serial correlations. This program sums data found in the ibox array for a given month with ibox data from another month. Thus, to derive the serial correlations of clouds at altitudes for the winter season, for example, the program first summed together all the information in the ibox arrays of .sav files for

75

December, January, and February. Then the program proceeded to
compute the serial correlations at the given levels into a two-
dimensional array called "$array_{1440,74}$" using the algorithm
detailed below.

```
        DO i = 10,74
          DO m = 1,1440
            a = ibox_{1,1,m,i}
            b = ibox_{2,1,m,i}
            c = ibox_{1,2,m,i}
            d = ibox_{2,2,m,i}
            sum=a + b + c + d
            if(sum .or. a .or. b .or. c .or. d .lt. 11) go to **
            a = a/sum
            b = b/sum
            c = c/sum
            d = d/sum
            array_{m,i} = tetra(a,b,c,d)
          ENDDO
   **   ENDDO.
```

Array was then sent to the contour routine to produce the
graphs of serial correlation of clouds at altitude.

## 4.4  Algorithm for Determining Probability of Vertical Cloud Thickness

Program TPQTHK was developed to compute probability of
vertical cloud thicknesses using the cloud/no cloud image data
created by the TPQAVG program. Program TPQTHK utilized an array
named and dimensioned $isum_{73,73}$ to store 1) the number of
continuous cloudy cells (n) found within 2) the given height
level where a cloud originates (i). Also array $p_{73}$ was set aside
to store population values of each cell. The $SHOT_{73}$ array was
the buffer for storing 73 cloud/no cloud bytes from the cloud/no
cloud image data storage input file. The algorithm for
distributing these parameters is as follows:

```
        DO 20 i=9,73
        p_i = p_i + 1
```

```
      if(SHOT_i .eq. CLEAR .or. SHOT_{i-1} .ne. CLEAR) go to 20
         DO j=i,73
         if(SHOT_j .eq. CLEAR) then
             n = j - i
             isum_{n,i} = isum_{n,i} + 1
             go to 20
         ENDDO
 20   ENDDO.
```

Another array named and dimensioned $ary_{73,0:16}$, where "0:" allows 0 subscripting, was utilized to compress the isum data to a suitable size for graphical display of the cloud thickness statistics. Thus, the loop below was performed to compress results in the isum array (cells 10 thru 73) into the ary array.

```
         DO i = 10,73
         ii = .25*float(i-9) + .75
            DO j = 1,73
               ary_{j,ii} = ary_{j,ii} + isum_{j,i}
            ENDDO
         ENDDO.
```

Since population values of all cell heights are equal, the variable DIV used below was set to the population of $p_{10}$ x 4. (It is multiplied by 4 because of the compression of the data by 4 above). The ary array was then set to probability values of cloud thickness by the following loop.

```
         DO j=1,73
            DO i=1,16
               ary_{j,i} = ary_{j,i} / DIV
            ENDDO
         ENDDO.
```

The ary array was finally plotted out in a format shown in the graphs of probability of cloud thickness.

## 4.5 Algorithm for Determining Probability of Cloudy or Clear Run Lengths

Program TPQRUN was designed to compute probabilities of cloudy or clear run lengths. A preprocessing program called

TPQRU was actually used initially to get the cloud/no cloud image data files into a format for efficient processing using TPQRUN. This preprocessing program reformatted the cloud/no cloud image data for a given monthly set of observation episodes into the format described below.

| Byte | Value | Parameter |
|------|-------|-----------|
| 1 | "t" | Data delimiter. |
| 2-3 | 0 - 23 | Begin time Hour, |
| 4-5 | 0 - 59 | Minute |
| 6-7 | 0 - 59 | Second |
| 7-n | "0" or "1" | 0 = Clear, 1 = Cloudy cell. |
| . | . | |
| . | . | |
| . | . | |
| n | "t" | Beginning of next observation episode. |
| . | . | |
| . | . | |
| . | . | |
| EOF | | End of file. |

The new data were written onto permanent output files called tpqjun.run, tpqjul.run, tpqaug.run, tpqdec.run, tpqjan.run, or tpqfeb.run.

Program TPQRUN read the selected .run files above to compute and display the probability of cloudy or clear run lengths. (The program was run separately for cloudy or clear conditions.) An array named and dimensioned $icount_{1441}$ was utilized for summing up occurrences of 1-minute runlengths, and array $p_{1441}$ was used to store final probability values of run lengths. Several counters

were used for bookkeeping such as the variable "kount" used to count the runs. Variable "pop" was used for summing populations, "numcas" keeps count the number of cases or episodes and "iclcd" the number of cloudy or clear cells encountered. In fact, these counters were displayed in the sentence above each of the graphs in Figures 35-38. Thus, the sentence showing these variable names instead of numbers would look like, "FOR pop ONE MINUTE OBS THERE WERE iclcd CLEAR (or CLOUDY) OBS COMBINED INTO kount RUNS DURING numcas OBSERVATION EPISODES". In general, the documentation of the program is listed below.

Processing begins by selecting certain input option values for loop controls.

1) Input the number of monthly cases, "ncases". (usually 3 for processing seasonal statistics).

2) Input which runs to process either Cloudy ("1") or Clear ("0"). The choice is stored into variable "test".

```
      DO 9898 nn=1,ncases
      kount=0
c      Input name of month to process. For example,
c      tpqjun.run.
c      Open the requested input file as unit 1.

      DO k=1,40000
      read(1,100,end=999) ibyte
100   format(a1)
          if(ibyte.eq."t") then
              read(1,101,end=999) hour,minute,second
              numcas=numcas + 1
              if(kount .ne. 0) icount_{kount} = icount_{kount} + 1
              kount=0
          else
              pop=pop+1
```

79

```
                  if(ibyte.eq.test) then
                      kount=kount + 1
                      iclcd=iclcd + 1
                  else
                      if(kount.gt.1440) kount=1441
                      if(kount.ne.0) icount_kount=icount_kount + 1
                      kount=0
                  endif
              endif
          ENDDO
999       CONTINUE
          if(kount.gt.0) then
             if(kount.gt.1440) kount=1441
             icount_kount=icount_kount + 1
          endif
9898      close unit 1


c Computation of the probabilities of run lengths is next.

c         Sum up the counts.
          kount=0
          DO i=1,1441
              kount = kount + icount_i
          ENDDO


c         Compute probabilities.
          DIV = kount
          DO i=1,1441
              p_i = float(icount_i)/DIV
          ENDDO


c         Backward cumulative probabilities.
          n=1440
          DO i=1,1440
            p_n = p_n + p_{n+1}
```

80

```
n = n - 1
ENDDO.
```

At this point, the p array is sent to the plotter routines for display of the probability of cloudy or clear run lengths.

On option, the icount array can be saved as a separate file on a diskette at the end of each program run. In fact, this has been done for both the winter and summer clear and cloudy cases. The values stored are the run length variables $N_j$ in Section 3.2.8. A readme file has been stored onto the same diskette that documents the formats of the files so that interested users can program reading of the data.

As mentioned earlier, recording episodes of continuous 1-minute averages were at the most 24-hours long and many were shorter. The breaks in recording affect the run lengths making them appear somewhat shorter than they actually are. The number of episodes is also given so that this bias could, in principle, be estimated. However, only the raw statistics are given here.

## 5. SUMMARY

For the first time, climatological cloud layer statistics derived from echo intensities received by a 35-GHz vertical propagating radar have been compiled and presented. Most of the statistics compiled were for cloud conditions occurring at vertical heights of the atmosphere extending from 1,350-10,950 meters (4,428-35,916 feet). The radar was actually capable of observing the atmosphere from the surface to about 18 km or 60,000 feet. But, echoes below about 1,300 meters were too noisy to process and cloudy occurrences above about 11 kms were considered too low for stable statistical computations.

Each cloud layer within the vertical radar beam was defined to be 150 meters or 492 feet in height. Radar data acquisition rate at the site was one beam "shot" at about one second each. These shots were averaged into 1-minute averaged groups for deriving the statistics. Each cloud layer was considered to be either cloudy or clear based on a dBZ threshold that was determined subjectively as outlined in Section 3.1.

A summary of the statistics presented in this report is discussed as follows.

1)    The monthly probabilities of clouds aloft for individual winter and summer months show estimates of the extent of the monthly variability in the frequency of clouds aloft.  Monthly and seasonal curves give insight as to how high into the atmosphere clouds can extend before they become nearly extinct over the New England area.  The curves appear to give good monotonic decreasing sequences of probabilities of clouds aloft from 5,000-36,000 feet.

2)    The diurnal cloud layer analysis or probabilities of clouds aloft over a 24-hour period for both winter and summer cases show an intriguing decrease in the amount of cloud cover during the morning hours at conventional cloud layers for middle and high clouds over New England.  This phenomenon may be due to a low data capture rate where data capture = (Number of data values actually captured)/(Number of data values proposed).  However, since the phenomenon is consistent for both seasons perhaps it should be further investigated.

3)    The graphs of probability of vertical CFLOS and cloud layer correlation between two heights show the kind of graphical representation that should help fill the requirement for determining these statistics for at least the vertical CFLOS between two points when both points are aloft.

4)    The serial correlation of clouds at altitudes when combined with probabilities of clouds aloft can lead to statistics pertaining to cloudy or clear reoccurrences.  As expected, higher correlation values shown in the graphs for winter episodes appear to last longer than those for summer episodes.

5)    Probability of vertical cloud thickness for clouds with bases between indicated altitudes is a relatively new statistic made possible by the TPQ11 radar.  The cloud thickness probabilities can be beneficial toward predicting the success of certain sensor designs.

82

6)      Probabilities of cloudy or clear run lengths for both seasons show dramatic decreases in probable occurrences of these sky conditions lasting one hour or less.  Very small probabilities (less than .07) of cloudy or clear conditions are shown for run lengths lasting 1 hour or more up to 24 hours. This information can be beneficial for simulating the persistence of cloud cover and CFLOS conditions.

Some of the shortcomings involved with deriving the statistics using the radar data are discussed next.

1)     A larger data capture rate would have been more desirable for deriving the climatological cloud layer statistics.

2)     The initial beam width of the radar is only about .26 degrees, which limits the atmospheric scale to which results apply.

3)     Although great care was utilized in determining a cloud/no cloud threshold for defining the data for subsequent statistical processing, these thresholds are somewhat subjective and obviously can have considerable influence on the final statistics.

4)  Serial correlations can be influenced by radar operations. For example, in some cases the radar may have been turned on during the last minute of a lengthy time persistent cloudy or clear condition over the radar beam.

Finally, recommendations for future TPQ11 35-GHz radar data acquisition are listed below.

1)     Define cell width, beam extension height and data sampling rate up front and don't change it.  If these parameters for some reason must be changed then documentation of the changes should be made available.

2)     Acquire data over uninterrupted periods of time for up to three or four consecutive days if possible.  If long periods of data acquisition are impossible, then do shorter periods at **random** intervals.

3)    Make sure that date/time groups such as Julian days, hours minutes and seconds for labeling digital data records are consistently correct.

4)    Document all important activities such as downtime, program changes, and format changes.  This document should accompany the data when they are released to other investigators.

The statistics presented here provide a good first step approach for the development of probability and correlation statistics of cloud cover, and CFLOS, in layers or at specified levels of the atmosphere using 35-GHz radar data.  It would be desirable to collect 35-GHz radar data at several other sites located in the tropics, subtropics and at several mid and high latitudes. Such a network of observations would give further insight on cloud layer statistics over a global scale.

# REFERENCES

Biswas, K.R., and P.V. Hobbs, 1988: Preliminary Evaluation of the Use of a 35-GHz Radar for Measuring Cloud Base and Cloud Top Heights. AFGL-TR-88-0098, Air Force Geophysics Laboratory, Hanscom AFB, MA. 01731-5000. ADA 199133.

Gringorten, I.I., 1982: Climatic Probabilities of the Vertical Distribution of Cloud Cover. AFGL-TR-82-0078, Air Force Geophysics Laboratory, Hanscom AFB, MA. 01731-5000. ADA 118753.

Kantor, A.J., and D.D. Grantham, 1968: A Climatology of Very High Altitude Radar Precipitation Echoes. AFCRL-68-0630, Air Force Surveys in Geophysics, No. 207, Hanscom AFB. AD 681107.

Petrocchi, P.J., and W.H. Paulsen, 1966: Meteorological Significance of Vertical Density Profiles of Clouds and Precipitation Obtained with the AN/TPQ-11 Radar. *Preprint Volume of the 12th A.M.S. Conference on Radar Meteorology*, Norman, OK.

Petrocchi, P.J., 1990: Private communication. Phillips Laboratory, Atmospheric Structures Branch (GPAA), Hanscom AFB, MA.

Smyth, A., J. Willand, and J. Steeves, 1991: Graphical Analysis of Bertoni's LOS Data. PL-TR-91-2172, Phillips Laboratory, Air Force Systems Command, Hanscom AFB, MA 01731-5000. ADA 251592.

United Aircraft Corporate Systems Center With Technical Assistance Of ARACON GEOPHYSICS CO., 1964: Preliminary Operational Application Techniques for AN/TPQ-11. Published by Air Weather Service (MATS), United States Air Force, Technical Report 180.

Willand, J.H., and J. Steeves, 1990: "Sky-Cover Correlation within a Sky Dome," *Journal of Applied Meteorology, 30, 7, July 1991.*